Faculty of Science and Engineering
Department of Civil Engineering

Biologically Induced Cementation for Soil Stabilisation

Donovan Mujah Anak Bernard Lium

This thesis is presented for the Degree of
Doctor of Philosophy
of
Curtin University

June 2019

Declaration

To the best of my knowledge and belief, this thesis contains no material previously published by any other person except where due acknowledgment has been made.

This thesis contains no material which has been accepted for the award of any other degree or diploma in any university.

Signature : _____

Date : _____

Abstract

Bio-cementation through microbially induced calcite precipitation (MICP) has gained considerable research interests globally for improving the mechanical properties of soils. MICP leads to precipitation of calcite crystals that bind soil particles together, thereby increasing the soil strength and stiffness. In this research, the effects of some important environmental factors that affect the successful implementation of MICP for field application were investigated, including the treatment temperature, soil pH, freeze-thaw (FT) cycles and rainwater flushing. It was found that MICP treatment favours the ambient temperature over the much colder and hotter temperatures due to the different crystal structures formed with the various rates of crystal nucleation and growth. In addition, the neutral initial soil pH was found to facilitate the progressive inclination of the MICP process in achieving super-saturation conditions. Bio-cemented well-graded sand was also found to be more durable than uniformly-graded fine and coarse sands due to the unique characteristics of having a high number of inter-particle contact points (attributed to the presence of fine sand particles) and high permeability, as well as large pore size (attributed to the presence of coarse sand particles). The results also suggested that bio-cemented soils encountered rainwater flushing during the treatment process was partly cemented, or completely non-cemented owing to the bacteria flush out because of the premature bacteria attachment to the nucleation sites of the soil grains.

Despite the large number of studies carried out on MICP for soil stabilisation, little attention has been paid to the effect of different calcite crystal precipitation patterns on improving the strength of bio-cemented soils. In this research, the effect of the $CaCO_3$ crystal precipitation patterns on the geotechnical properties of bio-cemented sand was examined. Different concentrations of bacterial culture (BC) and cementation solution (CS) were utilised to achieve different $CaCO_3$ crystal precipitation patterns.

It was found that the combination of high BC (32 U/mL) and low CS (0.25 M) was optimum in producing the most effective $CaCO_3$ crystal precipitation patterns, evaluated through the unconfined compressive strength (UCS) test and considering a broad range of cementation levels. This finding was confirmed by a microstructural study using scanning electron microscopy (SEM) analysis, which explained the precipitation mechanism and revealed the unique characteristics of the $CaCO_3$ crystal pattern, such as having larger crystal size compared to the previously reported $CaCO_3$ crystal and rhombohedral in shape that favours the strategic spots of soil pore throats for precipitation.

The geotechnical properties of the bio-cemented sand were further assessed through the consolidated undrained (CU) triaxial tests, considering the effect of different confining pressures and stress paths. The results revealed an enhancement in the shear strength parameters of bio-cemented sand, and different soil behaviour was observed under the different applied stress paths. An analytical model was developed to predict the strength improvement of the optimised bio-cemented sand. The developed analytical model was able to predict the experimental data well. A comparative study was also conducted to assess the strength improvement and permeability retainment between the bio-cemented sand and the conventional ordinary Portland cement (OPC) treated sand. It was found that the bio-cemented sand outperforms the OPC treated sand due to the efficacy of the $CaCO_3$ crystal precipitation patterns of the bio-cemented sand samples.

Publications

The following publications have been prepared as a result of this research:

Refereed Journal Papers

1. **Donovan Mujah**, Mohamed A. Shahin, and Liang Cheng (2016). "State-of-the-art review of bio-cementation by microbially induced calcite precipitation (MICP) for soil stabilization." *Geomicrobiology Journal*, 34(6): 524-537.

2. Liang Cheng, Mohamed A. Shahin, and **Donovan Mujah** (2017). "Influence of key environmental conditions on microbially induced cementation for soil stabilization." *Journal of Geotechnical and Geoenvironmental Engineering*, 143(1) doi: 10.1061/(ASCE)GT.1943-5606.0001586

3. **Donovan Mujah**, Liang Cheng, and Mohamed A. Shahin (2019). "Microstructural and geo-mechanical study on bio-cemented sand for optimisation of MICP process." *Journal of Materials in Civil Engineering*, 31(4) doi: 10.1061/(ASCE)MT.1943-5533.0002660

4. **Donovan Mujah**, Mohamed A. Shahin, and Liang Cheng (2019). "Experimental study and analytical model for strength behaviour of bio-cemented sand." *Proceedings of ICE - Ground Improvement* (under review).

Refereed Conference Paper

1. **Donovan Mujah**, Mohamed Shahin and Liang Cheng (2016). Performance of biocemented sand under various environmental conditions. In *Proceedings of XVIII Brazilian Conference on Soil Mechanics and Geotechnical Engineering, COBRAMSEG,* 19-22 October 2016, Belo Horizonte, Brazil ISSN: 2595-0843 doi: 10.20906/CPS/GJ-05-0002.

Acknowledgements

I am indebted to my supervisor, Associate Professor Mohamed Shahin, for his guidance, and help in all aspects throughout this research. Personally, his invaluable comments, constructive criticisms, and suggestions have made this research conceivable. I am also thankful to my co-supervisor Professor Liang Cheng, for his early guidance in teaching me the essence of microbiology, kind suggestions and productive comments during my candidature. Coming from a pure engineering background, this multi-disciplinary research involving microbiology is quite challenging to me, but their guidance and encouragement have made this journey worthwhile.

Heartfelt acknowledgments are extended to those amazing technicians in the Geomechanical Laboratory, especially Mr. Mark Whittaker, Mr. Mirzet Sehic and Mr. Darren Isaac, for all their help and tireless assistance during my research work in the laboratory. Sincere appreciation is expressed to my fellow postgraduate (Dr. Wasiul Bari and Dr. Md. Abu Sayeed) and undergraduate (Lorenzo Lorio, Taka Kobayashi, Benjamin Duong, Samuel Cook and Katelyn Jamieson) comrades for their friendship and company.

The scholarship awarded to this research project under the Curtin University International Postgraduate Scholarship (CIPRS) provided by Curtin University and the top-up extension scholarship provided by the Department of Civil Engineering, Curtin University are sincerely acknowledged.

Special thanks also extended to my friends the Nham's (Du Vinh, Robyn, Sophie and Toby), the Lucero's, (Nino and Emylane), the Dharmaratne's (Dhanuka and Reshan), Dr. Aditya Nugraha, Leung Keet Khoo, Dr. Alex Goh, Johnny A. Phillip, Jacques Olivier, the Sorna's (Eddie and Steward), the Marwick's (Clinton and Brock), Chol Machmachic, members of the International Bible Fellowship (IBF) and the members of the Woolworths Perth Regional Distribution Centre for their friendship in Perth.

Finally, I am forever grateful to my parents, the late Mr. Bernard Lium Anak Barundang and Mdm. Seliah Anak Awan. My late father has always believed in the power of education to elevate one's life but sadly, he could not share the moment when I am officially become a 'doctor' because he has been called to be with The LORD. I hope I am making you proud dad, and this PhD thesis is dedicated to you.

Very special gratitude is offered to my siblings, Mr. Robinson Seludang, Ms. Sylvia Layam, Ms. Liza and Mr. Wilson Rentap, their spouses, my nieces and nephews and grandnieces for their constant love that became the pillar of my strength throughout my PhD journey. I thank you all.

'Pemujur dalam sekula enggau pengidup ukai bepanggai ba mimpi tauka peturun, ukai mega utai dibai ari ada, tang ketegal pengeransing ati serta basa enggau apai indai'– an old Iban Language adage.

Table of Contents

List of Figures

Chapter 3 : Bio-Cemented Samples Preparation and Testing

Chapter 5 : Geotechnical Behaviours of the Optimised Bio-Cemented Sand

List of Tables

List of Symbols

α	Cohesion value in *q-p'* space
a	Model parameter
A	Cross-sectional area of specimen
β	Ratio between uniaxial compressive and tensile strengths
c'	Effective cohesion value
Ca^{2+}	Calcium ion
$CaCl_2$	Calcium chloride
$CaCO_3$	Calcium carbonate (calcite)
C_{iv}	Percentage of cement volume over the total volume of the specimen
$CO(NH_2)_2$	Urea
CO_3^{2-}	Carbonate ion
C_c	Curvature coefficient
C_u	Uniformity coefficient
D_{10}	Grain diameter associated with 10% finer
D_{30}	Grain diameter associated with 30% finer
D_{60}	Grain diameter associated with 60% finer
E	Soil elastic modulus
e_{max}	Maximum void ratio
e_{min}	Minimum void ratio
ε	Axial strain
ε_r	Radial composite strain
ε_a	Axial composite strain
G_s	Specific gravity
h	Hydraulic height difference
I_B	Brittleness index
k	Coefficient of permeability
K_c	Cement stress ratio
K_{sp}	Solubility product
L	Length of specimen
M	Critical state strength
M^*	Peak strength
n	Porosity
NH_3	Ammonia
NH_4^+	Ammonium ion
NH_4Cl	Ammonium chloride
OD_{600}	Optical density at 600 nm wavelength
p	Total mean
p'	Mean effective stress
σ_c	Confining pressure
Q	Volume of water discharge

q_p	Peak shear stress
q_r	Residual shear stress
q_u	Peak strength
S	Degree of saturation
SI	Saturation index
$\gamma_{d\max}$	Maximum dry density
t	Discharge time
u	Pore water pressure
Δ_u	Change in pore water pressure
q	Deviatoric stress
V_s	Shear wave velocity
ϕ'	Effective friction angle
n_{cs}	Critical state porosity
σ	Failure state of the bio-cemented soil composite
σ_m	Failure state of the soil matrix phase
σ_c	Failure state of the cement phase
σ_c^c	Uniaxial compressive strength
σ_c^t	Uniaxial tensile strength
σ_3	Minor principal stress
μ_m	Volumetric concentration of soil
μ_c	Volumetric concentration of cement
ψ	Ratio between the current density with the density at the critical state
ν	Bio-cemented soil composite Poisson' ratio
ν_c	Cement Poisson' ratio
ζ	Friction angle in *q-p'* space

Abbreviations

ATP	Adenosine Triphosphate
BC	Bacteria Culture
BE	Bender Elements
CS	Cementation Solution
CCE	Calcite Chemical Efficiency
CPT	Cone Penetration Test
C-S-H	Calcium Silicate Hydrate
CSL	Critical State Line
CU	Consolidated Undrained
DI	Deionised
DF	Dilution Factor
EBSD	Electron Backscatter Diffraction
EDS	Energy Dispersive X-Ray Spectroscopy
ESP	Effective Stress Path
FS	Fixation Solution
FT	Freeze Thaw
IAP	Ion Activity Products
LVDT	Linear Variable Displacement Transducers
MICP	Microbially Induced Calcite Precipitation
OD	Optical Density
OMC	Optimum moisture content
OPC	Ordinary Portland Cement
PVC	Polyvinyl Chloride
SEM	Scanning Electron Microscope
SP	Poorly Graded Soil
SPT	Standard Proctor Test
TSP	Total Stress Path
UCS	Unconfined Compressive Strength
USCS	Unified Soil Classification System
UTM	Universal Testing Machine

Chapter 1

Introduction

Upon touching sand, may it turn to gold.

Greek Proverb

1.1 Preamble

Construction over loose sand has become inevitable, owing to the exponential population growth and land scarcity. Loose sand is usually characterised by its low bearing capacity and high compressibility. Conventional pre-construction treatments such as geosynthetics, chemical grouting, prefabricated vertical drains and micropiles are used to improve in-situ subsoil strength and stiffness, thus eliminating the risk of excessive post-construction deformations and concomitant instability issues. One of the major drawbacks of these soil improvement techniques is the requirement of substantial amount of energy for their production and installation. Hence, a more cost-effective and environmentally friendly soil stabilisation method is warranted.

Nature provides its own soil stabilisation solution through a process called diagenesis – natural lithification of sediments as a result of physical, biological and chemical processes that turns sediments into rocks. The deposited sediments get compacted in consecutive layers and cemented by the precipitated minerals from groundwater. Naturally, the transition process of sediments into a rock-like material takes extremely long time, depending on the cementation process. However, in the presence of certain microorganisms, the cementation process could be accelerated as they actively induce biochemical reactions, leading to the alteration of the subsurface environment that promotes the precipitation of inorganic minerals.

Biologically induced cementation by minerals such as calcium carbonate (or calcite - $CaCO_3$) successfully consolidated loose sand in nature. Example of such occurrence can be found in the several meters tall weathered limestone pillars called The Pinnacles that rise out of yellow sand dunes in Nambung National Park, Western Australia (Figure 1.1).

Figure 1.1: The Pinnacles, Nambung National Park, Western Australia

Observations from nature have paved the way towards the exploration of a novel soil improvement technique called microbially induced calcite precipitation (MICP) that harnesses the metabolic pathway of ureolytic bacteria to create an in-situ cementation agent in the form of $CaCO_3$. Precipitated $CaCO_3$ binds sand grains together, thereby increasing both the strength and stiffness of the otherwise uncemented material (Whiffin, 2004; DeJong et al., 2006; Al-Thawadi, 2008; van Paassen, 2009; Chou et al., 2011; Cheng, 2012). Due to its potential as a sustainable soil stabilisation technique, MICP has recently gained unduly interest in geotechnical engineering applications. Two notable applications, bio-cementation (the generation of particle binding) and bio-clogging (the production of pore filling materials via microbial processes in situ) have been explored (Ivanov & Chu, 2008).

Bio-cemented sand treated with MICP was reported to increase the engineering properties (strength and stiffness) of soils (DeJong et al., 2006; Whiffin et al., 2007; Chou et al., 2011; Rong et al., 2012; Cheng et al., 2013; Ng et al., 2013; Montoya & DeJong, 2015; Shahrokhi-Shahraki et al., 2015; Cheng & Shahin, 2016), reduce foundation settlement (DeJong et al., 2010; van Paassen et al., 2010a), minimise the effect of liquefaction (Montoya et al., 2013; Montoya & DeJong, 2015), promote erosion controls (Jiang & Soga, 2014; Maleki et al., 2016; Salifu et al., 2016), repair cracks in soil healing (Montoya & DeJong, 2013; Harbottle et al., 2014) and reduce soil permeability due to bioclogging (Ivanov & Chu, 2008; Chu et al., 2013). Few attempts have been previously made to study the different factors affecting the MICP treatment process for improving the engineering properties of bio-cemented soils and the $CaCO_3$ distribution uniformity (Al Qabany et al., 2012; Al Qabany & Soga, 2013; Martinez et al., 2013; Ng et al., 2014; Zhao et al., 2014a). Previously, it was believed that the strength of the bio-cemented soil is governed by the $CaCO_3$ distribution uniformity in the soil matrix (Fujita et al., 2000; Okwadha & Li, 2010; Al Qabany & Soga, 2013). However, Cheng et al. (2013) demonstrated that higher strength per mass of $CaCO_3$ can be achieved through the precipitation of effective $CaCO_3$ (relatively larger, rhombohedral-shaped and non-uniformly distributed crystals precipitation) in the partially saturated sample condition. This suggests that the alteration of calcite crystal precipitation patterns can have significant effects on the geotechnical response of bio-cemented soils. Most of the previous studies used the conventional unconfined compressive strength (UCS) test to verify the strength improvement of bio-cemented soils due to the simplicity of the technique, which allows a large number of samples to be treated simultaneously (Al Qabany & Soga, 2013).

Recent studies performed triaxial tests under monotonic loading (Lin et al., 2015; Montoya & DeJong, 2015; Feng & Montoya, 2016) and dynamic loading using a centrifuge (Montoya et al., 2013) to assess the improved engineering properties of bio-cemented soils. Nevertheless, the scarcity of experimental results that cover a wide range of cementation levels and shearing conditions represents a serious gap in the literature.

Previous research proved the potential of using the MICP method for field applications. One study by van Paassen et al. (2010b) showed that bio-cementation through MICP can significantly improve the stiffness of granular soils in a large-scale laboratory experiment (100 m^3). This was further echoed by Gomez et al. (2014), who performed field-scale bio-cementation tests using surficial application of MICP, aimed to provide surface stabilisation for dust control and future revegetation and enhancement of the erosion resistance of loose sand deposits. Despite the successful cementation to certain column depths, uniform distribution of the produced $CaCO_3$ within the soil still proves to be a great challenge (DeJong et al., 2010). A review of the literature indicated that the surface percolation method introduced by Cheng & Cord-Ruwisch (2012) successfully mobilised a homogeneous cementation along a 1 m column depth.

The main issue of successful execution of the MICP procedure that can produce uniformly distributed calcite is not on how to transport the bacterial along the sand column, but it actually relates to the lack of understanding of the different precipitation pattern mechanisms, especially the aspect of crystal growth (Terzis et al., 2016). This aspect is of major interest, because it governs the size of the precipitated $CaCO_3$ crystals within the soil matrix. Understanding the mechanisms associated with a specific precipitation pattern would certainly help engineers to design better recipes that can meet certain specifications.

1.2 Objectives and Scope of the Study

The primary aim of this research is to optimise the process that leads to precipitation of $CaCO_3$ by exploring the various precipitation patterns and the relationship between their microstructural characteristics and the corresponding strength of the bio-cemented soil post-treatment. The results of this research will have implications for the design of MICP for field applications. The specific objectives of this study are:

1. To quantify the factors affecting the treatment optimisation in extreme environmental conditions such as the treatment temperature, soil pH, freeze-thaw (FT) cycles and rainwater flushing through UCS testing, including the recipe to produce effective $CaCO_3$.
2. To elucidate the precipitation mechanism (evolution) and identify the specific microstructural features of the effective $CaCO_3$ crystal precipitation patterns through microstructural studies. Understanding the specific microstructural features will allow achieving specific targets for field applications.
3. To study the geotechnical response of the bio-cemented sand using triaxial tests, considering the influence of the different confining stresses and stress paths on the strength and stiffness. A simple theoretical derivation to predict the peak strength (q_u) value of the bio-cemented sand based on the effective $CaCO_3$ precipitation will also be presented.

For this research, the term 'effective $CaCO_3$' will refer to mineralisation of the relatively large, rhombohedral-shaped and non-homogeneously precipitated $CaCO_3$ crystals at the soil pore throats. Furthermore, the engineering properties of the bio-cemented sand imbued with the effective $CaCO_3$ will be assessed through UCS and triaxial tests. Figure 1.2 shows the summarised scope of the research.

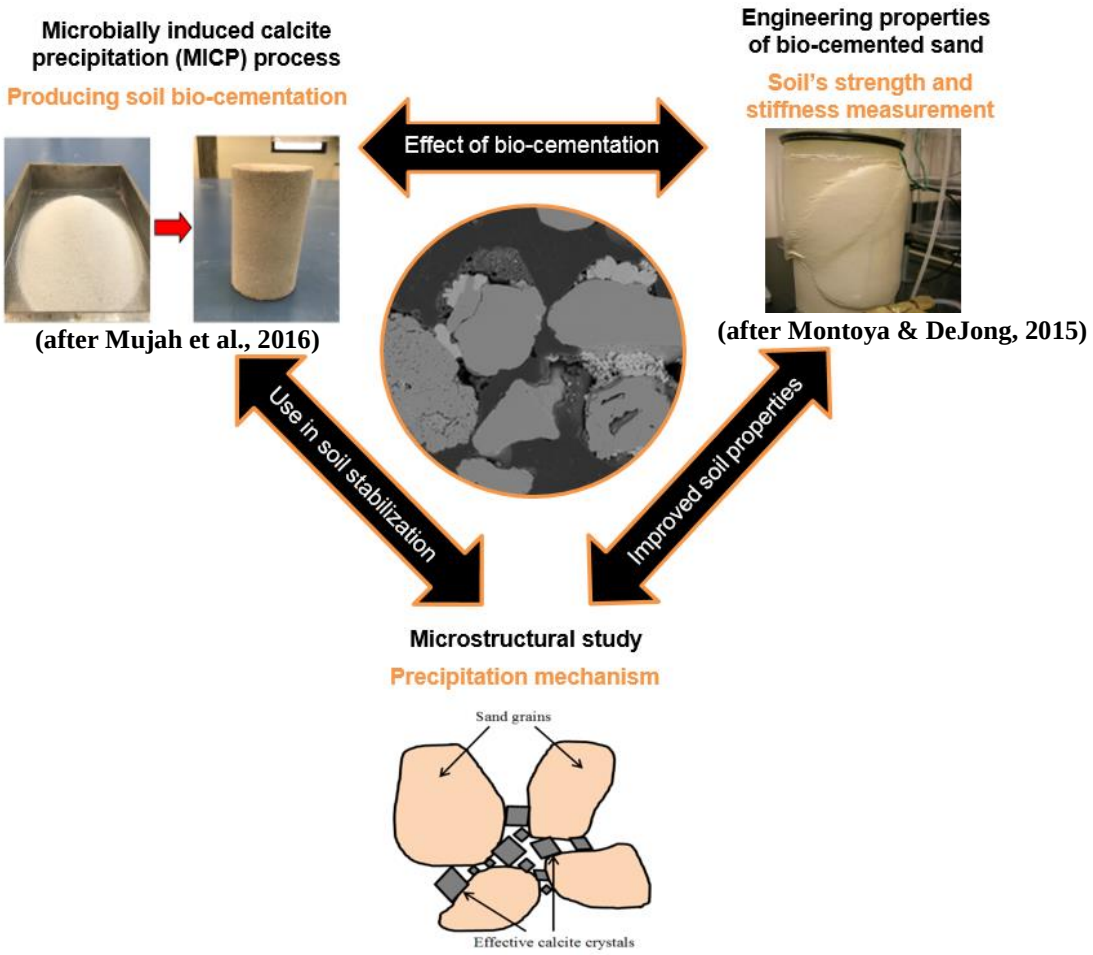

Figure 1.2: Scope of the current research

1.3 Thesis Structure

This thesis is divided into six diverse chapters. Chapter 1 describes a brief background of the study and highlights the gap in the literature. Also, the main aim, the specific objectives and the scope of the research are outlined in this chapter.

Chapter 2 presents a state-of-the-art review of the literature associated with the presented work. The comprehensive review focuses on the history, development, process optimisation, primary factors affecting $CaCO_3$ bio-mineralization and the application of MICP for soil stabilization. In the same chapter, the fundamental principles involving multidisciplinary fields such as microbiology, chemistry and engineering were briefly discussed to ensure sufficient understanding between their interactions.

Most of the recent literature dealing with soil bio-cementation was critically discussed and their limitations were highlighted to identify the rationale of this study. The inherent advantages and the potential drawbacks of the MICP for soil stabilisation were also considered.

Chapter 3 describes the materials used for the design of the bio-cemented samples and the methodology to commission the experimental programs for verification of the results. The first section relates to the sample preparation part that deals with the procedures to extract, inoculate, grow and harvest the microorganisms prior to the MICP treatment process. Next, the relevant calibration charts, key parameters for the urea hydrolysis reaction and set up for the batch analysis were presented. Small column split moulds and the stop-flow injection method procedures were detailed at length. The bio-cemented sand samples underwent UCS and triaxial testing to determine the effective $CaCO_3$ content and to capture the strength and stiffness of the MICP treated sand post shearing. The measurement of the $CaCO_3$ content, permeability, ammonia produced and the microstructural observation through the scanning electron microscopy (SEM) were all described in detail.

Chapter 4 discusses some key environmental factors that affect the successfully implementation of MICP treatment for field applications. These factors include the environmental temperature, soil pH, freeze-thaw (FT) cycles and rainwater flushing. Also, the optimum combination of bacteria culture and cementation solution concentrations that produced the most effective $CaCO_3$ crystal was identified. Various $CaCO_3$ crystal precipitation patterns were explored by altering CS and BC concentrations during injection. Samples were treated to represent various cementation levels for UCS testing. The optimum combination was predicted to produce the highest UCS and permeability retention values owing to the precipitation of the effective $CaCO_3$ crystals. The evolution and the specific microstructural features of the effective $CaCO_3$ crystals were observed under the scanning electron microscope (SEM). The optimised bio-cemented samples were compared to the ordinary Portland cement (OPC) treated samples.

Chapter 5 explores the geotechnical behaviours of the optimised bio-cemented sand employing the proposed optimum combination suggested by the current study. Consolidated undrained (CU) tests under different confining pressures (100, 200 and 400 kPa) and stress paths were performed. The stress path analyses include the conventional triaxial axial compression and constant-*p* loading paths. Accordingly, the experimental data were compared with the available published literature in terms of their respective shear strength parameters i.e. the effective friction angles (ϕ') and the effective cohesion values (c'). A theoretical formulation/model to predict the q_u values of the bio-cemented sands was also derived and presented. The model is based on the superposition of failure strength contributions of the soil and cement phases. The model assumes that the soil follows the critical state soil mechanics while the strength of the cemented phase is described using the Drucker-Prager failure criterion. In this model, q_u of the bio-cemented sand is a function of the adjusted porosity/cement parameter. The model data was compared with experimental results for further validation in Chapter 5.

Summary of the research findings, including the conclusions and recommendations for further studies were presented in Chapter 6. Lastly, a list of references and appendices were presented at the end of Chapter 6.

Chapter 2

Soil Bio-Cementation by MICP: A Review

2.1 Introduction

In order to produce a successful soil bio-cementation by MICP, a detailed understanding that encompasses the fundamentals of microbiology, basic soil improvement and the theory of superposition of failure strength contributions is warranted. This chapter was modified from a published article; the full reference of the article is: Donovan Mujah, Mohamed A. Shahin, and Liang Cheng (2016) 'State-of-the-Art Review of Biocementation by Microbially Induced Calcite Precipitation (MICP) for Soil Stabilization' *Geomicrobiology Journal*, 34(6): 524-537 (authorship attribution is appended in Appendix A). This chapter presents an updated comprehensive review of the relevant literature regarding the use of bio-cementation for soil stabilisation. Also, the primary components, treatment and the major factors affecting the MICP process were discussed. The potential applications, advantages, limitations, some primary challenges dealing with MICP for soil stabilisation and the current research focus were outlined in this chapter.

2.2 MICP Process

MICP is a biologically driven $CaCO_3$ precipitation technology that uses microbial cementation to form soil particle binding material as a result of the chemical reaction between microbes and specific chemical additives in the soil. Although many processes available in nature that are mediated by microbial pathway, namely reduction, oxidation and dissolution, only mineralisation of inorganic substances can produce stable and strong binding material in the soil matrix (Ivanov & Chu, 2008).

For soil stabilization purposes, the most commonly adopted microbial pathway is through a process called urea hydrolysis in the presence of highly active ureolytic bacteria. Al-Thawadi (2011) stated that urea hydrolysis is the most preferred $CaCO_3$ precipitation method due to its ability to generate up to 90% of the chemical conversion efficiency (CCE) of the precipitated $CaCO_3$ in a short period of time. Also Dhami et al. (2013), reported that the overall process of $CaCO_3$ mineralisation in the urea hydrolysis is straightforward and can be easily controlled deeming it to be superior to other microbial pathways. Attempts have also been made using denitrifying bacteria to produce $CaCO_3$ precipitation (van Paassen et al., 2010a; Martin et al., 2013; Hamdan et al., 2016). Although denitrifying bacteria managed to precipitate $CaCO_3$ all over the soil column, the amount of the $CaCO_3$ produced was reportedly much lower than the total converted amount, leading to non-homogenous $CaCO_3$ precipitation inside the soil column (van Paassen et al., 2010a). Pham et al. (2016) specified that the occurrence of inhibitive intermediates (nitrite and nitrous oxide) at high concentrations and the much slower reaction rate of denitrification process compared to that of urea hydrolysis eliminates the denitrification as a practical soil stabilisation technique.

2.3 Microorganisms Screening for MICP

Ureolytic bacteria can be found ubiquitously in nature. Nevertheless, only bacteria that possess high urease activity, thus producing high amount of $CaCO_3$ precipitates within a short period of time, are desired for MICP (Wei et al., 2015). Currently, the most commonly used bacteria for MICP are *Sporosarcina pasteurii*, *Bacillus megaterium* and *Bacillus sphaericus*. Ivanov & Chu (2008) described *S. pasteurii* as a type of aerobic bacteria able to hydrolyse urea into ammonia by generating adenosine triphosphate (ATP) through the secretion of urease enzyme. Figure 2.1 shows the physical difference between the bacteria usually utilised in MICP process.

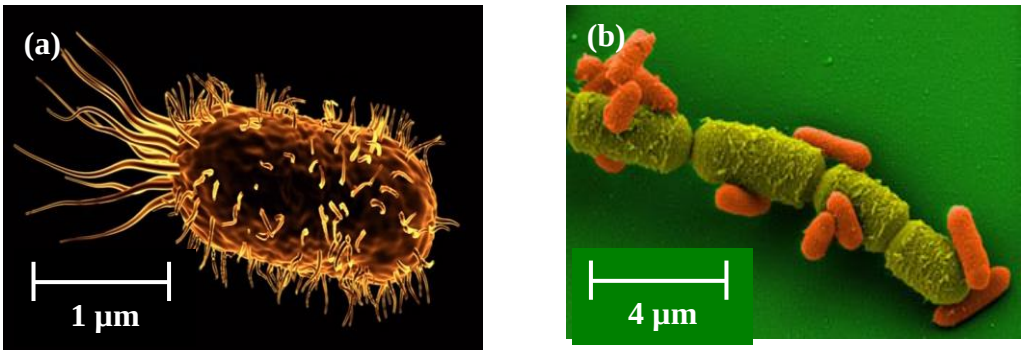

www.shareahack.com www.mobitec.com

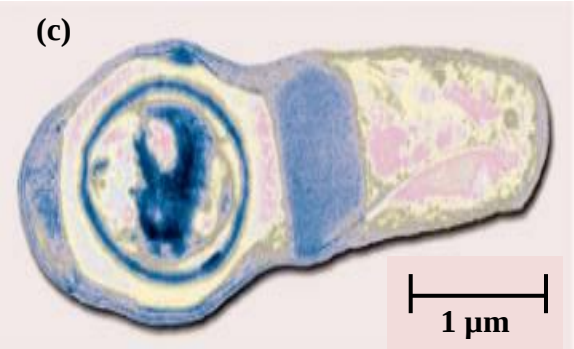

www.lifesci.sussex.ac.uk

Figure 2.1: Different types of bacteria commonly used in MICP: (a) *Sporosarcina pasteurii*, (b) *Bacillus megaterium*, and (c) *Bacillus sphaericus*

Ivanov & Chu (2008) consider facultative anaerobic bacteria as the most suitable agent for in-situ MICP soil stabilisation due to their unique characteristics. Facultative anaerobic bacteria remain active under both aerobic and anaerobic conditions and possess Gram-positive cell walls, which are highly resistant towards the changes in osmotic pressure. Although these types of bacteria can be found effortlessly in the environment, Al-Thawadi (2008) highlighted that only pure ureolytic bacteria strains, which are cultivated under sterile conditions and contamination are compatible with MICP due to the presence of the high urease enzyme that mediates the urea hydrolysis catalysis. Burbank et al. (2012) stated that only pure ureolytic bacteria cultures (BC) can produce highly active urease enzyme metabolic activity; the authors claimed that the desired urease activity of pure ureolytic BC for soil stabilisation is 4 – 50 mM urea/min.

Burbank et al. (2011) proposed the use of enrichment mediums containing molasses, urea, sodium acetate trihydrate, ammonium chloride and yeast extract to enrich the production of indigenous, highly active ureolytic bacteria in-situ and successfully induce soil bio-cementation. Recently, Cheng & Cord-Ruwisch (2013) produced highly active ureolytic bacteria by cultivating non-sterile chemostat cultures in a medium with pH = 10 and urea concentration = 0.17 M. These conditions helped the growth of urease active bacteria and facilitated the continuous reproduction of enriched bacteria on-site.

2.4 Calcite Precipitation by Urea Hydrolysis

Precipitation of $CaCO_3$ by urea hydrolysis has been explained in detail in several previous studies (Hillgartner et al., 2001; Hammes et al., 2003a; Burbank, 2010; Waller, 2011; Cheng, 2012; Martinez, 2012; Montoya, 2012). In general, the process can be categorised into two main stages: (1) urea hydrolysis stage; and (2) $CaCO_3$ precipitation. The following general chemical reactions of the urea hydrolysis process were presented by Cheng et al. (2013):

$$CO\left(NH_2\right)_2 + 2H_2O \rightarrow 2NH_4^+ + CO_3^{2-} \qquad \text{Equation 2.1}$$

$$Ca^{2+} + CO_3^{2-} \rightarrow CaCO_3 \qquad \text{Equation 2.2}$$

During the urea hydrolysis stage, 1 mole of urea ($CO(NH_2)_2$) is hydrolysed to produce 2 moles of ammonium ions (NH_4^+) and 1 mole of carbonate ion (CO_3^{2-}). Next, the calcium ion (Ca^{2+}) derived from the calcium chloride ($CaCl_2$) of the cementation solution (CS) reacts with the carbonate ion (CO_3^{2-}) to form 1 mole of calcium carbonate ($CaCO_3$) crystals. Figure 2.2 shows highly active ureolytic bacteria catalyse the generation of $CaCO_3$ crystals in three main phases (Ferris et al., 2004): (1) the development of a supersaturated condition; (2) nucleation at the point of critical saturation; and (3) spontaneous crystal growth on the stable nuclei.

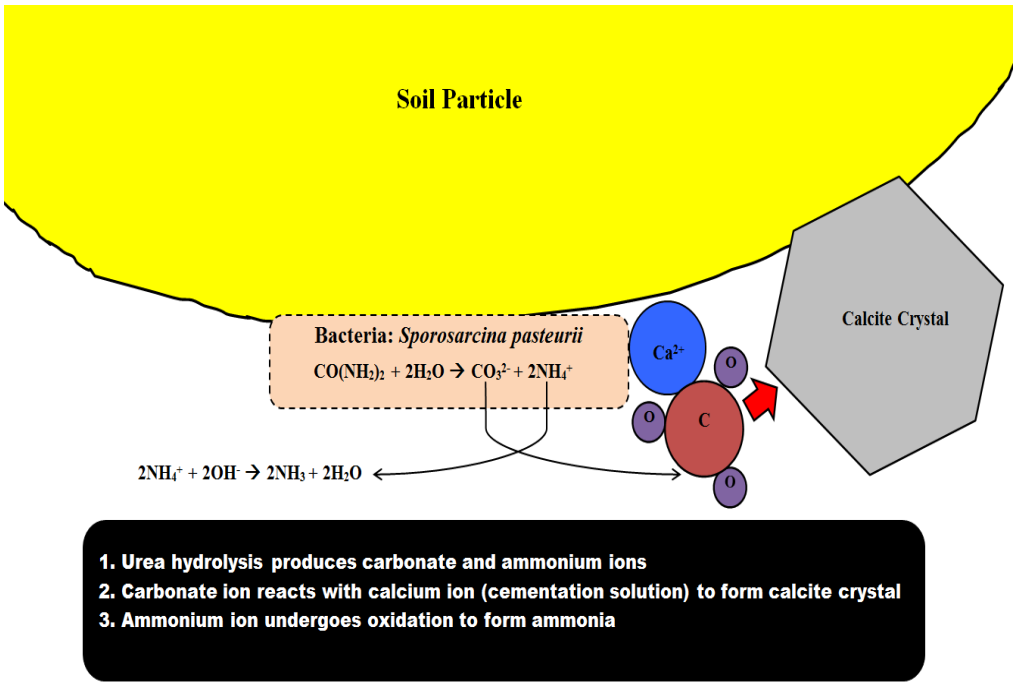

Figure 2.2: Schematic diagram showing $CaCO_3$ precipitation mechanism in the microscopic level during urea hydrolysis

Since the precipitation process of $CaCO_3$ by urea hydrolysis obeys the domino theory, where each stage is dependent on one another, a supersaturation condition must be initially present. Al-Thawadi & Cord-Ruwisch (2012) suggest that the $CaCO_3$ precipitation rate is a linear function of the concentration of the ion products (Ca^{2+} and CO_3^{2-}) and generally obeys the second order kinetics. However, the first order kinetics governs the precipitation rate if one of the reactants is in excess. The supersaturation condition is achieved when the concentrations of Ca^{2+} and CO_3^{2-} exceed the solubility product (K_{sp}) based on Equation 2.3 (Al-Thawadi & Cord-Ruwisch, 2012). The higher the supersaturation index (SI), the more likely the $CaCO_3$ precipitation is to take place.

$$SI = \frac{\left[Ca^{2+}\right]\left[CO_3^{2-}\right]}{K_{sp}} \qquad \text{Equation 2.3}$$

Where; $\left[Ca^{2+}\right]\left[CO_3^{2-}\right]$ are the ion activity products (IAP) and K_{sp} is the $CaCO_3$ solubility product.

After the supersaturation condition is reached, the $CaCO_3$ crystals start to form until the critical saturation. At the point of critical saturation, the $CaCO_3$ minerals grow spontaneously on the previously stable nuclei, precipitating larger $CaCO_3$ crystals. The understanding of these phases is crucial, particularly for soil stabilization, since the interplay of each phase would lead to different mechanical responses from the bio-cemented soil as a result of the diverse $CaCO_3$ crystals precipitation patterns (i.e. type, shape, size and distribution). Previous studies showed that different $CaCO_3$ crystal polymorphs, such as calcite, vaterite and aragonite, can affect the strength of the bio-cemented soil post-treatment (Al-Thawadi, 2013; Dhami et al., 2013). Mitchell & Ferris (2006) proposed that the size of the $CaCO_3$ crystals can be increased by propagating more concentrated ureolytic BC during the nucleation phase. More recently, Cheng & Shahin (2016) showed the influence of some precipitation patterns on the geotechnical response of the bio-cemented soil. The research demonstrated the multifaceted potential of urea hydrolysis by showing it to be one of the most viable pathways to tailor the $CaCO_3$ production for practical purposes.

2.5 Soil Bio-Cementation by MICP

Soil bio-cementation mimics natural events through the lithification process of sediments over a long period of time (Stocks-Fischer et al., 1999). In the case of MICP, the artificially produced $CaCO_3$ is accelerated through the continuous supply of BC and CS. The combination of BC and CS is fortunate because both elements can be found in nature (Fujita et al., 2000). The production of $CaCO_3$ in the soil matrix alters the engineering properties of the bio-cemented sand as it metamorphoses from natural sand into bio-sandstone (Achal et al., 2015). Figure 2.3 shows the transformation of natural sand into bio-sandstone after MICP treatment.

"Publication has been removed due to copyright restrictions"

Figure 2.3: Sand metamorphoses: (a) natural sand; and (b) bio-sandstone (after Mujah et al., 2016)

2.6 Soil Treatment Process by MICP

The retention capacity and the mobilisation of the urease enzyme, resulting from the introduction of ureolytic bacteria into the soil matrix, hold the key to the successful MICP application for soil stabilization. Without these qualities, inapt bacteria mobilization could lead to uneven urease enzyme distribution, which results in a non-uniform $CaCO_3$ precipitation along the column depth and negatively impacts the global bio-cemented soil strength. An increased bacteria retention capacity enables the bacteria adherence towards the sand particles to mitigate the bacteria nucleation sites detachment as a result of a continuous injection of the CS. The introduction of bacteria into the soil can be attained by the injection method, the surface percolation method or the pre-mixing method. In the injection method, BC is flushed following a top-down direction, while a certain retention period is observed (depending on the concentration of the supplied CS) to ensure sufficient bacteria attachment onto the sand grains before the CS is injected. In the surface percolation method, both BC and CS are percolated by gravity and capillary forces. The pre-mixing method warrants mechanical mixing of the soil and bacteria prior to the introduction of CS. Each method is discussed in the following sections.

2.6.1 Injection Method

The injection method was first introduced by Whiffin (2004) in treating a 2 m long column of natural sand. In this method, both BC and CS were injected alternately by half of the void volume, from top to bottom, following the vertical flow path regulated by a peristaltic pump. Since then, the injection method was used by many researchers (Burbank, 2010; Chou et al., 2011; De Muynck et al., 2011; Akiyama & Kawasaki, 2012; Martinez et al., 2013; Gomez et al., 2014; Wei et al., 2015; Cheng et al., 2016) to introduce BC and CS into a sand column. One of the key steps of the injection method is the attachment of the bacteria onto the sand grain surface prior to the supply of CS. Initially, this was achieved by allowing a retention period (normally 3 hours after introducing BC to the sand column) (Whiffin et al., 2007). However, Harkes et al. (2010) added a fixation solution (FS), in the form of a 50 mM calcium chloride ($CaCl_2$) solution, after injecting BC and found that the increase in calcium ions promoted bacteria attachment as a result of the bacterial absorption onto the sand grain surface (Torkzaban et al., 2008). van Paassen et al. (2010b) demonstrated that the injection method also functions well in the horizontal flow direction. Although they reported high variations of UCS values along the sand volume transversely, they managed to fairly reinforce a large-scale experiment comprising of 100 m^3 of sand volume. The schematic diagram of the most recently adopted injection method is presented in Figure 2.4.

The injection method is the most preferred MICP treatment method because the main parameters of BC and CS, flow, pressure and hydraulic gradient, can be controlled during the test using pumps. The flexibility of the method allows injection of fluids either vertically or horizontally. Also, this method permits the control of the soil's degree of saturation (S) to be either fully saturated (S = 100%) or partially saturated (S < 100%) since the flow of the fluids is controllable (Cheng et al., 2013).

"Publication has been removed due to copyright restrictions"

Figure 2.4: Schematic diagram of the injection method set-up (after Whiffin et al., 2007)

Despite the control provided by the injection method, nonhomogeneous $CaCO_3$ distribution resulting from uneven bacteria distribution poses the risk of non-uniform soil strength throughout the soil column length, therefore representing a serious disadvantage of the injection method for soil stabilization using MICP (Mujah et al., 2016). Ginn et al. (2001) explained that the uneven bacteria distribution was partly due to the filtering effect of the sand particles as the bacteria were injected through the pore space. Some bacteria might be suspended along the injection path as the bacteria concentration reduces linearly with depth. Al Qabany et al. (2012) described this phenomenon, known as pore plugging, as one of the potential reasons for the uneven bacteria distribution. Pore plugging occurs when a localised cementation occurs at the region near to the injection source (top part of the sand column if applied top-down). The localised cementation ensues when the repeatedly supplied CS reacts with the trapped bacteria near the injection point. Pore plugging at the injection source hinders the transport of the subsequent BC injection into other regions of the sand column, ultimately leading to the uneven bacteria distribution.

Whiffin et al. (2007) recommended an increase in the CS injection rate as a countermeasure to pore clogging to allow more fluids to reach further in the sand column. It is believed that the higher CS injection rate provides greater BC mobilisation into the soil depth, although no studies have proven this claim. Harkes et al. (2010) suggested the use of FS (high salinity $CaCl_2$ solution), immediately injected after the initial BC injection, to retard the movement of bacteria and facilitate bacteria absorption onto the sand grains surface. The next injection of CS (less saline than the FS) would remobilise the bacteria into the deeper locations of the sand column as they return to the liquid phase. Tobler et al. (2012) found that the two-staged injection method (alternate injection of BC and CS) was more effective than the parallel injection (CS is immediately injected after BC) as the latter greatly promotes pore plugging near the injection source.

2.6.2 Surface Percolation Method

The surface percolation method was introduced by Cheng & Cord-Ruwisch (2014) to allow for the treatment of an unsaturated sand. In this method, BC and CS were vertically introduced from the top opening of the sand column. No caps were provided on both sides of the column to permit fluid passage through the column. The fluids were transported into the column depth by gravity and capillary forces. Figure 2.5 shows a schematic diagram of the surface percolation method. Cheng & Cord-Ruwisch (2014) found that by applying multiple alternating layers of BC and FS and then incubating the sample, bacteria could be mobilised into a 1 m sand column depth due to a higher percolation rate. This would imply that a reasonable $CaCO_3$ distribution homogeneity would be observed. In terms of the degree of saturation, the pendular regime (lower water content region) produced three times higher local strength per mass of $CaCO_3$ over the samples taken from the funicular regime (higher water content region). This indicates that the cost of strengthening using the surface percolation method is three times lower than that of the traditional injection method, which always requires the sample to be fully saturated.

"Publication has been removed due to copyright restrictions"

Figure 2.5: Schematic diagram of the surface percolation method set-up (after Cheng and Cord-Ruwisch, 2012)

Despite such appraisal, application of the surface percolation method is limited to coarse-grained soil. Fine-grained soils, such as silt and clay, have low fluid infiltration rates and permeability, hence limiting the transport of bacteria into the deeper locations of the column. The bulk of the soil deposits present deep in soil strata are fine-grained soils. To date, no study has shown the potential of using the surface percolation method in fine-grained soils.

2.6.3 Pre-Mixing Method

In order to achieve better $CaCO_3$ distribution uniformity, Yasuhara et al. (2012) mechanically pre-mixed bacteria powder, in enzyme form, with sand. After pre-mixing, CS was injected into the sand column. Zhao et al. (2014a) found that 83% of $CaCO_3$ precipitated in their bio-cemented sample was homogenously distributed throughout the 1 m sand column depth.

Recently, Zhao et al. (2014b) applied the pre-mixing method in MICP treatment to stabilize natural sand. The sand mixture was compacted into geotextile mould and wrapped around the sand column before full submersion into a mechanically operated tank containing CS. In this method, CS could freely diffuse into the sand column through the perforated geotextile due to the difference in the concentration gradients by the action of the robust magnetic stirring. The schematic diagram of the pre-mixing method is presented in Figure 2.6.

"Publication has been removed due to copyright restrictions"

Figure 2.6: Schematic diagram of the pre-mixing method set-up (after Zhao et al., 2014b)

The advantage of this method over the traditional injection method is that it helps to promote more uniform $CaCO_3$ distribution deeper into sand column depth. This is accomplished by rigorously mixing the bacteria (can be in the liquid or solid powder form) with the sand prior to the introduction of CS. The mixing process ensures the homogenous placement of the bacteria inside the sand and afterwards guarantees the precipitation of homogeneous $CaCO_3$ distribution. Ivanov et al. (2015b) successfully utilised this method to strengthen marine clay and found that the $CaCO_3$ was fairly distributed along the column depth in the presence of fine-grained soils.

However, one of the major drawbacks of this method is that it is impractical to apply the diffusion technique in the field, as it requires the installation of geotextile wrapping around the massive soil bulk and the fitting a huge mechanical stirrer to accelerate the diffusion rate of the CS into the treated sample. It is also argued that the integrity of the treated soils in terms of the pseudo stress history may be disturbed by the instalment of the geotextile wrapping, hence contributing to inaccurate prediction of the soil's strength.

2.7 Geotechnical Engineering Properties of Bio-Cemented Sand

2.7.1 Permeability

MICP can be used to regulate soil permeability through a process called bio-clogging, which completely blocks inter-particle pores in the soil. The concept of bio-clogging was introduced by Ivanov & Chu (2008) at which, significant permeability reduction was observed (5×10^{-5} m/s to 1.4×10^{-7} m/s) at high $CaCO_3$ content. Similarly, Chu et al. (2013) found that bio-clogging mechanism only occurs after 9.6% $CaCO_3$ content or higher. The generated $CaCO_3$ is responsible for clogging the soil pores, thereby restricting the flow of water and thus decreasing the soil permeability (Glatstein & Francisca, 2014; Kanmani et al., 2014; Amin et al., 2017). Bio-clogging has practical geotechnical engineering applications, including the prevention of leachate penetration from landfill sites to the surrounding soil and as a support barrier that averts the displacement of backfill materials in construction of dams. The ability to control the permeability of porous materials is highly desirable because it can prevent the development of excess pore pressure during loading (Farah et al., 2016). Cho et al. (2006) stated that the packing density of the soil inter-particles at a microscopic level affects the drainage condition of the porous materials. To achieve a good drainage condition, Chu et al. (2013) suggested that a permeability value of at least 1×10^{-4} m/s must be maintained to ensure a full penetration of bacteria and cementation solution to the desired soil depth. This is crucial to guarantee a homogeneous $CaCO_3$ distribution along the treated soil column.

Cheng et al. (2013) compared the permeability characteristics of bio-cemented sand with ordinary Portland cement (OPC) treated sand and found that the bio-cemented samples have significantly higher permeability retention compared to the OPC treated samples (Figure 2.7). It was noted that the hydraulic conductivity for the sand used was 10×10^{-5} m/s. At cement content of 7%, permeability reduction values of 50% and 98% were recorded for the bio-cemented and OPC treated samples, respectively. It was also noted that at a cement content greater than 9.6%, considerably poor drainage behaviour was demonstrated by the OPC treated samples with a permeability value less than 1×10^{-6} m/s while the bio-cemented samples successfully maintained permeability value $\geq 4 \times 10^{-5}$ m/s. Cheng et al. (2013) suggested that the mineralisation of insoluble hydrates that occupies the pore spaces as a result of the cement hydration reaction between OPC and water molecules was the cause for the permeability loss in the OPC treated samples. Compared to the insoluble hydrates, the $CaCO_3$ crystals cause slight volume change in the pore space hence, allowing better drainage passage in the soil matrix.

Figure 2.7: Comparison of permeability reduction between bio-cemented and OPC treated samples (after Cheng et al., 2013)

Using 0.5 M cementation solution, van Paassen (2009) reported 60% permeability reduction at 100 kg/m^3 $CaCO_3$ content whereas, Ivanov et al. (2010) recorded 50 – 99% permeability reduction using a 1 M cementation solution. Al Qabany & Soga (2013) compared the effect of using different cementation solution concentrations (0.25, 0.5 and 1 M) towards the permeability reduction. They found that high CS concentration produced sudden clogging in the biocemented soil samples as a result of the biomass plugging that occurred in the vicinity of the accumulated bacteria cells producing large clusters of $CaCO_3$ crystals (Stewart & Fogler, 2001). This resulted in non-uniform flow of the subsequent chemical injection, leading to non-homogenous $CaCO_3$ precipitation in the soil matrix. Low CS concentration promotes the precipitation of $CaCO_3$ at the soil contact points due to the tendency of the bacteria cells to be amassed at the soil pore throats (DeJong et al., 2010). The accretion of the bacteria cells near to the pore throats produced relatively small $CaCO_3$ crystals, leading to much more stable chemical flow, hence encouraging more homogeneous $CaCO_3$ crystals precipitation in the soil matrix. The different precipitation patterns and the corresponding effect of the pore clogging towards the chemicals flow are presented in Figure 2.8.

2.7.2 Stiffness

Soil stiffness or better known as soil elastic modulus (E) is the ratio of stress over strain and is associated with the bonding strength induced by adjacent soil grains. Cheng et al. (2013) showed that E increases with the amount of the precipitated calcite content in an exponential fashion, although the precipitation patterns affect the mechanical response of the bio-cemented samples. Montoya & DeJong (2015), Lin et al. (2015) and Feng & Montoya (2016) studied the stress-strain behaviour of biocemented sand in a triaxial machine and found that E noticeably was improved with the increase in the cementation levels.

"Publication has been removed due to copyright restrictions"

Figure 2.8: Schematic diagram of pore clogging in MICP: (a) high cementation solution concentration; and (b) low cementation solution concentration (modified after Al-Qabany & Soga, 2013)

Cheng et al. (2013) compared *E* values of different types of geomaterials such as concrete, gravel and soft rock with MICP treated sand, as shown in Figure 2.9. Their results revealed that the MICP cemented coarse sand showed the most flexible behaviour compared to other types of geomaterials. This characteristic of artificially cemented materials proves to be very useful in earthquake prone areas, where less stiff soil is able to provide extra time for evacuation purposes due to its ability to sustain significant residual strength post failure (Montoya et al., 2013). In the event that stiffer soil conditions are desired, Ismail et al. (2002a) suggested that more reagent flushes are required so that *E* values approach that of concrete. It is worth to note that the rate of stiffness can be influenced by the different stress paths (SP) of soil in a way that particular SPs could reduce *E* resulting from the cementation degradation over time, prior to failure. Montoya & DeJong (2015) discussed this mechanism and found that SPs play an important role in determining the actual *E* response of bio-cemented sand. Ruistuen et al. (1999) related the shear-enhanced compaction of the SP condition to weakly cemented soil and how it loses stress sensitivity despite the increase in the cementation levels.

Figure 2.9: Relationship between *E* and q_{ucs} of the biocemented sand compared with other geomaterials (after Cheng et al., 2013)

2.7.3 Shear Strength

Shear strength parameters refer to the cohesion value (c) and the friction angle (ϕ) of the bio-cemented sand samples. Montoya & DeJong (2015) showed that the cohesive intercept for bio-cemented sand samples is equal to zero in the Mohr-Coulomb failure criteria diagram because the MICP treated samples having shear wave velocity, V_s = 1000 m/s or higher (heavily cemented samples) were able to retain their shape under self-weight. Also, Lee et al. (2009) mentioned that the corresponding cohesion intercept greatly depends on the confining stress levels. A constant cohesion intercept is normally found at low confining stress levels; meanwhile a gradual decrease in the cohesion intercept is witnessed after a breaking point (transition zone) due to the breakage of the cementation bonds observed at high confining stresses (Figure 2.10). The peak effective ϕ was observed to increase with an increase in the cementation levels, leading to a transition in the stress-strain behaviour from strain hardening to strain softening (Montoya & DeJong, 2015). The large increase in the peak effective ϕ shown in Figure 2.11 was argued to be related to the increase in the particle roughness as the cementation level increases during the bio-chemical cementation process.

Figure 2.10: Cohesion value of the cemented sand idealisation (after Lee et al., 2009)

"Publication has been removed due to copyright restrictions"

Figure 2.11: Peak effective ϕ' in relation to the various cementation levels measured using bender element (after Montoya & DeJong, 2015)

Furthermore, Feng & Montoya (2017) showed that no significant influence was observed in the peak effective ϕ in the lightly-cemented and moderately-cemented samples. It is worthy to note that the degree of saturation affects the shear strength parameters of the bio-cemented soils, i.e. coarse and fine grained, as confirmed by Cheng et al. (2013). It was demonstrated that the precipitated $CaCO_3$ crystals under the low saturation degree condition improved the shear strength parameters of the tested soils significantly. In the case of the coarse sand, this is attributed to the formation of the $CaCO_3$ crystals which were concentrated only near the soil pore throats (the smallest pore space connecting two large pore cavities). The effective placement of the $CaCO_3$ crystals in the interparticle connections assists the enhancement of shear strength in bio-cemented soils. On the other hand, the improvement in shear strength in the fine sand is related to the compounding benefits of much smaller particles, such as precipitation of more effective $CaCO_3$ crystals and lower particle contact stresses.

2.7.4 Unconfined Compressive Strength (UCS)

The unconfined compressive strength (UCS) test is currently the most preferable strength test to describe the mechanical response of the bio-cemented soil, particularly because the test permits a large number of bio-cemented samples to be tested at the same time, easing the characterisation of sample strengths (Al Qabany et al., 2012). Figure 2.12 shows the comparison of UCS values and the corresponding calcite contents from different studies using a consistent cementation solution concentration, i.e. 1 M. There exists an exponential relationship between the precipitated $CaCO_3$ content with the UCS values. Based on Figure 2.12, it can be deduced that the mechanical response of the bio-cemented samples can vary remarkably despite having the same amount of $CaCO_3$ content. Currently, no literature has embarked on explaining this observation; hence this study will attempt to elucidate this with the theory of effective $CaCO_3$ crystal formation, which is discussed at length in Chapter 4.

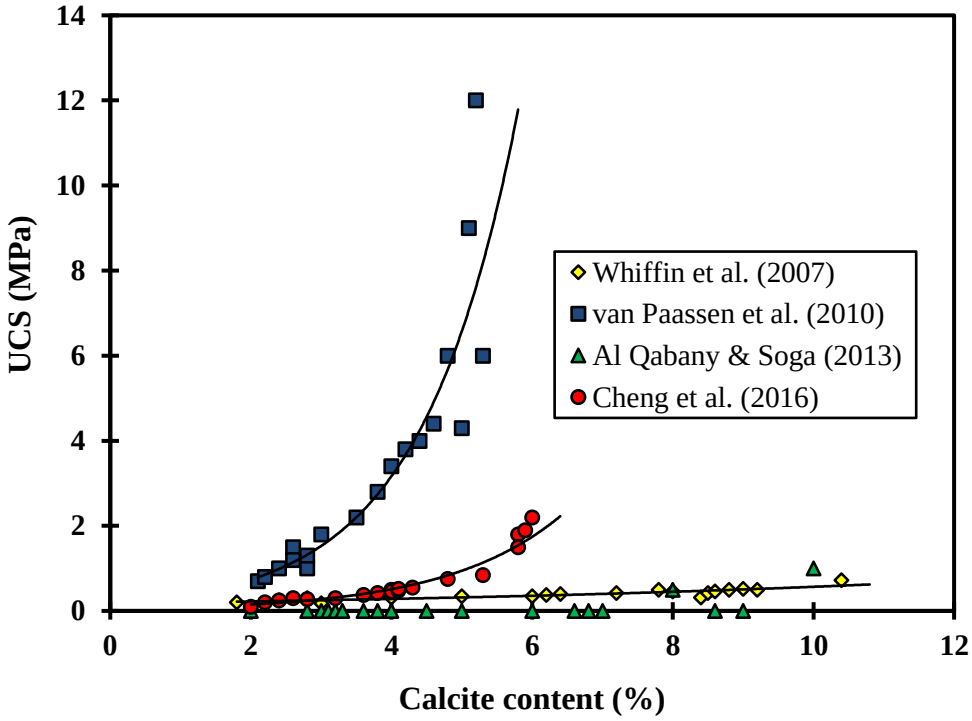

Figure 2.12: Relationship between the UCS values and the calcite content comparison between different studies

2.7.5 Microstructural Characteristics

The improvement mechanism of the bio-cemented samples in the microscopic level could be explained through the scanning electron microscopy (SEM) imaging technique. This aspect is particularly crucial since it was noted by Sham et al. (2013) and Terzis et al. (2016) that different precipitation pattern structures at a microscopic level could influence the macroscopic response of bio-cemented samples differently. DeJong et al. (2010) presented two $CaCO_3$ crystals precipitation distribution alternatives within the soil pore spaces, e.g. (1) uniform distribution at which the $CaCO_3$ crystals form almost an equal thickness layer of envelope surrounding the sand particles resulting in a relatively small contact bonding area between the neighbouring sand particles; and (2) preferential distribution which highlights the agglomeration of the precipitated $CaCO_3$ crystals near to the vicinity of the soil pore throats. However, based on the observation through SEM images by many researchers (De Muynck et al., 2011; Akiyama & Kawasaki, 2012; Rong et al., 2012; Tobler et al., 2012; Cheng et al., 2013; Rong & Qian, 2013; Park et al., 2014a; Sel et al., 2014; Cheng et al., 2016), the actual distribution of $CaCO_3$ crystals precipitation is a combination of both alternatives, as shown in Figure 2.13. Furthermore, DeJong et al. (2011) associated the spatial distribution of the precipitated $CaCO_3$ crystals in the bio-cemented soil pore spaces to the biological behaviour of the bacteria and the liquid filtering process. Bacteria are prone to smaller space area such as near to the soil pore throats as a result of the reduced shearing stresses and the availability of more nutrients at the grain contact surface. The filtering process is the result of the formation and suspension of the $CaCO_3$ crystals in the soil pore fluid space because of the incessant supplement of the BC and CS. This process would force the $CaCO_3$ particles to re-attach to the region of the grain contact points as the supplied chemicals flow inside the soil pore fluid space. Its effect towards the formation of the $CaCO_3$ crystals near to the grain contact points becomes more pronounced since it governs the relative size of the suspended $CaCO_3$ crystals and the soil pore throat space which decreases under loading (Santamarina & Cho, 2004).

Figure 2.13: $CaCO_3$ crystals precipitation distribution in the soil pore space: (a) uniform distribution (modified after DeJong et al., 2010); (b) preferential distribution (modified after DeJong et al., 2010); and (c) actual distribution (after Lin et al., 2015)

Earlier studies correlated the strength improvement of the MICP treated samples to the amount of the $CaCO_3$ content enveloping the sand particles in the bio-cemented soil matrix (Fujita et al., 2000; Okwadha & Li, 2010). However, Whiffin et al. (2007) suggested that the shear strength of the bio-cemented samples may not be directly proportional to the amount of the $CaCO_3$ content present in the bio-cemented soil matrix. Further investigations by Cheng et al. (2013) and Cheng et al. (2017) demonstrated that the exponential increase in the UCS values of the bio-cemented samples is due to the precipitation of the effective $CaCO_3$ crystals.

Figure 2.14 shows the precipitation of the effective $CaCO_3$ crystals post MICP treatment. Based on the figure, it can be observed that among the most salient characteristics of an effective $CaCO_3$ crystal includes: (1) larger crystal size (approximately 20–50 μm); (2) rhombohedral in shape (calcite); and (3) distributed mainly at the soil pore throats which then fills in the gaps between two or more sand particles (Cheng et al., 2017). The $CaCO_3$ crystal precipitation patterns greatly influence the mechanical properties of bio-cemented samples according to the precipitated $CaCO_3$ crystals size, shape and structure as they accumulated in the soil pore throats (Al Qabany et al., 2012). In return, these unique characteristics could potentially implicate how MICP treatment can be applied more economically in engineering practice.

"Publication has been removed due to copyright restrictions"

Figure 2.14: Microstructure of the effective $CaCO_3$ crystals precipitation (after Cheng et al., 2017)

2.7.6 Shear Wave Velocity

Shear wave velocity measurement is a relatively new technique utilised in geotechnical engineering that employs the use of non-destructive test via using bender elements (BE) to determine the development of the progressive strength of the improved soil (Sharma et al., 2011). In MICP application, BE is used mainly to monitor the one-dimensional flow of the permeability reduction in the bio-cemented soil column (Martinez et al., 2013) and also to capture the change in the small-strain stiffness of the bio-cemented soil during shearing in the triaxial setup (Montoya & DeJong, 2015). Among the advantages of this technique include the ability to measure soil strength as a function of time in the real time domain and also the non-destructive examination of the bio-cemented samples (Piriyakul & Iamchaturapatr, 2013).

2.8 Factors Affecting the Formation of $CaCO_3$ Crystals in MICP Treatment

Al Qabany & Soga (2013), Terzis et al. (2016) and Cheng et al. (2017) noted that the different precipitation patterns could affect the mechanical response of bio-cemented soils depending on their crystallographic morphology (shape, size and distribution) in the bio-cemented soil matrix. Some critical factors affecting MICP treatment namely the bacteria culture concentration, cementation solution concentration, temperature, pH level and degree of saturation are discussed in this section.

2.8.1 Bacteria Culture Concentration

Bacteria culture concentration is related to the urease activity of the supplied bacteria. According to Whiffin (2004), urease activity can be measured based on the hydrolysis rate of urea by the ureolytic bacteria. In other words, the higher is the number of bacteria concentrated in a culture, the higher is the urease activity.

The increase in urease activity enhances the $CaCO_3$ production due to the more bacteria cells concentrated inside the culture acting as nucleation sites for $CaCO_3$ crystals precipitation (Nemati & Voordouw, 2003). Similarly, Hammes & Verstraete (2002) also confirmed that the availability of the nucleation sites is a vital governing factor in determining the amount of $CaCO_3$ production. DeJong et al. (2011) explained that the nucleation sites for $CaCO_3$ crystals precipitation occur as a result of the bacteria cells attachment to the soil grains surface at which, bacteria would catalyse the reaction between Ca^{2+} and CO_3^{2-} ions to form $CaCO_3$ that would ultimately bond two or more soil particles together as they grow in size. Since the availability of the nucleation sites greatly depends on the amount of the attached bacteria cells on the soil particles, it is imperative that the amount of the introduced bacteria cells (i.e. the BC concentration which then would affect the urease activity level) needs to be addressed. When more bacteria cells present in the soil matrix, precipitation of new $CaCO_3$ crystals can be anticipated due to the abundance of the bacteria cells accumulated at the soil pore throats (contact points) and also attached to the sand grains surface acting as the nucleation sites for the consumption of the Ca^{2+} and CO_3^{2-} ions to form new small $CaCO_3$ crystals instead of growing the existing ones. These several small crystals would progress to form dense layers which envelop the sand grains with the continuous supply of CS. In case of fewer bacteria cells introduced into the soil matrix, the nucleation of new $CaCO_3$ crystals is insignificant compared to the growth of the existing ones. The low number of nucleation sites present in the soil matrix facilitates the growth of individual crystals instead of formation of new ones. This claim is proved by Cheng et al. (2017) when they studied the effect of different urease activities on the UCS values of the bio-cemented samples, as shown in Figure 2.15. They claimed that bio-cemented samples treated with lower urease activity bacteria culture would produce higher strength gain compared to the higher urease activity bacteria culture at the same $CaCO_3$ content level due to the precipitation of larger $CaCO_3$ crystals.

"Publication has been removed due to copyright restrictions"

Figure 2.15: Effect of different bacteria culture concentrations on the bio-cemented soils UCS (after Cheng et al., 2016)

It is noted by Cheng et al. (2017) that using different strain of ureolytic bacteria would probably lead to different results than those presented because of the attainment of the same urease activity level requires different bacteria culture biomass, leading to different number of nucleation sites and therefore, potentially affecting the precipitated $CaCO_3$ crystals pattern. Further study is needed considering this issue because different $CaCO_3$ crystals precipitation patterns would lead to different strength gain after MICP treatment of soils.

2.8.2 Cementation Solution Concentration

Al-Thawadi & Cord-Ruwisch (2012) indicated that the precipitation of $CaCO_3$ crystals in the bio-cemented samples is affected by the cementation solution concentration. In their study using pure chemical $CaCO_3$ production, they showed that a higher cementation solution concentration would lead to produce larger $CaCO_3$ crystals. However, in the MICP treatment scheme, where the CS is introduced to the soil column in its liquid

form, Okwadha & Li (2010) observed that the precipitated $CaCO_3$ crystals were randomly distributed in the soil voids due to the faster rate of the precipitation process induced by the higher CS concentration. This finding is further echoed by Al Qabany & Soga (2013), which showed that more homogeneous $CaCO_3$ crystals distribution was observed in the bio-cemented samples using lower CS concentration. Their findings also suggest that the $CaCO_3$ precipitation homogeneity contributes towards the strength gain by the bio-cemented samples, as shown in Figure 2.16.

"Publication has been removed due to copyright restrictions"

Figure 2.16: Effect of different cementation solution concentrations on the bio-cemented soils UCS (after Al-Qabany and Soga, 2013)

Al Qabany & Soga (2013) conducted a study using different CS concentrations comprising of equimolar urea-calcium chloride, i.e. 0.1 M, 0.25 M, 0.5 M and 1 M. They found that the lowest concentration (0.1 M) produced higher UCS values compared to that treated with higher CS concentration. They argued that this is probably due to the precipitation of more homogeneously distributed $CaCO_3$ crystals at the particle contact points, hence, leading to strength improvement with minimum soil disturbance and permeability reduction.

No further explanation was provided as to why the use of 1 M CS provided no strength despite the high $CaCO_3$ content. Also, the fact that the authors linked the strength improvement with the $CaCO_3$ crystals distribution homogeneity does not fully explain why 1 M CS produced samples with null strength. Further investigation into the microstructural characteristics especially in terms of the evolution of the precipitated $CaCO_3$ crystals and their relationship with the progressive bio-cemented sample strength is necessary. Their findings are further supported by Ng et al. (2014) who found that 0.5 M CS provided higher strength improvement on the bio-cemented residual soil as compared to that of 1 M CS concentration. Also, Cheng et al. (2014) used low concentration of Ca^{2+} ion source, i.e. seawater to produce bio-cemented sand columns. They noted that, in order to achieve the same amount of $CaCO_3$ crystals precipitation using seawater, greater number of injections is needed compared to that of using the normal equimolar CS.

2.8.3 Degree of Saturation

It was suggested by Cheng & Cord-Ruwisch (2012) that the $CaCO_3$ crystals distribution patterns can be controlled by manipulating the degree of saturation of the bio-cemented soils during the MICP treatment. This is made possible by restricting the $CaCO_3$ precipitation only at the vicinity of the soil pore throats. It was hypothesised that the ability to precipitate $CaCO_3$ at the soil pore throats leads to the formation of $CaCO_3$ crystals that link two or more sand grains together at their contact points. Hence, Cheng et al. (2013) conducted a series of experiment investigating the effectiveness of MICP treatment at various degrees of saturation (20%, 40%, 80% and 100%). The study found that the 20% degree of saturation proved to be the most effective (highest UCS value at 5% $CaCO_3$ content) compared to 40%, 80% and 100%, as shown in Figure 2.17. Cheng & Cord-Ruwisch (2012) attributed this to the precipitation of the $CaCO_3$ crystals, which were concentrated at the soil pore throats as a result of the air occupation in the partially saturated condition (Tuller et al., 1999).

The materialisation of the menisci shaped cementation solution at the soil pore throat has led to the formation of the $CaCO_3$ crystals at the contact points between the soil grains, contributing to the strength improvement. Meanwhile, in the case of fully saturated condition, the $CaCO_3$ crystals are free to precipitate without being restricted to the location as the MICP solution occupies the entire pore space. This condition propels the agglomeration of $CaCO_3$ crystals to be formed on both the host grain surface and the grain gaps thus, leading to the much scattering pattern of the $CaCO_3$ crystals precipitation in the fully saturated condition. The SEM images showing the difference of the precipitation patterns in the two extreme saturation degree conditions is shown in Figure 2.18.

"Publication has been removed due to copyright restrictions"

Figure 2.17: Effect of different degree of saturation on the bio-cemented soil strength improvement (after Cheng et al., 2013)

"Publication has been removed due to copyright restrictions"

Figure 2.18: $CaCO_3$ crystals precipitation patterns: (a) fully saturated condition; and (b) partially saturated condition (20%) (after Cheng et al., 2013)

2.9 Large Scale MICP Experiments

Attempts have been made to upscale the use of bio-cementation for field application. For example, van Paassen (2009) treated 100 m^3 of natural sand (Figure 2.19) and found that the strength of the bio-cemented sand was significantly increased after the MICP treatment. However, a distinct $CaCO_3$ precipitation spatial heterogeneity was noted. Possible reasons for the non-homogeneously distributed $CaCO_3$ in the bio-cemented soil mass include: (1) non-homogenously distributed bacteria cells as a result of the lacking in both the retention time and the fixation solution, to ensure the attachment of bacteria into the sand grains before the subsequent injection of cementation solution which might wash away some of the injected bacteria cells; (2) the amount of the supplied reagents and the way that they are introduced into the soil mass (e.g. injection or surface percolation; and (3) flow of reagents into the soil depth which might follow the preferential flow path along the phreatic surface.

"Publication has been removed due to copyright restrictions"

Figure 2.19: 100 m^3 scaled up experiment set up (after van Paassen, 2009)

The transport of reagents in the preferential flow path leads to higher $CaCO_3$ content precipitated in that area, which is prone to receive more reagents where the flow resistance is much lower. The locally precipitated $CaCO_3$ crystals located in the soil pore throats reduce the permeability of the bio-cemented sand and thus, causing an increase in the flow resistance and leading to the development of a new preferential flow path (DeJong et al., 2011).

Martinez (2012) performed an up-scaled experiment to investigate the three-dimensional flow regime pattern developed by the MICP treatment in the scaled well-to-well treatment model. The scaled well-to-well model simulates the flow condition found in a repeated five-spot well pattern, commonly used in oil recovery applications to achieve efficient oil recovery over a target subsurface zone. It was found that the two-phase MICP treatment scheme utilised to consolidate the system has adequately improved the target treatment (0.5 m × 0.5 m × 0.15 m) zone with small spatial variation. The small spatial variation was attributed to the uniformly distributed $CaCO_3$ crystals along the soil subsurface as a result of the uniformly distributed bacteria and nutrients along the flow regime.

Gomez et al. (2014) conducted a field-scale bio-cementation test focussing on the surficial application of MICP to provide surface stabilisation and to improve the erosion resistance of loose sand deposits (Figure 2.20). The results indicated that the treated soil was improved to a depth of approximately 28 cm after 20 days of treatment. Also, it was shown that the treated soil exhibited moderate degradation at 298 days post-treatment following a harsh winter condition. This signals the potential use of MICP treatment to strengthen soil in cold regions. The result also showed that the low-concentration treatment solutions provided the greatest improvement; no apparent reason was discussed to explain this finding. However, this indicates that the use of low-concentration treatment solutions can result in a relatively lower cost of MICP treatment installation in the field due to the use of less concentrated reagents.

Figure 2.20: Field scale set up using uniform, loose and poorly graded sand (after Gomez et al., 2014)

Recently, Phillips et al. (2016) used MICP to seal fracture due to fluid leakage near the subsurface wellbore environment. As discussed by Ivanov & Chu (2008) and Chu et al. (2013), MICP can act as either bio-cementing or bio-clogging agent depending on the targeted usage. In fracture sealing mechanism, MICP treatment is used to produce $CaCO_3$ crystals that perform as bio-clogging agent to provide fracture plugging and permeability reduction in porous materials. It was highlighted that the $CaCO_3$ sealant is advantageous over cement-based sealant due to the lower viscosity of the reagents needed to produce $CaCO_3$ crystals thus, enabling their ease of transport into the targeted well fracture.

Gomez et al. (2016) performed a large scaled bio-cementation experiment to study the improvement difference when using two different types of bacteria: (1) bio-augmented using the commercially available bacteria, i.e. *S pasteurii*; and (2) bio-stimulated approach (natural bacteria in the soil) (Figure 2.21). Their results suggested that MICP treatment using bio-stimulation approach provided comparable resistance towards CPT with an increase in tip resistance of 419% after treatment signifying the potential economic gains using the bio-stimulation concept.

Figure 2.21: Large scale experiment set up using bio-augmented and bio-stimulated MICP approaches (after Gomez et al. 2016)

2.10 Envisioned Applications of MICP for Soil Improvement

Present research on soil bio-cementation basically revolves in the MICP process and treatment optimisation at the experimental scale level. Table 2.1 presents the envisioned application of MICP exploring its plausibility as other alternatives for geotechnical engineering soil improvement technique. Each envisioned application is tailored to its specific function and the possible mechanism is explained in brief.

Table 2.1: Envisioned Applications of MICP for Soil Improvement

Envisioned application	Improvement mechanism	References
Soil stabilisation	The produced $CaCO_3$ crystals bind sand particles together hence, increasing soil's shear strength and stiffness	Whiffin et al. (2007); DeJong et al. (2010); Al Qabany et al. (2012); Cheng et al. (2013); Chu et al. (2013); Ivanov et al. (2015a); Smith et al. (2017)
Slope stabilisation	The produced $CaCO_3$ crystals help to strengthen the failure plane surface by providing additional stability needed to inhibit slope failure	DeJong et al. (2011); DeJong et al. (2013); Salifu et al. (2016)
Settlement reduction	The produced $CaCO_3$ crystals increased the bearing capacity of the foundation thus, reducing the primary settlement	van Paassen et al. (2010a); van Paassen et al. (2010b); Pham et al. (2016)
Erosion control	The produced $CaCO_3$ crystals increase the soil resistance against the forces of water along the sea shores/riverbanks and wind for surficial soil protection	Jiang et al. (2016); Maleki et al. (2016); Jiang & Soga (2017)
Liquefaction prevention	The post-shearing loads could re-initiate the MICP process hence, preventing further liquefaction damages	Montoya et al. (2013); Montoya & DeJong (2015); Han et al. (2016)
Self-healing of soil	The produced $CaCO_3$ crystals degraded when loaded beyond its yield strength. The bio-cemented sand properties can be returned to its pre-sheared level condition by re-initiating the MICP process	Montoya & DeJong (2013); Harbottle et al. (2014)

2.11 Advantages of MICP for Soil Bio-Cementation

2.11.1 Cost Effectiveness

One of the reasons why MICP is yet to be applied in the real field application is due to the misleading belief that its implementation would be costly. Table 2.2 provides the cost comparison to treat 1 m^3 of soil sample based on the various cementing agents available in the literature against MICP. Although, it is noted by Whiffin et al. (2007) that the initial cost of the implementation of MICP in terms of the bacteria placement and the cementation solution introduction into the targeted soil stratum is slightly more compared to other cementing agents, soil bio-cementation by MICP process is deemed to be cost-saving in the long run because the bacterial enzyme can be reused in subsequent treatment applications using the same cementation solution provided that no major bacterial cells flushed out during the treatment.

Table 2.2: Cost Comparison of Various Cementing Agents

Cementing agent	Yield strength (MPa)	Cost per m3 treatment ($)*	References
MICP	0.5 – 2.5	20 – 60	Cheng (2012)
Portland cement	0.5 – 3.8	NC	Ismail et al. (2002b)
Gypsum	0.2 – 1.8	NC	Ismail et al. (2002b)
Chemical grout	NM	2 – 72	Ivanov & Chu (2008)

NM = not measured
NC = not calculated
$ = Australian dollar

Based on Table 2.2, the cost to treat 1 m^3 of soil differs according to the cementing agents used. While MICP seemed to be incurring the highest cost at the moment, it poses no detrimental effects to the environment as opposed to the use of other cementing agents such as Portland cement, gypsum and chemical grout, which according to Ivanov & Chu (2008) could be toxic to the environment.

Alternatives have been suggested in the literature to reduce the cost of MICP implementation for field application. For example, Cheng (2012) successfully showed that the cost of the sterile bacteria production could be further minimised with the production of non-sterile chemostat culture containing high urease active bacteria cultivated at high pH = 10 and high urea concentration of 0.17 M. The preparation of the non-sterile chemostat culture allows the enrichment of bacterial cells to be reproduced continuously on site. Also, Cheng et al. (2014) demonstrated that the calcium ions (Ca^{2+}) available in the seawater could potentially act as substitution for the commercial calcium chloride ($CaCl_2$) source for the production of the cementation solution. The use of seawater would reduce the cost of MICP implementation since the source of Ca^{2+} occurs naturally, plus the concept would work well if the targeted soil treatment is located near to the seashore where the soil is prone to erosion.

2.11.2 Promoting the Concept of Sustainability

MICP process used in soil bio-cementation promotes the concept of sustainability in the sense that it uses natural material ubiquitously available in nature such as microorganism (bacteria) as the primary source of the cementing agent. The supplied bacteria can be reused to re-initiate MICP process up to three times injection of the cementation solution provided that bacteria flushed out can be kept to the minimum. Harkes et al. (2010) suggested the use of fixation solution to ensure the permanence of bacteria attachment to the sand particles to prevent bacteria detachment, as a result of the initial cementation solution injection. MICP process has been successfully applied in the construction industry mostly as cementing agent to heal concrete cracks (Van Tittelboom et al., 2010; Achal et al., 2011; Achal et al., 2013) and retrofitting historical structures (Reddy et al., 2012; Yang & Cheng, 2013). The myriad use of MICP signals its novelty as the plausible material for future purposes.

Although it has been pointed out that the end product of urea hydrolysis i.e. ammonia, can be detrimental to the environment, especially if it is able to permeate into the groundwater chains and reportedly cause the 'blue baby' syndrome (Qiu et al., 2017). It is also learnt from nature that ammonia helps to enrich plants' nutrients intake. The release ammonia could be properly collected, managed and fed back into the surroundings as possible source of fertilizer to nourish plants' growth. This eventually could open new horizon into looking at the aspect of vegetation growth on top of soil treated with MICP. For example, vegetation growth could improve slope stability with its roots anchorage system that grips the soil surface (Hooke & Sandercock, 2017; Shen et al., 2017).

2.11.3 Bacteria Reliability

One of the most fundamental advantages of MICP for soil bio-cementation is the fact that the bacteria used for the catalyst of the ureolytic process could be sourced from and is abundance in nature. The availability of the bacteria in the MICP process indicates that the $CaCO_3$ crystals precipitation is an active process. Unlike other cementing agents, which are generally considered inert, the process of bio-cementation continues to occur as long as the bacteria cells remain active in the soil matrix system (bacteria activity is measured in terms of their urease enzyme production) (Cheng et al., 2013). The ability of the bacteria to remain active in the soil matrix even after several cementation solution injections could further be harnessed into the concept of soil healing. Soil healing is made possible through MICP by means of bacteria re-activation upon loading. The degraded $CaCO_3$ bonds developed in the bio-cemented soil as a result of the subsequent loading could be healed by re-introducing the cementation solution into the cracked bio-cemented sample (Harbottle et al., 2014). The supplied cementation solution would infiltrate the cracked bio-cemented sample through the degraded $CaCO_3$ bonds by preferential flow. The dormant bacteria available in the bio-cemented sample are re-activated through the supply of growth medium or buffer solution that would re-initiate the MICP process.

The healing ability of MICP in soil improvement can be utilised to minimise primary and secondary settlements of structures and soils during earthquake as well as the subsequent additional settlement due to aftershocks (Montoya and DeJong 2013). This specific healing property of MICP derived soil improvement technique denotes the reliability of bacteria as the precursor to the whole MICP process reaction.

2.12 Limitations of MICP for Soil Bio-Cementation

2.12.1 Bio-Cemented Soil Treatment Uniformity

$CaCO_3$ crystals precipitation uniformity along the soil depth remains the most integral part in the successful implementation of MICP in the field. $CaCO_3$ crystals precipitation uniformity could not be achieved if the bacteria cells were not uniformly distributed along the intended treated soil column (Whiffin et al., 2007; Okwadha & Li, 2010; Akiyama & Kawasaki, 2012; Cheng et al., 2013; Montoya & DeJong, 2015). It was identified through the literature that there are two ways to achieve the bacteria cells homogeneity, i.e. (1) adoption of two-phase injection strategy; and (2) introduction of fixation solution (FS). For instance, Whiffin et al. (2007) introduced the two-phase injection method at which, the bacteria and the cementation solutions were injected alternately into the treated soil samples. It was found that the two-phase injection method produced more homogeneous $CaCO_3$ crystals formation compared to the simultaneous injection for both reagents. Simultaneous injection of BC and CS leads to immediate bacteria flocculation that results in the precipitation of primary $CaCO_3$ crystals that tend to precipitate near the region of the injection point hence, causing local clogging. Subsequent introduction of BC and CS into the treated sample would further increase the size of the initially precipitated $CaCO_3$ crystals. The gradual increase in the $CaCO_3$ crystals size would then retard the passage of the subsequent BC and CS injections into the treated column.

As previously mentioned, the key issue in achieving a homogenously distributed $CaCO_3$ crystals precipitation along the treated soil column relies upon the ability to spread out the bacteria cells evenly across the entire column depth. One of the main challenges to achieve $CaCO_3$ crystals precipitation uniformity is the gullibility of the bacteria to be flushed away during MICP treatment. Harkes et al. (2010) introduced the application of fixation solution (consisting of high salinity solution i.e. 50 mM $CaCl_2$ solution) after the initial bacteria culture injection. It was observed that the high salinity solution promoted the increased in the ionic strength of Ca^{2+} ions available in the CS thus; enhancing bacteria cells attachment to the sand grains Torkzaban et al. (2008). Bacteria cells attachment to the sand grains increases the chances of the bacterial absorption onto the sand grains surface, hence, eliminating the possibility of bacteria cells washed out as a result of the subsequent reagents injection as the treatment process continues (Tobler et al., 2012). Employing this injection scheme, followed by the injection of the FS, Zhao et al. (2014a) reported that almost 85% of precipitated $CaCO_3$ crystals were uniformly distributed along the bio-cemented sample upon the calcite content measurement.

2.12.2 Ammonia Production

In the presence of urease active bacteria, urea ($CO(NH_2)_2$) is hydrolysed into ammonia (NH_3) and carbamic acid (NH_2COOH), as shown in Equation 2.4. Due to its instability, carbamic acid (NH_2COOH) spontaneously hydrolyses into ammonia (NH_3) and carbonic acid (H_2CO_3), as shown in Equation 2.5. In the presence of water, ammonia (NH_3) and carbonic acid (H_2CO_3) can reversibly turn into ammonium (NH_4^+) and hydroxide (OH^-) ions (Equations 2.6 and 2.7). Bicarbonate (HCO_3^-) ions equilibrium can easily be altered forming carbonate (CO_3^{2-}) ions by the production of hydroxide (OH^-) ions, as a result of the pH increase (Equation 2.8). In the presence of calcium source, i.e. from the cementation solution, calcium (Ca^{2+}) ion would react with carbonate (CO_3^{2-}) ion to form calcium carbonate ($CaCO_3$) crystals (Equation 2.9) (Hammes et al., 2003b).

$$CO(NH_2)_2 + H_2O \rightarrow NH_2COOH + NH_3$$ Equation 2.4

$$NH_2COOH + H_2O \rightarrow NH_3 + H_2CO_3$$ Equation 2.5

$$2NH_3 + 2H_2O \Leftrightarrow 2NH_4^+ + 2OH^-$$ Equation 2.6

$$H_2CO_3 \Leftrightarrow HCO_3^- + H^+$$ Equation 2.7

$$HCO_3^- + H^+ + 2NH_4^+ + 2OH^- \Leftrightarrow CO_3^{2-} + 2NH_4^+ + 2H_2O$$ Equation 2.8

$$Ca^{2+} + CO_3^{2-} \rightarrow CaCO_3$$ Equation 2.9

As can be seen from Equations 2.4 – 2.6, for 1 mole of urea hydrolysis, 2 moles of ammonia are produced. To date, no study has been found in the literature, which specifically addresses the issue of ammonia production as the by-product of MICP process. Ammonia can be detrimental to human health and safety and has obnoxious odour. The severity of the health impact of ammonia to the human body has been outlined in the National Health and Medical Research Council (2011) for drinking water source, which limits the amount of less than 0.5 mg/L ammonia is to be consumed at a time. It has been reported that, incessant consumption of ammonia in the drinking water beyond this limit could lead to 'blue baby syndrome' in infants that could consequently lead to infant fatality if no proper immunisation scheme is to be initiated at the early stage. Hence, moving forward, it is fundamental to devise strategies to deal with ammonia production through MICP treatment. Lately, Yasuhara et al. (2012) and Zhao et al. (2014a) proposed the use of urease enzyme extracted from plant, i.e. jack bean as substitute towards urease active bacteria to catalyst the process of urea hydrolysis. It was reported that although the strength improvement of the urease enzyme mediated treatment was almost 5 times lower than that of the traditional MICP treatment using urease active bacteria, the amount of ammonia produced could be significantly reduced by employing urease enzyme as ureolysis catalyst.

2.12.3 Geometric Soil-Bacteria Compatibility

One of the key issues that limit the use of MICP as general solution towards soil improvement is the geometric compatibility between the soil and the bacteria. Geometric compatibility refers to the condition whereby bacteria can freely move from one pore space to another through the soil pore throats in the bio-cemented soil matrix. Mitchell & Santamarina (2005) argued that there are two major factors that govern the geometric compatibility, i.e. (1) soil pore throat size; and (2) agglomeration of the $CaCO_3$ crystals.

Soil pore throat size affects the movement of bacteria in the soil matrix. DeJong et al. (2010) suggested that the soil pore throat size could approximate to be 20% of the soil particle size that corresponds to 10% passing in the sieve analysis. In other words, should the size of the soil pore throat be less than the size of the bacteria used in the treatment, MICP process could not function properly as local pore clogging would occur near to the inlet of the MICP reagents injection (Al Qabany et al., 2012). Pore clogging occurs as a result of the accumulation of bacteria cells that eventually turn into $CaCO_3$ precipitates aligning themselves near to the vicinity of soil pore throat, which is rich in nutrient and presumably features the least stressed area (DeJong et al., 2011). As the soil pore throat is impeded by the accumulation of the $CaCO_3$ precipitates, further supply of MICP reagents would contribute into either the $CaCO_3$ crystals growth or the agglomeration of $CaCO_3$ crystals instead of the transport of the bacteria into the column depth thus, rendering $CaCO_3$ crystals precipitation distribution non-uniformity.

Agglomeration of $CaCO_3$ crystals from primary individual circular-shaped crystals into the secondary clustered rhombohedral-shaped mesocrystals would create a natural filter for the subsequent MICP reagents injection. Since the filtering process is dependent on the relative size between the pore space and the $CaCO_3$ crystals size as they aggregated, the effect would be more pronounced in a comparatively smaller soil pore throat size.

DeJong et al. (2010) mentioned that the size of the microorganisms typically used in soil bio-cementation ranges from 0.5 – 3 μm. It is noted that the microorganisms' selection takes into consideration the soil pore throat size in the soil matrix. This is to accommodate for the relatively small allowance of passageway the microorganisms took as they move from one pore space to another via the soil pore throat (Mitchell & Santamarina, 2005). On the other hand, soil is classified into two major categories, i.e. coarse and fine-grained soils. Although most of the soil bio-cementation treatment was applied to sandy soil due to its most convenient geometric compatibility, more attempts were directed into improving finer-grained soils (e.g. silt and clay) or even coarser soil (e.g. gravel) in the laboratory scale experiments. Table 2.3 lists the most currently use soils for MICP available in the literature.

Table 2.3: Current Soil Types Treated Using MICP Process

Soil type	**Soil size**	**References**
Gravel	2 – 6 mm	Amini & Hamidi (2014); Jiang et al. (2016); Jiang & Soga (2017)
Sand	0.06 – 2 mm	Mitchell & Santamarina (2005); Whiffin et al. (2007); Harkes et al. (2010); Burbank et al. (2011); Al Qabany et al. (2012); Burbank et al. (2012); Cheng & Cord-Ruwisch (2012); Yasuhara et al. (2012); Cheng et al. (2013); Yang & Cheng (2013); Zhao et al. (2014a); (Park et al., 2014b); Montoya & DeJong (2015); Cheng et al. (2017); Choi et al. (2016); Pham et al. (2016); Terzis et al. (2016); Cheng & Shahin (2017); (Feng & Montoya, 2017); (Terzis & Laloui, 2018)
Silt	0.002 – 0.06 mm	Lee et al. (2013); Ng et al. (2014); Keykha et al. (2014); Grabiec et al. (2017)
Clay	< 0.002 mm	Ivanov et al. (2015b)

2.13 Current Research Focus

Unlike other cementing agents, $CaCO_3$ crystals precipitated through MICP process could be tailored into their specific usage according to their precipitation patterns, i.e. (1) small crystals to clog the soil pores (Ivanov & Chu, 2008; Al Qabany et al., 2012; Chu et al., 2013); and (2) large crystals such as effective $CaCO_3$ crystals formation at soil pore throats that bind soil particles together, hence, improving the bio-cemented soil's strength (Cheng et al., 2013; Terzis et al., 2016). Cheng et al. (2013) has pointed out that the various precipitation patterns are closely related by the interplay between the concentration of the bacteria culture and the cementation solution injected into the treated sample.

No study has ever embarked on the microstructural characteristics of the different precipitation patterns and their relationship towards the macro strength improvement properties of the bio-cemented samples. So far, the production of $CaCO_3$ crystals whether in the laboratory scale or in the field relies heavily on the so-called MICP process optimisation, e.g. treatment injection scheme, treatment cycle, use of urease active bacteria or urease enzyme extracted from plant, source of cementation solution (i.e. magnesium or calcium) and various environmental factors (Harkes et al., 2010; Mortensen et al., 2011; Al Qabany et al., 2012; Tobler et al., 2012; Martinez et al., 2013; Zhao et al., 2014a; Cheng et al., 2017). Although the optimised version of MICP utilising these recommendations exhibited improved strength properties; however, the production of specific $CaCO_3$ crystal pattern still yet to be cost-effectively produced due to the failure to understand the mechanism of achieving different patterns of $CaCO_3$ crystals precipitation in the laboratory and field scale levels.

The current study aims to artificially produce effective $CaCO_3$ crystals that can improve both the strength improvement and the permeability retention of the bio-cemented sand. This was achieved by mixing various concentrations of BC and CS. The main goal of the present study was to identify which combination of the different BC and CS that would produce the most effective $CaCO_3$ crystals. The different $CaCO_3$ crystals precipitation is crucial because they could serve different purpose for field application. For instance, small $CaCO_3$ crystals that cover the surface of the sand grains would be ideal for embankments and dams' consolidation to prevent dissipation of liquid. Meanwhile, the precipitation of effective $CaCO_3$ crystals would serve the traditional superstructure foundation's reinforcement, ground improvement and pavement base stabilisation.

The microstructural properties of various $CaCO_3$ crystals precipitation were then observed under the SEM to explore their evolution phases and the specific microstructural features. While the evolution study will show the transformation of the primary and secondary $CaCO_3$ crystals and the associated binding mechanism of the soil particles, the microstructural analysis will pinpoint to the unique characteristics of the proposed effective $CaCO_3$ crystals in this study.

2.14 Summary

A thorough review of the process and the influencing factors affecting the effectiveness of MICP process for soil bio-cementation was addressed in this chapter. Different approaches adopted to treat soil samples using MICP together with the geotechnical engineering properties of the bio-cemented soils and their microstructural characteristics were discussed at length. Different factors affecting the effectiveness of the MICP process which include the process and treatment optimisation were presented. Field application of soil bio-cementation were duly acknowledged and earlier experimental works available in the literature were described and criticised with some details highlighting their limitations, in order to justify the present research. The envisioned applications of MICP for soil improvement, their advantages and limitations were also discussed.

The review into the literature reveals that very few studies have examined the relationship between the different precipitation patterns with the engineering properties of the bio-cemented samples, as explained in Section 2.12. The ability to produce different precipitation patterns within a controlled environment (in this case, the effective $CaCO_3$ crystals), and then specifically tailor their purpose for field application is desirable. Therefore, there is a need to explore the necessary procedures and treatment regime to achieve the effective $CaCO_3$ crystals. In the following chapter, the materials and methodologies used to prepare the bio-cemented samples together with the associated testing program to assess the engineering properties improvement are discussed in detail.

Chapter 3

Bio-cemented Samples Preparation and Testing Program

3.1 Introduction

This chapter describes the materials (bacteria, growth medium, cementation solution and OPC) and test procedures (batch analyses, UCS, permeability, triaxial, SEM) utilised in the present study. Unlike previous studies, which focused on the mechanical behaviour of the bio-cemented soils in the macroscale level (Al-Thawadi, 2013; DeJong et al., 2014; Duraisamy & Airey, 2015; Gomez et al., 2016; Smith et al., 2017) and the MICP process optimisation (Al Qabany et al., 2012; Duan & Zhu, 2012; Chu et al., 2013; Martinez et al., 2013), the current study considers the effect of the $CaCO_3$ crystal precipitation patterns and their relationship on the strength improvement of the bio-cemented soils at a microscopic level.

The microstructural study will focus on two main issues: (1) the evolution of the $CaCO_3$ crystal during the MICP process, which includes the propensity of the bacteria cells to align themselves near the soil pore throats, the availability of the nucleation sites, the birth of new crystal and the growth of the available crystal; and (2) the specific microstructural features of the effective $CaCO_3$ crystals that would pinpoint to their unique characteristics compared to the previously discovered precipitation patterns.

3.2 Methodology Framework

Three phases of experimentation setup were executed to achieve the objectives of the present study. The different staged experiment outlined in the research work is crucial in the interest of producing, examining and understanding the effect of the effective $CaCO_3$ crystals towards the bio-cemented soils engineering properties. Concisely, the three phases experimentation setup proposed herein can be described as follow:

1. Optimisation in terms of batch analyses to assess the bio-cementation kinetics to obtain the most optimum parameters for an effective MICP process;

2. The optimised $CaCO_3$ crystals and their relationship with the strength improvement of the bio-cemented sand in the microscopic level; and

3. UCS and triaxial tests to quantity the strength and stiffness of the bio-cemented sand columns reinforced with the optimised $CaCO_3$ crystals.

Details of the above steps are presented in the methodology framework, as shown Figure 3.1. The test program was carefully designed to justify the research objectives relevant to the current research scope. The goal of conducting batch analyses was to determine the most optimum parameters for an effective MICP process. Factors such as initial soil pH and temperature were assayed. In the next phase, the optimised $CaCO_3$ crystals and its relationship on the strength improvement of the bio-cemented sand were assessed. The examination was made particularly in the microscopic level to study the inter-particle bonding mechanism as well as the corresponding failure criteria. Different BC and CS concentrations were used to produce different precipitation patterns at which, the most effective $CaCO_3$ crystals precipitation and their impact on the strength and stiffness improvement of the bio-cemented sand samples were examined. Finally, the correlation between the amount of the precipitated $CaCO_3$ content with the strength and stiffness enhancement were determined through the UCS and triaxial tests.

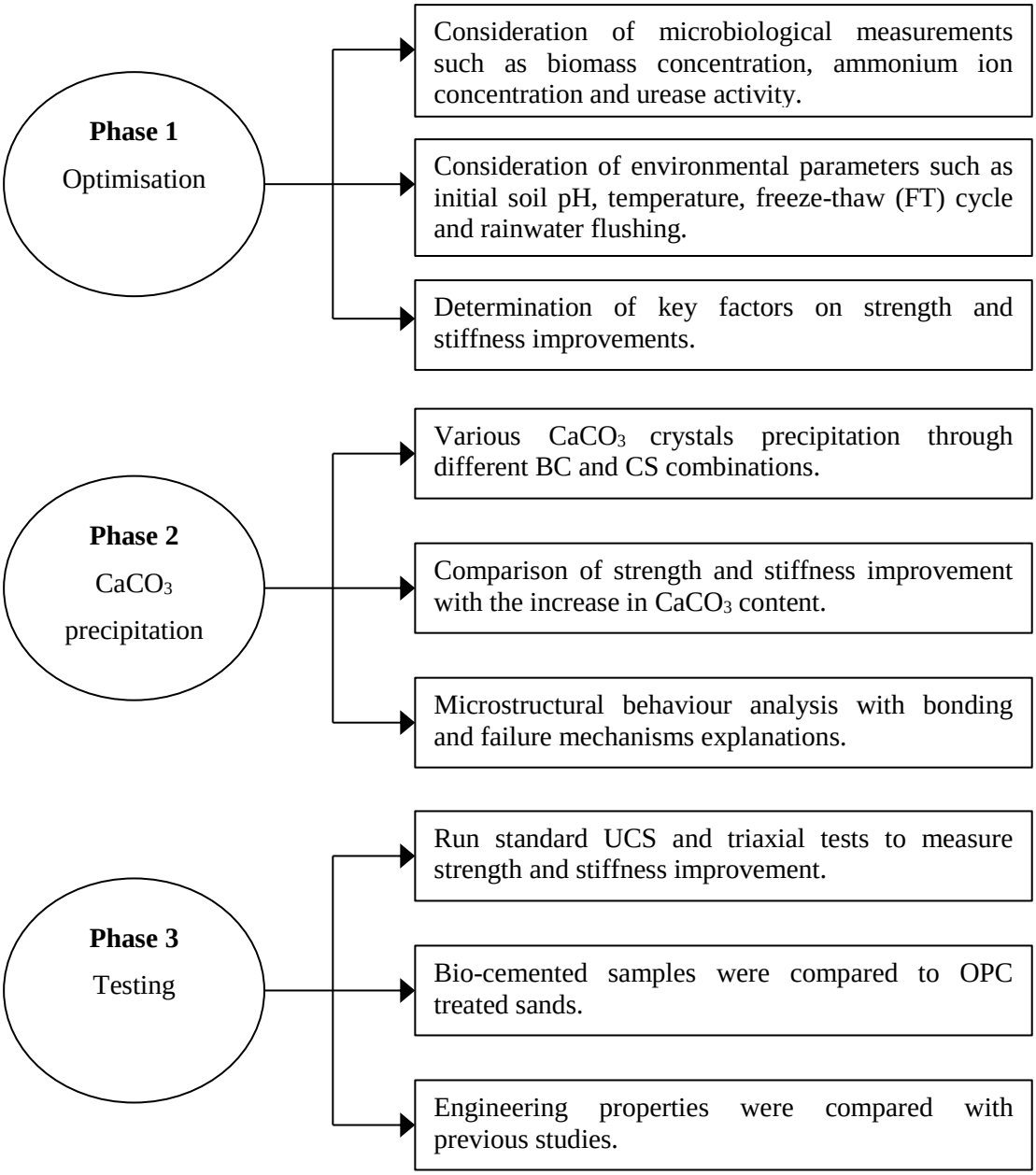

Figure 3.1: Methodology framework

3.3 Materials

3.3.1 Bacteria

The urease-producing bacteria used in the current study are called *Sporosarcina pasteurii*. *S. pasteurii*, which are Gram-positive, rod-shaped bacteria commonly found in soil and have unique characteristics. The main reason for choosing *S. pasteurii* in this study is their highly active urease production characteristics. As discussed in Chapter 2, highly active urease-producing bacteria contributed directly towards the high amount of the $CaCO_3$ precipitates in the MICP process (Tobler et al., 2014; Wei et al., 2015; Bhaduri et al., 2016; Harris et al., 2016). Another crucial reason is their tolerance to high temperature and chemicals due to the availability of their resistant endospores, which then maintain their permanence in the soil for a long period of time. Most importantly, *S. pasteurii* pose no harm to humans, as they are categorised as a non-pathogenic type of bacteria. Figure 3.2 shows the proximate view of *S. pasteurii*.

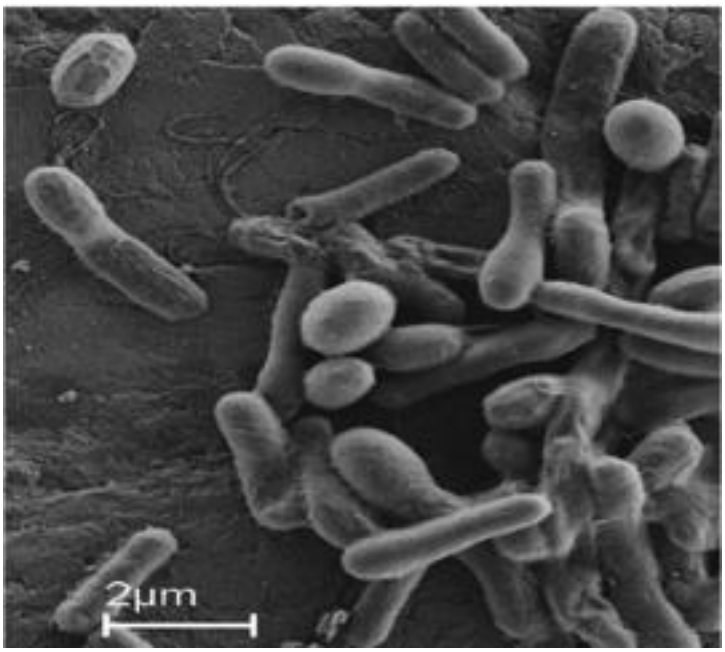

Figure 3.2: A proximate view of *Sporosarcina pasteurii*

(www.alchetron.com**)**

3.3.2 Urea

Urea is a colourless crystalline compound that has the chemical formula $CO(NH_2)_2$. In the presence of water, $CO(NH_2)_2$ can be reduced to form carbonate and ammonium ions. The released carbonate ion in return becomes a crucial factor in the formation of the $CaCO_3$ crystals. The index properties of $CO(NH_2)_2$ are given in Table 3.1.

Table 3.1: Index properties of $CO(NH_2)_2$

Property	Value
Molar mass	60.06 g/mol
Density	1.32 g/cm^3
Solubility in water	1079 g/L at 20°C
Gibbs free energy	-47.12 kcal/mol
Flash point	Non-flammable
Hazards identification	Hazardous

3.3.3 Calcium Chloride

Calcium chloride ($CaCl_2$) is an inorganic compound that has the chemical formula $CaCl_2$. It is colourless and highly soluble in water. In the presence of water, the $CaCl_2$ compound can be reduced to form calcium ions and chlorine gas. The released calcium ions are important in the formation of the $CaCO_3$ crystals. The index properties of $CaCl_2$ are listed in Table 3.2.

Table 3.2: Index properties of $CaCl_2$

Property	Value
Molar mass	147.02 g/mol (dehydrate)
Density	1.85 g/cm^3 (dehydrate)
Solubility in water	134.5 g/L (dehydrate)
Gibbs free energy	−748.81 kcal/mol
Flash point	Flammable
Hazards identification	Hazardous

3.3.4 Ordinary Portland cement

Ordinary Portland cement (OPC) has a grey; fine powder form produced by heating limestone and clay minerals in a kiln by grinding to form clinker. In the current study, OPC was used to prepare cemented samples for comparison of UCS and permeability values with those obtained from bio-cementation. Table 3.3 outlines the mixture design of the OPC treated samples. The sand used for this experiment was silica sand of uniform size 0.425 mm, classified as poorly graded sand (SP) by the Unified Soil Classification System (USCS).

Table 3.3: Mixture design for the OPC treated sands

Sample ID	Cement Content (g)	Sand Content (g)	Water Content (mL)	Dry Density (g/cm^3)
1	7	350	45	1.8 – 1.83
2	14			
3	21			
4	28			
5	35			
6	38.5			
7	42			
8	49			

3.3.5 Soil

Natural silica sand obtained from Cook Industrial Minerals Pty Ltd, Western Australia was used in the present study. Unless specified elsewhere in the thesis, natural silica sand was used as the key soil in this study. The basic soil physical properties are given in Table 3.4. According to the Unified Soil Classification System (USCS), the sand used is classified as poorly graded sand (SP). This type of sand was used in the current study because it exhibits undesirable engineering behaviour for most geotechnical engineering applications.

Table 3.4: Properties of the sand used in the current study

Property	Value
D_{10} (mm)	0.17
D_{30} (mm)	0.21
D_{60} (mm)	0.28
C_u	1.65
C_c	0.84
G_s	2.71
e_{min}	0.48
e_{max}	0.71
OMC (%)	12
$\gamma_{d\text{-}max}$ (kN/m^3)	16.3
n (%)	40
k (x 10^{-5} m/s)	80 ± 0.5
USCS classification	SP

OMC is the optimum moisture content with respect to the standard Proctor test (SPT)
$\gamma_{d\text{-}max}$ is the sand maximum dry density
n is the sand porosity
k is the sand permeability

3.4 Bacteria Culture Preparation

3.4.1 Growth Medium

S. pasteurii isolated from a previous work by Al-Thawadi & Cord-Ruwisch (2012) at Murdoch University, Australia, was used as the mother culture for the bacteria supply needed for the current study. Hence, other microbiological activities such as the pure strain bacteria cultivation were not conducted. The ingredients of the typical growth medium are listed in Table 3.5.

Table 3.5: Ingredients of the typical growth medium

Ingredient	Quantity
Yeast extract	20 g
Ammonium sulfate	18 g
Nickel chloride hexahydrate	500 μL
Sodium hydroxide	To adjust pH until 9.25
Distilled water	1 L

The procedures to produce the growth medium are demonstrated in Figure 3.3. Firstly, 20 g of yeast extract and 18 g of ammonium sulfate were measured and mixed inside a 2000 mL glass beaker, as shown in Figure 3.3(a). Then, 1 L of distilled water was added, and the mixture was mixed well until all the chemicals powder were completely dissolved [Figure 3.3(b)]. Next, a 500 μL of nickel (II) chloride hexahydrate solution was added using a pipette into the well-mixed solution [Figure 3.3(c)]. It should be noted that the initial pH of the solution should be slightly acidic ($6.5 < pH < 7.0$) at this point. Sodium hydroxide 10 M solution was introduced into the mixture using a 5 mL pipette, to adjust the final pH to 9.25 [Figure 3.3(d)]. Once the final pH reached a value of 9.25, the mixture was then equally divided into 2 sets of conical flasks containing, 200 mL mixture poured into the first set of 500 mL conical flasks and 300 mL mixture poured into the final set of 1 L conical flasks [Figure 3.3(e)]. Finally, all conical flasks were purified in the steriliser at 121°C for 40 minutes [Figure 3.3(f)]. The sterilisation step is important to ensure that the growth medium is free from contamination.

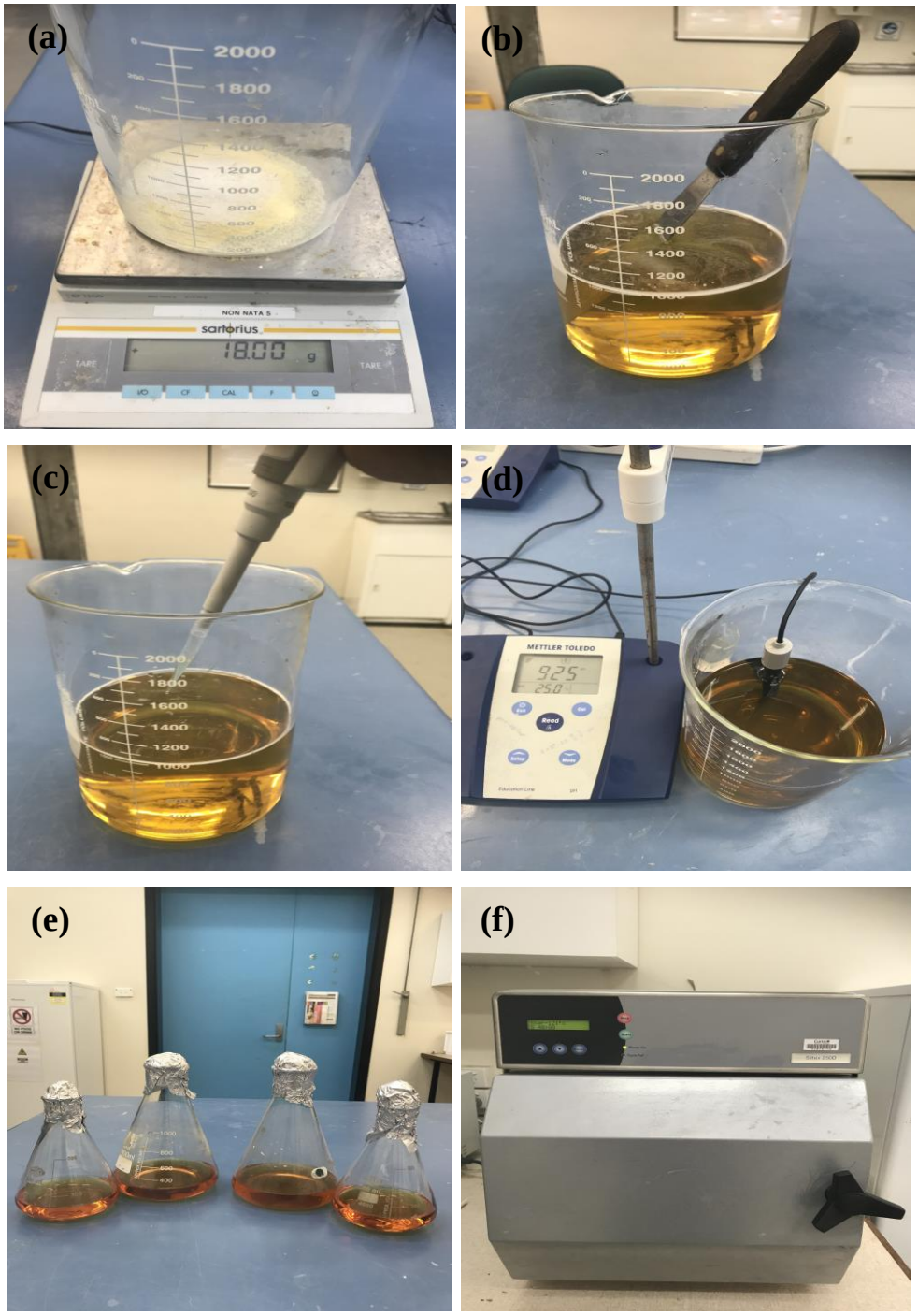

Figure 3.3: Growth medium preparation procedures: (a) yeast extract and ammonium sulfate measurement; (b) addition of 1 L distilled water and mixing; (c) addition of 500 µL of nickel (II) chloride hexahydrate; (d) addition of 10 M sodium hydroxide until the final pH is 9.25; (e) dividing the growth medium equally into several conical flasks; and (f) sterilising the medium at 121°C for 40 minutes

3.4.2 Bacteria Inoculation

It is critical to ensure that a clear growth medium is formed, as shown in Figure 3.4(b) by repeating the procedures stated in Section 3.4.1 prior to bacteria inoculation. This was assessed by monitoring any change in the colour of the solution after 24 hours; any change in the growth medium was recorded and a decision was made according to the quality of the solution. For example, if the growth medium showed slight turbidity, as shown in Figure 3.4(a), it was deemed contaminated and hence discarded. After the growth medium has cooled down and the bacteria sub-culture temperature reached ambient temperature, the inoculation process was started, as shown in Figure 3.5. Initially, the laminar flow cabinet was turned on and disinfected with 70% ethanol [Figure 3.5(a)]. Then, the tip of the conical flask containing the bacteria sub-culture was heated up using the Bunsen burner to ensure that the sub-culture remains sterile [Figure 3.5(b)]. Next, a few drops of the bacteria sub-culture were transferred into the growth medium flask, whose lid was closed immediately after the transfer [Figure 3.5(c)]. Finally, the inoculated growth medium was transferred into the water bath shaker to continue the growing phase. During this step, the water bath was set to 30°C (optimum temperature for bacteria growth) and allowed to shake (aerobic condition) for at least 72 hours until the specific urease activity of the desired BC was achieved [Figure 3.5(d)].

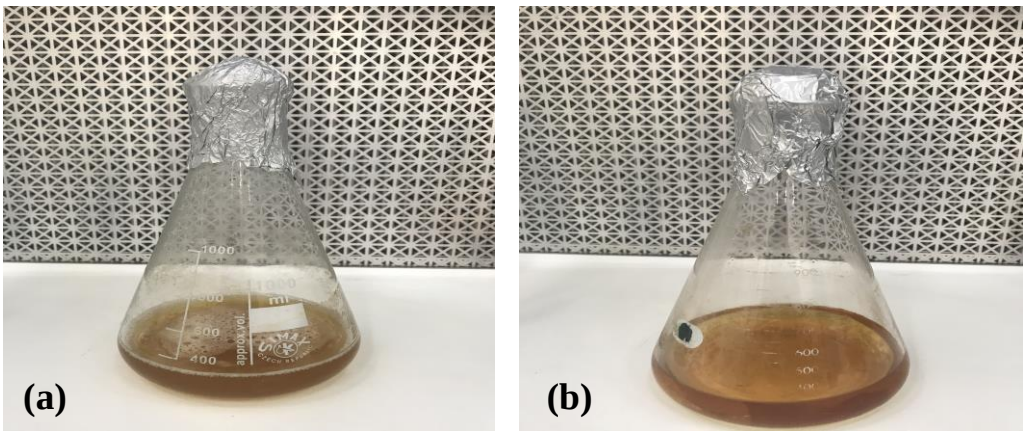

Figure 3.4: Growth medium indication: (a) contaminated sample characterised by a change in turbidity; and (b) a clear growth medium, a characteristic of successful preparation

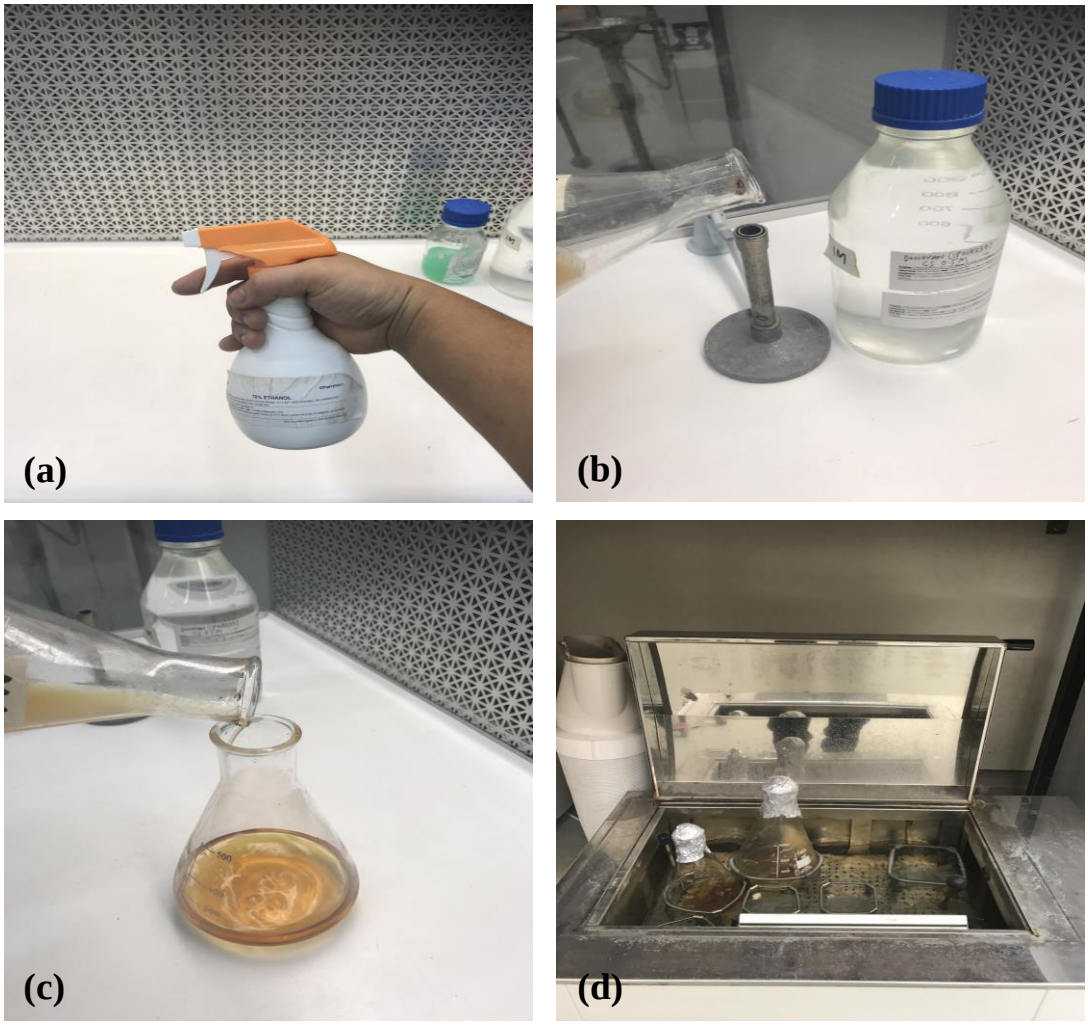

Figure 3.5: Bacteria inoculation procedures: (a) disinfecting laminar flow cabinet working area with 70% ethanol to avoid other impurities; (b) heating up the bacteria sub-culture flask tip to ensure that the sub-culture remained sterile; (c) addition of a few drops of bacteria sub-culture into the growth medium; and (d) growing the inoculated bacteria inside a water bath shaker at a constant temperature of 30°C for at least 72 hours

3.5 Cementation Solution

3.5.1 Recipes

The cementation solution used in the current study consisted of equimolar of $CO(NH_2)_2$ and $CaCl_2$ anhydrous. A total of three final CS concentrations were considered, namely 0.25 M, 0.5 M and 1 M. Higher CS concentration above 1.5 M was found to result in a reduced $CaCO_3$ content, according to Whiffin (2004). Concentrations below 0.25 M were not tried since more CS treatment cycles would have been required to produce adequate amounts of $CaCO_3$ crystals. Table 3.6 details the amount of each chemical used to achieve the different concentrations above. Once the desired CS concentration was achieved, the CS was then transferred into glass bottles and labelled prior to use.

Table 3.6: Cementation solution recipes

$CO(NH_2)_2$ (g/L)	$CaCl_2$ (g/L)	Molarity (M)
15.1	36.75	0.25
30.1	73.5	0.5
60.2	147.02	1

3.5.2 Cementation Solution Preparation

The exact amount of each of the two chemicals $CO(NH_2)_2$ and $CaCl_2$ needed to obtain the desired CS molarity listed in Table 3.6 was strictly used to ensure an equimolar distribution of each chemical in the CS combination. For instance, in order to prepare 1 M CS, 60.2 g of $CO(NH_2)_2$ was initially mixed with 500 mL of distilled water, resulting in a 2 M $CO(NH_2)_2$ solution. At the same time, 147.02 g of $CaCl_2$ was mixed with 500 mL distilled water, resulting in 2 M of $CaCl_2$ solution. After about 5 minutes, once all the $CO(NH_2)_2$ and $CaCl_2$ powder were completely dissolved in the mixture, both solutions were added simultaneously into a 1 L measuring cylinder and shaken vigorously to ensure that the CS was homogeneously mixed to produce a final molarity of 1 M CS. This procedure was repeated to produce others CS molarities.

3.6 Microbiological Consideration

Microbiological consideration assessing the suitability of the microorganism to be used as the source of the ureolytic bacteria is needed. Three calibration charts were established in order to calibrate the biomass of the grown bacteria, the concentration of the ammonium ions and the urease activity of the ureolytic bacteria used during the study.

3.6.1 Biomass Concentration Measurement

Routine biomass growth monitoring was carried out by applying the optical density (OD) measurement method using a spectrophotometer. OD is the measurement of a refractive medium to slow or delay the transmission of light. In MICP application, it is measured by passing the ultraviolet light through the cuvette containing bacteria suspension, forcing the light to scatter. The speed of light affecting the wavelength of a given light wave was then analysed and translated to the biomass concentration. Typically, a greater scattering degree indicates more bacteria present in the liquid. The spectrophotometer then analyses the amount of light scatter and translates it into a numeric value that could be read through the monitor display of the spectrophotometer. Generally, in order to determine the biomass concentration, the OD is set to a wavelength of 600 nm (OD_{600}) with deionised (DI) water used as blank sample. All cuvette samples are diluted to a range between 0.2 – 1.0 of the absorbance prior to measurement (Cheng, 2012). Figure 3.6 shows the standard curve used to determine the biomass concentration (recorded as the biomass dry density) at any given OD_{600} below 3. The correlation between the dry density of the biomass and OD_{600} is expressed by Equation 3.1 with a correlation strength, R^2 = 0.9974.

$$Biomass\ dry\ density\ \left(\frac{g}{L}\right) = 0.4155OD_{600} + 0.0112 \qquad \text{Equation 3.1}$$

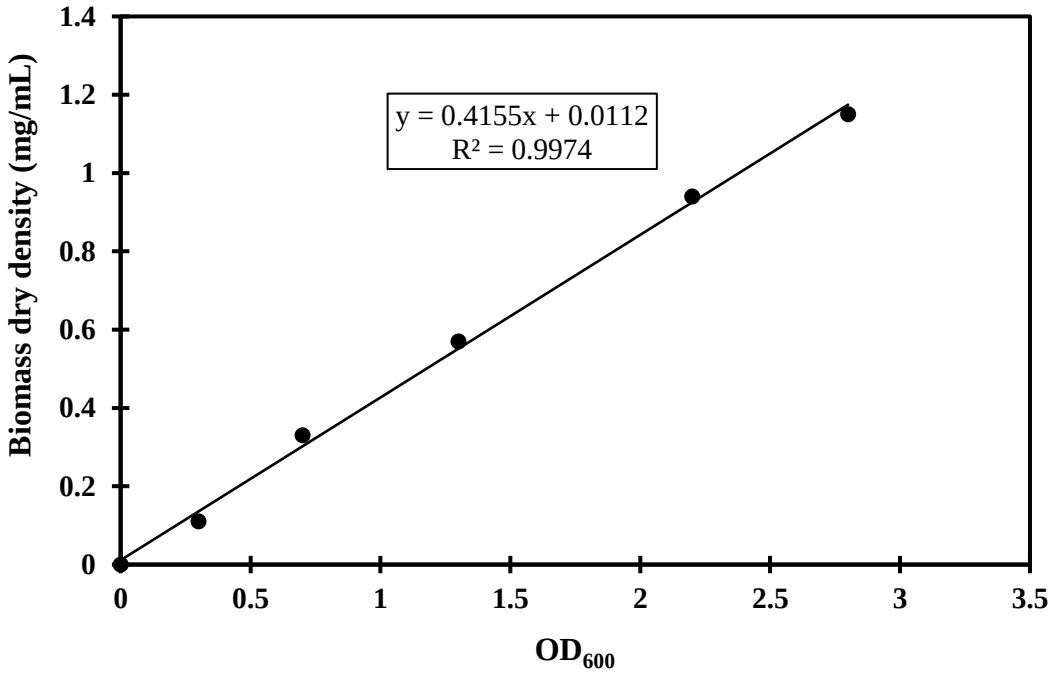

Figure 3.6: Standard curve of biomass dry density versus OD_{600}

3.6.2 Ammonium Ion Concentration Measurement

In the MICP process, determination of the ammonium ion (NH_4^+) concentration is crucial, as it relates to the amount of ammonia (NH_3) released as a by-product; such substance is detrimental to the environment if no proper measures are taken to mitigate its impact. The impact of NH_3 releases into the environment was discussed at length in Section 2.11.2. The procedures outlined by Whiffin (2004) and Cheng (2012) in accordance with the modified Nessler's Method was utilised to determine the NH_4^+ concentration using the spectrophotometer. All cuvette samples were diluted to a range of 0 – 0.5 mM of the absorbance prior to measurement (Whiffin, 2004). Then, 2 mL of the diluted sample was mixed with 100 µL of Nessler's reagent and left to react for exactly 1 minute in the cuvette. The cuvette was then placed inside the spectrophotometer and a reading was taken at a wavelength of 425 nm. The spectrophotometer reading was compared to the standard curve obtained using the calibration chart of analytical grade ammonium chloride (NH_4Cl) (Figure 3.7).

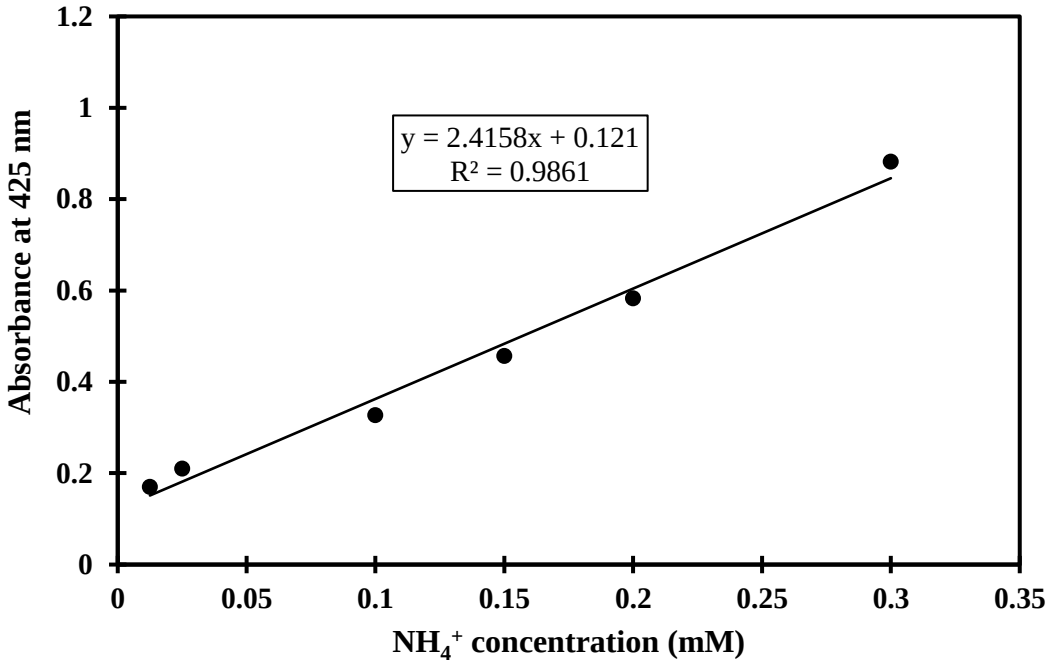

Figure 3.7: Standard curve of the absorbance versus NH_4^+ concentration

Based on Figure 3.7, the correlation between absorbance at 425 nm and NH_4^+ concentration maybe expressed by Equation 3.2 with a correlation strength, R^2 = 0.9861.

$$Absorbance_{425nm} = 2.4158 NH_4^+ concentration + 0.121 \quad \text{Equation 3.2}$$

3.6.3 Urease Activity Measurement

The urease activity of the bacteria was determined based on the urea hydrolysis rate using the conductivity meter technique. The conductivity meter measures the electrical conductivity to determine the amount of nutrients in a liquid. In this study, the conductivity meter technique was used to calculate the concentration of NH_3 and NH_4^+ over time during the batch analyses. The urease activity was determined from the rate of change of conductivity that takes place during the conversion of NH_3 to ionic products, i.e. NH_4^+ and CO_3^{2-} under the standard conditions of 1 atm pressure and 298 K temperature (Whiffin, 2004).

According to Rebata-Landa (2007), a typical bacteria growth curve consists of 4 distinct phases (Figure 3.8). (1) The 'lag' phase is where bacterial cells begin to adapt to their new environment after inoculation, characterised by a limitation of the amount of the cells division. (2) The 'exponential' phase is where the cells consume the provided substrates optimally characterised by fast duplication of the bacteria cells. (3) The 'stationary' phase is where the cells reach their maximum population density. (4) The 'death' phase is where the bacteria die due to the combination of several factors namely the nutrients depletion, oxygen exhaustion, unfavourable pH condition and waste accumulation. Therefore, it is imperative to measure the urease activity of the bacteria either at the end 'exponential' or stationary phases to determine the accurate activity of the bacterial cells.

Figure 3.8: A typical growth curve of bacteria population in a batch culture (after Rebata-Landa, 2007)

In order to measure the urease activity of the bacteria used in the present study, 1 mL of bacterial suspension was collected from the culture and 5 mL of 3 M $CO(NH_2)_2$ solution together with 4 mL of DI water were added to the mixture. The conductivity change was recorded for a period of 5 minutes at 25°C until the incremental rate of the conductivity achieved a constant rate. Figure 3.9 shows the conductivity of the different BC concentrations used in the current study.

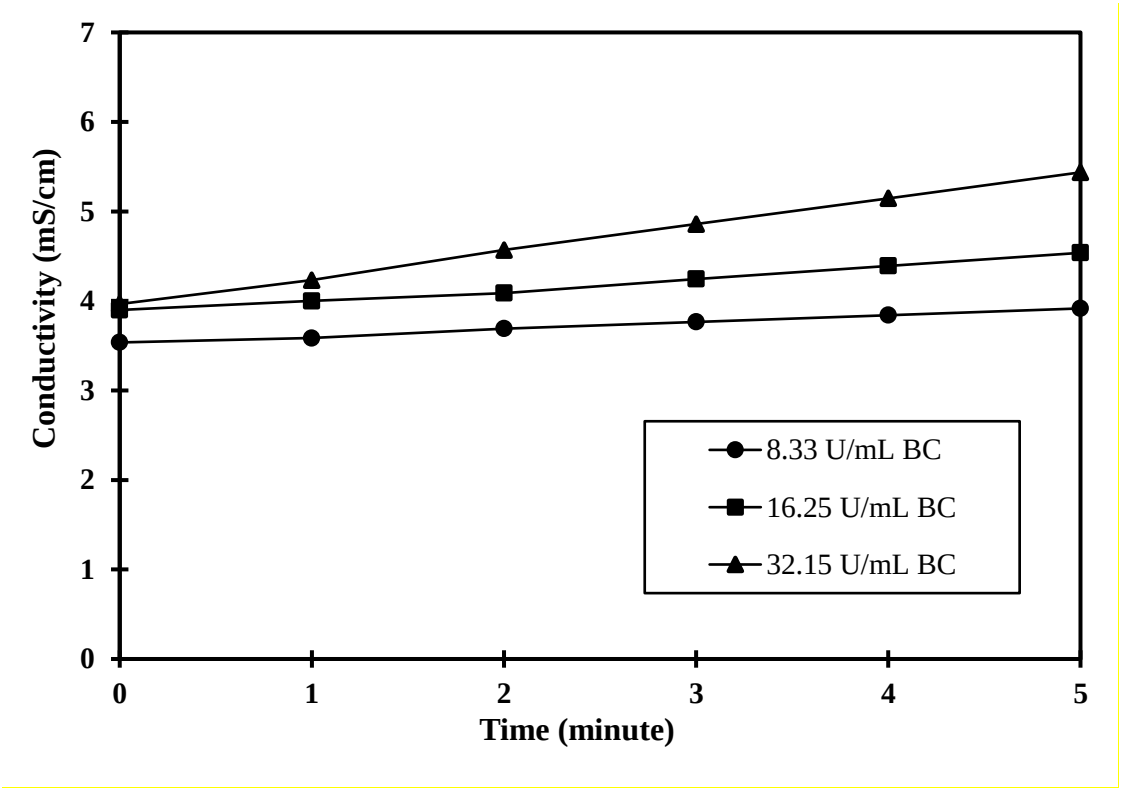

Figure 3.9: Conductivity rate of various BC concentrations

According to Whiffin (2004), urease activity can be calculated using Equation 3.3, which indicates that a rate of 1 mS/cm/min corresponds to 11.11 mM urea/min and a dilution factor DF = 10. Table 3.7 presents the bacteria culture recipes used in the current study. It is worth to note that the specific urease activities of the different types of BC used were similar, with ±0.01 tolerance in order to ensure consistency of the experiments.

$$Urease\ activity\ \left(\frac{U}{mL}\right) = Conductivity\ rate\ \left(\frac{\frac{mS}{cm}}{\min}\right) * 11.11 \frac{mMurea}{min} * DF$$

Equation 3.3

Table 3.7: Bacteria culture recipes

ID	Bacteria culture		
	Biomass concentration, OD_{600}, (cell density, g/L)*	**Urease activity (U/mL)†**	**Specific urease activity (U/mL/OD_{600})#**
1	1.21 (0.615)	8.33	6.88
2	2.36 (1.093)	16.25	6.89
3	4.66 (2.048)	32.15	6.90

*The OD_{600} and cell density were calculated based on Equation 3.1
†The urease activity was calculated based on Equation 3.3
The specific urease activity was calculated as 'urease activity/OD_{600}'

3.7 MICP Treatment Process

The method outlined by Martinez et al. (2013) and Cheng & Cord-Ruwisch (2014), i.e. the two-phase injection method, was employed for the MICP treatment in this study. The method was carried out by injecting a half void volume of BC, followed by injecting a half void volume of CS during the first cycle of treatment. The sample was left to cure for 24 hours to allow the bacteria cells to adhere to the soil particles. After 24 hours, a full void volume of CS was then injected into the sand column. The sample was left to cure for 24 hours to allow for formation and precipitation of the $CaCO_3$ (second injection). After 24 hours, another full void volume of CS was supplied, and the sample was left to cure for 24 hours (third injection). These procedures were repeated several times for each individual sand column in order to produce different levels of cementation. The NH_4^+ content and the bacterial activity were constantly monitored after each treatment using the methods discussed in Section 3.6. Figure 3.10 shows the MICP treatment set-up used in this study.

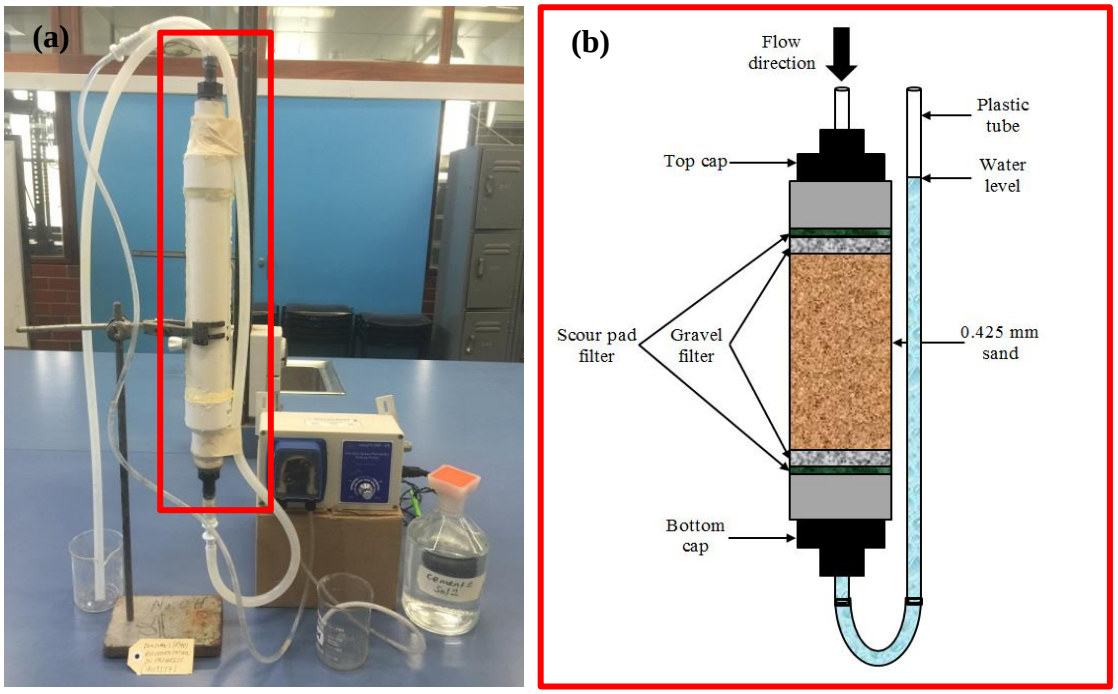

Figure 3.10: MICP treatment set-up: (a) upward flow injection during saturation process; and (b) downward flow injection during MICP treatment

The sand column was fully saturated with water (S = 100%) using the upward flow method [Figure 3.10(a)]. The upward flow method facilitates removal of air voids from inside the soil sample, thus maintaining the fully saturated soil condition. The MICP treatment was then initiated using the two-phase downward flow injection strategy [Figure 3.10(b)]. In order to maintain the full saturation status of the sand column throughout the MICP treatment process, the water head in the free tube attached to the bottom of the sand column was kept at the same level of the top part of the sand column.

3.8 Key Environmental Parameters

Some of the key environmental parameters that may affect the performance of the MICP in real field application were investigated in the current study. This included the initial soil pH, the degree of the surface temperature, the freeze-thaw (FT) cycles and the rainwater flushing.

3.8.1 Initial Soil pH

Harkes et al. (2010) pointed out that the pH of the surrounding environment at which the MICP process occurred can influence the bacteria transport and attachment in the soil matrix. In this study, the sand was flushed with 2 L of 1 M citric acid to achieve the initial soil pH = 3.5 (acidic), 2 L of 1 M sodium hydroxide adjusted to achieve the initial soil pH = 9.5 (basic) whereas, pH = 7 (neutral) acts as a control. The flushed sand samples were then prepared and tested accordingly to the procedures described in Sections 3.11, 3.12 and 3.13 for UCS, $CaCO_3$ content measurement and SEM analysis, respectively.

3.8.2 Surface Temperature

Ng et al. (2012) reported that the urease activity would increase with the increase in temperature from 10°C to 60°C. While, Nemati & Voordouw (2003) showed that an increase in temperature (from 20°C to 50°C) improved both the $CaCO_3$ crystals production rate and the extent of CS conversion in a batch system. However, the effectiveness of $CaCO_3$ crystals formed at different degrees of temperature was not investigated. In the current study, three different temperature scenarios were examined in particular 4°C to simulate the surface temperature in cold regions, 25°C to simulate the surface temperature in tropical regions, and 50°C to simulate the surface temperature in arid regions. Table 3.8 summarises the experimental conditions for this study. The sand samples were prepared and tested accordingly to the procedures outlined in Sections 3.11, 3.12, and 3.13 for UCS, $CaCO_3$ content measurement and SEM analysis, respectively.

Table 3.8: Experimental conditions for surface temperature study

Temperature (°C)	Representation	Condition
4	Cold region	Left for treatment inside 4°C refrigerator
25	Tropical region	Left for treatment at room temperature
50	Arid region	Left for treatment inside 50°C oven

3.8.3 Freeze-Thaw (FT) Cycles

Destruction of porous materials as a result of freezing and thawing becomes a great concern for people living in cold regions. The action of FT cycles could affect the durability of the soil in question due to the loss in the soil mass caused by the repeated actions of freezing and thawing. Therefore, current study examines the effect of FT cycles on three types of soils: (1) fine grained soil (0.15 mm diameter); (2) coarse grained soil (1.18 mm diameter); and (3) well-graded sand (0.053 – 2.36 mm diameter). The properties of the sand used for FT cycles study is presented in Table 3.9.

Table 3.9: Sands used for FT cycles experiment

Property	**Fine Sand (0.15 mm)**	**Coarse Sand (1.18 mm)**	**Well-graded sand**
D_{10} (mm)	0.12	0.54	0.13
D_{30} (mm)	0.13	0.61	0.33
D_{60} (mm)	0.15	0.7	0.81
C_u	1.25	1.29	6.23
C_c	0.94	0.98	1.03
G_s	2.68	2.73	2.75
e_{min}	0.36	0.52	0.35
e_{max}	0.68	0.75	0.65
OMC (%)	17.41	15.54	11.5
γ_{dmax} (kN/m^3)	16.41	14.72	18.5
n (%)	35.91	40.23	30
k (10^{-5} m/s)	4.09±0.2	80.4±4.2	11.8±1.1
USCS classification	SP	SP	SW

OMC stands for optimum moisture content with respect to the standard Proctor test (SPT)
n stands for porosity
k stands for permeability
USCS stands for the unified soil classification system

Each bio-cemented sand column was prepared and tested according to the procedures detailed in Sections 3.11–3.13 followed by exposure to 4 and 10 FT cycles prior to UCS testing. Each FT cycle procedure was subjected to 12 hours freeze at -14°C followed by 12 hours thaw at room temperature (25 ± 1°C). All bio-cemented sand columns were fully immersed in water throughout the FT cycles to ensure full saturation conditions. The effect of FT cycles on the bio-cemented sand columns was evaluated by comparing the UCS values before and after the FT cycles.

3.8.4 Rainwater Flushing

In the current study, tap water with pH ranges from 6.8 to 7.2 was used to simulate the effect of heavy rain with rainfall intensity of 50 mm/hour on the MICP process according to the National Meteorological Library (2015). Sand columns were prepared accordingly to the procedures described in Section 3.7 followed by tap water flushing for approximately 12 hours. To examine the different effects of the rainwater, the tap water was flushed immediately or 24 hours after the bacterial placement while, a sample with no tap water flushing was prepared as a control. After treatment, the samples were prepared and tested accordingly to the procedures highlighted in Sections 3.11 and 3.12 for UCS and $CaCO_3$ content measurement, respectively. The extraction of the bio-cemented specimens from the PVC mould was made with great caution as to avoid the impact of soil disturbance on the bio-cemented specimens.

3.9 $CaCO_3$ Crystals Precipitation Patterns

It was suggested previously by DeJong et al. (2010) that the most desirable $CaCO_3$ crystals distribution within the pore space is the one which is significantly concentrated at the vicinity of the particle-particle contacts. This is due to the selective nature of the bacteria cells, which align themselves in small surface features due to their biological behaviour and the particle filtering processes. DeJong et al. (2010) explained that bacteria cells favour the small space due to reduced shear stresses and a greater availability of nutrients at the particle-particle contacts. A greater concentration of microbes near the particle-particle contacts results in

increased $CaCO_3$ crystals precipitation in the region. Another factor affecting the different $CaCO_3$ crystals precipitation is the bacteria filtering processes that occurred in the soil matrix as a result of the relative size of the suspended $CaCO_3$ crystals and the pore space (Valdes & Santamarina, 2006). As the pore fluid seeps through the soil matrix, the precipitated $CaCO_3$ crystals that were suspended within the pore fluid tend to re-attach near the particle-particle contacts as the pore fluid flows through the surrounding pore throats. This effect is more pronounced as the $CaCO_3$ crystals precipitation increases (the pore throat space decreases). Despite those findings, none of the previous studies ever examined this matter deeper due to the complexity of the BC kinetics inside the soil matrix. However, Cheng et al. (2013) found that precipitation of concentrated $CaCO_3$ crystals in the vicinity of the particle-particle contacts is indeed possible in partially saturated conditions. Moreover, concentration of the $CaCO_3$ crystals at the particle-particle contacts results in the formation of relatively large $CaCO_3$ crystals, which were found to be more effective in terms of strength improvement compared with conventional $CaCO_3$ crystals that are normally characterised by relatively smaller size. It is postulated that three main patterns exist for $CaCO_3$ in association with precipitation patterns: large, small and a mixture of both. Figure 3.11 shows a schematic diagram of these patterns. The different patterns were obtained using the combination of different BC and CS concentrations outlined in Sections 3.5 and 3.6.

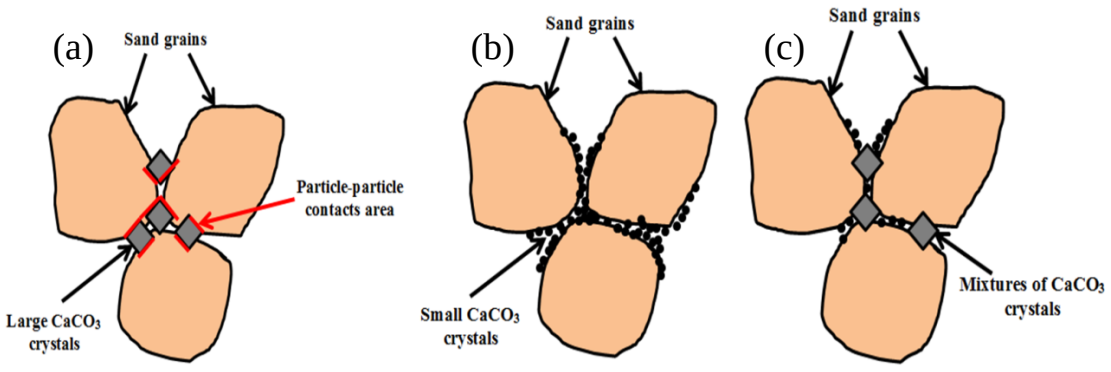

Figure 3.11: Various patterns of $CaCO_3$ morphology and precipitation within the soil matrix: (a) large $CaCO_3$ crystals that increase the particle-particle contact areas; (b) small $CaCO_3$ crystals that surround the sand grains forming a coating layer; and (c) mixture of $CaCO_3$ crystals

3.10 Permeability Test

Permeability testing was conducted for all specimens prepared by the MICP method, as described in Section 3.7. The test was conducted in accordance with the procedures described in the Australian Standards AS 1289.6.7.1 (2001). The bio-cemented specimens were kept inside the original PVC column split mould during the permeability test to avoid disturbance. The permeability value, *k* was measured before and after the MICP treatment to monitor its change due to the bio-cementation. The coefficient of permeability, *k*, was determined using Equation 3.4,

$$k = \frac{QL}{Ath} \qquad \text{Equation 3.4}$$

where; *Q* is the volume of the discharged water, *L* is the length of the specimen, *A* is the cross-sectional area of the specimen, *t* is the discharge time and *h* is the hydraulic head difference.

Two sets of permeability tests were conducted to investigate: (1) the effect of different precipitation patterns; and (2) the effect of using an optimised MICP recipe compared with traditional OPC, as an alternative cementation agent. The bio-cemented specimens covered the range of light, medium and heavy cementation discussed above. The effect of the various precipitation patterns on the hydraulic conductivity is of interest in this study for potential field application. The mixture designs for the OPC treated specimens are covered in Section 3.3.4. The results of the permeability experiments are presented and discussed in Chapter 4.

3.11 UCS Test

UCS tests were performed in this study in accordance with Australian Standards AS 5101.4 (2008). The UCS test was employed in this study as an indicator of the success of the MICP method to impart true cohesion to otherwise uncemented sands.

3.11.1 UCS Samples Preparation

The split mould used in the current study was made of cylindrical PVC of 40 mm diameter and 160 mm height. The height of the column was deliberately made to be 4 times the diameter so that the bio-cemented sample could be cut into two specimens of a height to diameter ratio of 1:2, as required in the UCS test standards. Figure 3.12 shows the sample preparation for UCS testing. Figure 3.12(a) shows the PVC column split mould used in the present study. Prior to sample preparation, the internal wall of the PVC mould was lubricated with silicon grease to minimise the friction between the sand and the mould wall. The split mould was sealed using silicon glue and the two halves were tied using a metal hose clamp. Prior to that, the sand underwent the standard Proctor test to determine the OMC, at which a given soil type will become most dense and achieve its maximum dry density. It was found that the OMC of the sand used for the current study was roughly 12%. The sand was carefully placed using a scoop and was tamped using a steel rod that was specifically designed to fit the diameter of the PVC column, as shown in Figure 3.12(b). The PVC column was filled with 3 equal thickness layers of sand at which, each layer was lightly tamped by the steel rod 20 times to produce specimens with consistent and uniform densities. The top surface was levelled and trimmed using a straight edge, as shown in Figure 3.12(c). Finally, the top part of the PVC column was sealed, and the specimen was treated using the MICP process, as described in Section 3.7. Figure 3.12(d) shows the extracted bio-cemented specimen ready for the UCS test.

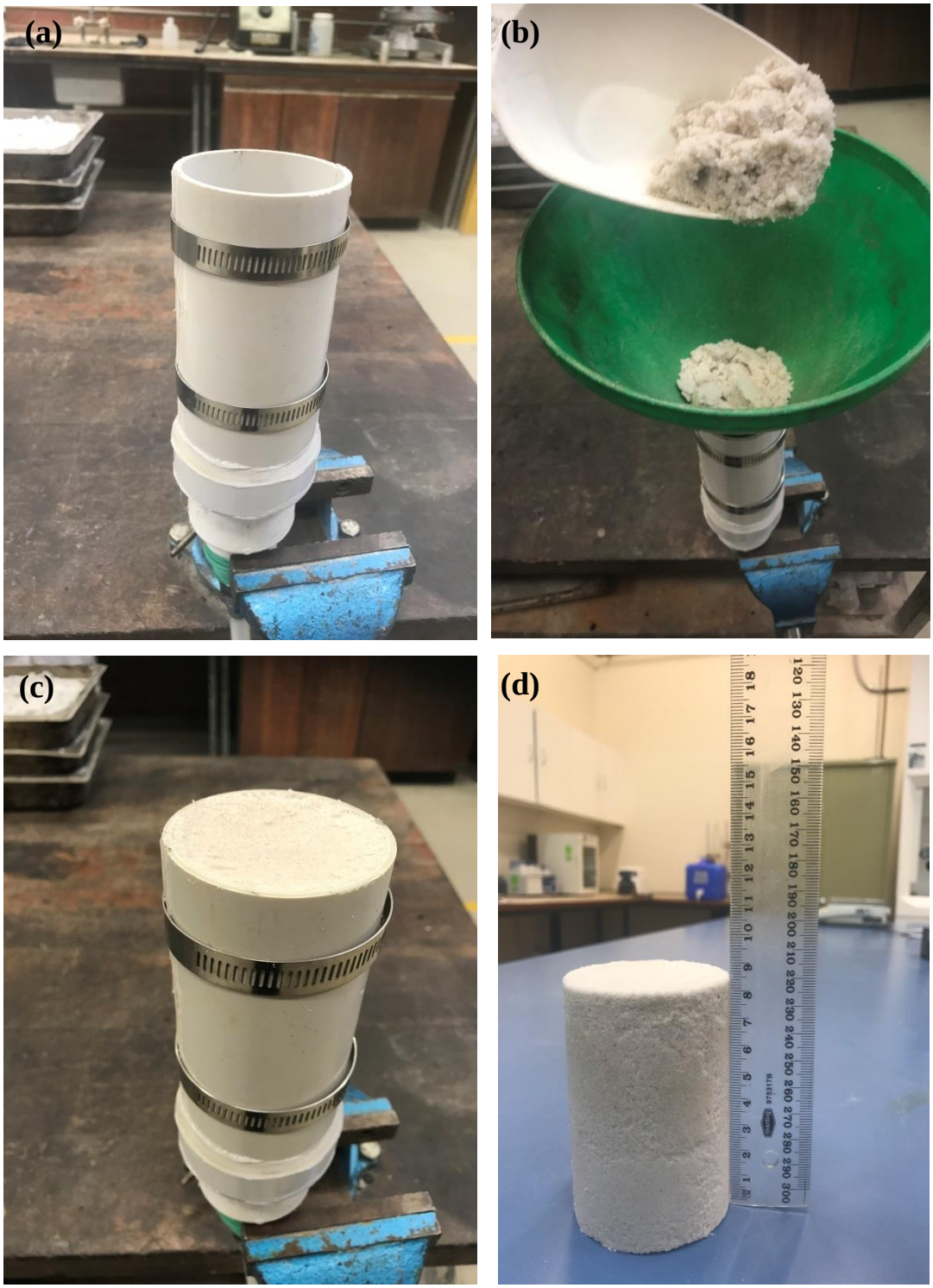

Figure 3.12: UCS sample preparation: (a) PVC column split mould; (b) addition of sand into the PVC column; (c) levelling of the tampered sand; and (d) extracted specimen ready for UCS test

3.11.2 UCS Testing Procedures

After extracting the bio-cemented specimens from the split mould, it was rinsed with 1 L of tap water to remove the excess salts from the surface. Immediately after that, the specimens were placed into the UCS apparatus. The UCS machine is completely automated and it was programmed to apply a constant rate of displacement of 1 mm/min, and the displacement was measured using a linear variable displacement transducers (LVDT) mounted on the platen. The axial load was applied at a constant rate of strain. The tests termination procedures were carried out either when the specimens failed at which, failure planes were clearly visible (noted by the sudden dropped in q_u after peak) or when the axial strain reached 20%, whichever comes first. Two distinct failure modes were generally observed after UCS testing, as shown in Figure 3.13. Failure with tension cracks (single crack) and local failure (multi cracks either at the top or bottom part of the bio-cemented specimen).

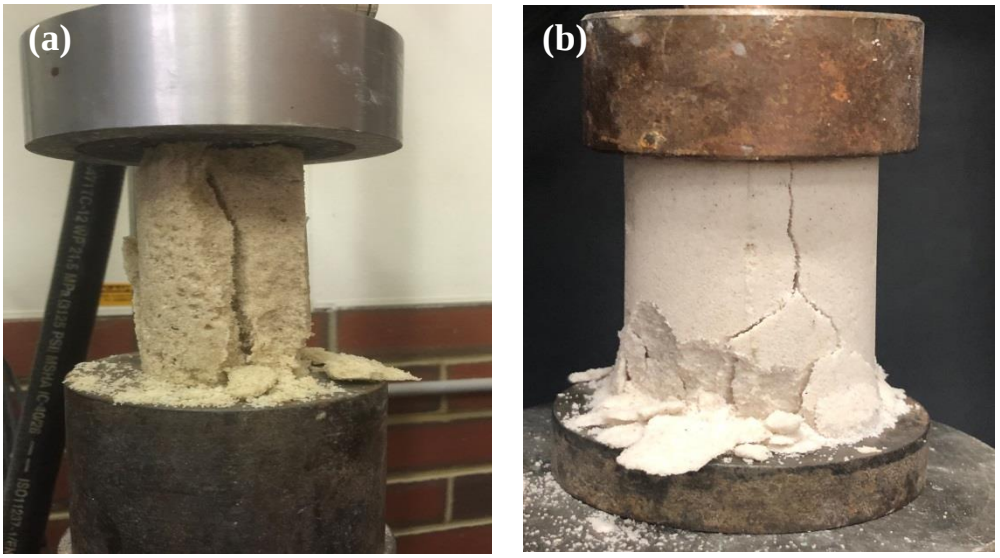

Figure 3.13: Typical failure modes of the bio-cemented specimens: (a) tension crack (single crack); and (b) local failure (multi cracks)

3.12 $CaCO_3$ Content Measurement

After UCS testing, the failed sample was collected, sealed and labelled inside a transparent plastic bag prior to measuring the $CaCO_3$ content. This was performed by mixing 2 ml of 2 M hydrochloric acid (HCl) to 0.5–2 g of the crushed specimen. In order to maintain the accuracy of the measurement, the $CaCO_3$ samples were taken at 3 different spots (top, middle and bottom), as shown in Figure 3.14. The $CaCO_3$ was calculated as the average of these 3 values.

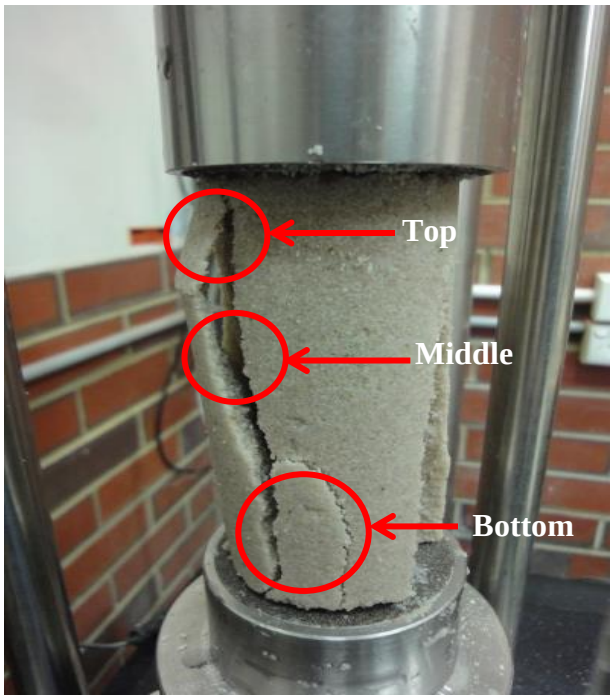

Figure 3.14: Sampling for measurement of the $CaCO_3$ content after UCS testing

The reaction between HCl and $CaCO_3$ within the crushed specimen produces carbon dioxide (CO_2). Whiffin et al. (2007) showed that the CO_2 gas emitted from this reaction can be captured using the U-tube manometer under standard conditions (25°C, 101.325 kPa atm), as shown in Figure 3.15. The actual amount of the $CaCO_3$ content was calculated based on the standard curve of the analytical grade $CaCO_3$ powder versus CO_2 gas production from the dissolution of $CaCO_3$ sample, as displayed in Figure 3.16.

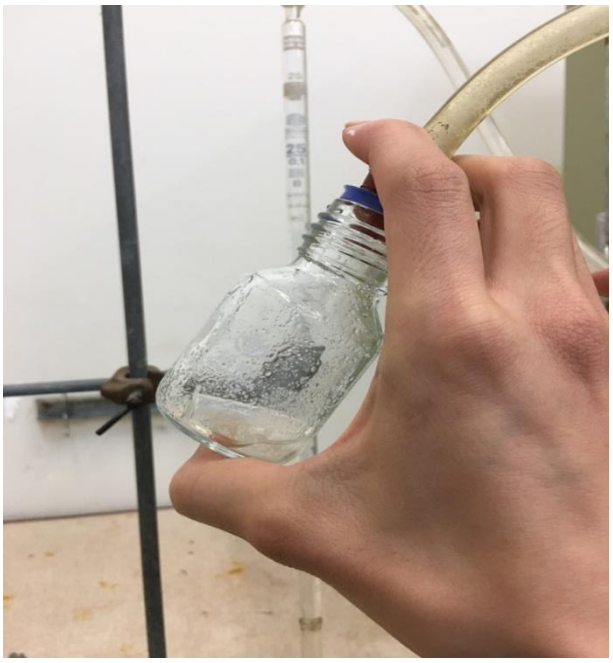

Figure 3.15: Capturing CO_2 gas using the U-tube manometer set-up

"Publication has been removed due to copyright restrictions"

Figure 3.16: Standard curve of the analytical grade $CaCO_3$ powder vs. CO_2 gas production for $CaCO_3$ content measurement (after Cheng, 2012)

Based on Figure 3.16, the correlation between the analytical grade $CaCO_3$ powder and the CO_2 gas production may be expressed by Equation 3.5 with correlation strength, $R^2 = 0.9993$.

$$CaCO_3\ content\ (g) = 0.0044 CO_2\ gas\ produced\ (mL) \quad \text{Equation 3.5}$$

3.13 Microstructural Study

Despite the large number of studies showing the bond mechanism associated with the $CaCO_3$ crystals in the bio-cemented sands, a detailed microstructural study is still needed involving the examination of: (1) the morphological structure of the $CaCO_3$ crystals; and (2) the evolution process associated with $CaCO_3$ crystals. The first morphological study will differentiate between the two most critically acclaimed $CaCO_3$ polymorphs that bind soil particles (i.e. calcite or vaterite), and the evolution study will show the transformation of the primary and secondary $CaCO_3$ crystals and the associated bonding mechanism to the soil particles. These are covered herein and the outcome will be used to identify the most effective $CaCO_3$ crystals for further mechanical testing. A variable pressure field emission scanning electron microscope (VP-FESEM) capable of analysing high resolution images with secondary electrons (SE) or/and backscattered electrons (BSE) was used at Curtin University.

Pieces of the crushed bio-cemented samples from the UCS test were rinsed with tap water to remove all soluble salts and oven-dried at 105°C temperature for 24 hours to remove the moisture. Then, the specimens were desiccated for 30 minutes inside a high-pressured vacuum to ensure they are completely dry and uncontaminated. Contamination in the form of oil can induce specimen charging inside the electron chamber leading to SEM images distortion. The tested specimens were placed on designated stubs and platinum coating was applied. This step improves the conductivity of the specimen to produce better SEM imaging quality. A conductive, double coated carbon tape was used as adhesive to mount the specimens onto the stubs. The stubs were then screwed into the steel mount and placed inside the electron chamber for imaging.

3.14 Triaxial Tests

Triaxial tests were performed in this study in accordance with Australian Standards AS 1289.6.4.2 (1998). The aim of the triaxial testing was to investigate the effect of different confining pressures of 100, 200, and 400 kPa and loading paths on the geotechnical response of the bio-cemented specimens.

3.14.1 Triaxial Samples Preparation

The triaxial samples were prepared in accordance to the procedures explained in Section 3.11.1. For triaxial testing, the sample was placed in a rubber membrane lining the PVC mould, to ease the removal of the bio-cemented specimen from the mould to the triaxial pedestal. After the sand was fully cemented under the effective $CaCO_3$ crystals, it was then removed from the PVC split mould and rinsed with tap water to remove any excess salt. The aspect ratio of the height to diameter was 1:2 for all samples. A total number of 6 specimens were prepared for each triaxial test. Figure 3.17 shows the typical triaxial test set-up used in the current study.

Figure 3.17: Triaxial test set-up used in the current study

3.14.2 Triaxial Testing Procedures

Conventional triaxial testing procedures were adopted using the 3 main stages of saturation, consolidation and shearing. The saturation phase ensures that all voids within the test specimen are filled with water. In this study, this was achieved by increasing the back pressure to force air into solution. During the saturation phase, the back pressure and cell pressure were increased simultaneously at the rate of 10 kPa/min, until the back pressure reached 300 kPa. All samples were saturated by maintaining a constant effective pressure recorded negligible change and the Skempton's B > 0.96. The B-value check was conducted by increasing the cell pressure by 10 kPa ($\Delta\sigma_3$) in undrained condition and the increase in pore pressure (Δu) was monitored. The B-value was calculated by calculating the ratio between $\Delta u/\Delta\sigma_3$. All the tested samples were having B-values of at least 0.98, signifying that the saturation phase was sufficiently achieved.

The consolidation stage is used to bring the specimen to the effective stress state required for shearing. Typically, the specimen was isotropically consolidated by increasing the cell pressure whilst maintaining a constant back pressure. This process was continued until the volume change, ΔV, of the specimen was no longer significant, and at least 95% of the excess pore pressure has dissipated. At the end of the consolidation phase, the sample was sheared undrained according to their designated loading paths, i.e. axial compression or constant-p. The excess pore pressures were recorded to calculate the effective stresses within the sample. The shearing rate for all the CU tests was kept at 0.016 mm/min (1%/hour) for all samples. However, for the constant-p test, the undrained tests were conducted under stress-controlled condition and the shear stress rates were set at +5 kPa/min (+300 kPa/hour) for the deviator stress, and -1.67 kPa/min (-100 kPa/hour) for the radial stress respectively. The stress-controlled condition in the constant-p test was performed in order to determine the effect of pore water pressure (liquefaction) to the bio-cemented sand at which, the constant total mean stress values of σ_c = 100, 200 and 400 kPa were maintained. The test was terminated when: (1) a pronounced shear plane was observed: or (2) the axial strain reached 20%, whichever occurred first.

3.15 Summary

In this chapter, details of the materials and the testing procedures for preparing, treating and testing the bio-cemented soil specimens were presented. The method of injection was implemented for the supply of both the BC and CS into the compacted soil column. Unlike previous treatment reported in the literature where the bio-cemented column was subjected to 24 hours of 104°C heat to remove the excess pore water prior to UCS testing, the current study skipped this step and immediately tested the treated bio-cemented column after removal from the split mould to mimic real field conditions. Relevant mechanical tests (UCS and triaxial) and microstructural analysis (SEM) were also outlined following the available standards. UCS tests were performed to determine the most optimum BC and CS concentrations producing the effective $CaCO_3$ crystal under a wide range of cementation level: light, medium and heavy. Triaxial tests (considering two stress paths, i.e. axial compression and the constant-*p*) were conducted to examine the behaviour of the bio-cemented specimen under these loading paths.

In the following chapter, the results from the study of crystal precipitation patterns in terms of the most applicable key environmental parameters for field application and the most effective $CaCO_3$ crystal precipitation were presented. The efficacy of the effective $CaCO_3$ crystal was determined using the SEM examination which focussed on their evolution and specific microstructural features. Understanding of the specific $CaCO_3$ crystals microstructure is imperative to suit their intended purpose for field application.

Chapter 4
Calcite Crystals Precipitation Patterns

4.1 Introduction

Limited research has been reported on the strength improvement of bio-cemented soils in relation to their calcite crystals precipitation patterns. To fill this gap, various sand samples were prepared in this study under the co-effect of different bacteria culture (BC) and cementation solution (CS) concentrations, to evaluate the optimum BC (u/mL) and CS (M) combination that yields the highest soil strength. Prior to that, some key environmental parameters were investigated to ensure the feasibility of MICP for field application. This work has formed the basis of the published article: Liang Cheng, Mohamed A. Shahin, and Donovan Mujah (2017) 'Influence of Key Environmental Conditions on Microbially Induced Cementation for Soil Stabilization' *Journal of Geotechnical and Geoenvironmental Engineering* 143(1) doi: 10.1061/(ASCE)GT.1943-5606.0001586 (authorship attributions in Appendix B) and refereed conference proceedings Donovan Mujah, Mohamed Shahin, and Liang Cheng (2016) 'Performance of Biocemented Sand Under Various Environmental Conditions' In Proceedings of XVIII Brazilian Conference on Soil Mechanics and Geotechnical Engineering, COBRAMSEG ISSN: 2595-0843, 19-22 October 2016, Belo Horizonte, Brazil doi: 10.20906/CPS/GJ-05-0002 (authorship attributions in Appendix E).

The bio-cemented specimens were examined in terms of their strength, stiffness and permeability. It is postulated that the effectively precipitated $CaCO_3$ crystals are characterised with their rhombohedral shape and large crystals size and were concentrated at the soil pore throats. On the other hand, the normal $CaCO_3$ crystals are characterised with their circular shaped, relatively smaller crystals size and were deposited on the individual sand grain surface. In order to determine the most optimum combination to produce the most effective $CaCO_3$ precipitation, the following were assumed:

- The combination that provided the highest UCS value is the most effective.
- The combination that provided the highest permeability value is the most effective.
- Only reagents that were able to sustain at least 50% chemical conversion efficiency (CCE) (i.e. urea to ammonia conversion) are considered effective.
- One full injection of CS (M) is equivalent to 24 hours reaction time.

Furthermore, the evolution and the specific microstructural features of the $CaCO_3$ crystals growth were presented via results obtained from SEM analysis. The ability to produce an effective CCPP that meets the specific need of a field application is extremely useful to design a treatment strategy that can provide successful improvement solution to the soil in question. In addition, the optimised CCPP (i.e. the bio-cemented specimen treated with the effective $CaCO_3$ crystals precipitation) was then compared with the conventional OPC treated soil in terms of their strength improvement and permeability retention. Some work presented in this chapter has formed the basis of the published article: Donovan Mujah, Liang Cheng, and Mohamed A. Shahin (2019). Microstructural and geo-mechanical study on bio-cemented sand for optimization of MICP process. *Journal of Materials in Civil Engineering*, 31(4) doi: 10.1061/(ASCE)MT.1943-5533.0002660 (authorship attributions in Appendix C).

4.2 Key Environmental Parameters

4.2.1 Initial Soil pH

Most of previous studies performed on the MICP method were conducted in basic condition where pH = 9.25, because the resulting $CaCO_3$ favours basic condition (explained in detail in Section 2.8.4). However, the natural soil environment is not necessarily basic. To understand the implications of pH values different from 9.25, the effect of initial soil values of pH = 3.5 (acidic), pH= 7 (neutral) and pH = 9.5 (extra basic) were investigated in terms of the geotechnical response of the cemented sand resulting from the treatment. The UCS values of all bio-cemented samples are shown in Figure 4.1.

"Publication has been removed due to copyright restrictions"

Figure 4.1: Strength improvement of bio-cemented sand under various soil pH conditions (after Mujah et al. 2016)

Based on Figure 4.1, the initial neutral soil condition provides the highest UCS value (325 kPa) at a $CaCO_3$ content of 0.025 g/g or equivalent to 2.5%. The next best UCS value resulted from the basic soil condition (170 kPa) at $CaCO_3$ content of 0.013 g/g or 1.3%. The initial acidic soil condition recorded the lowest UCS value (80 kPa) at a $CaCO_3$ content of only 0.005 g/g or 0.5%. It was also observed that, regardless of the initial soil pH value, the final soil pH value after MICP treatment ranged between 7.5 and 9.5 for all treated soil samples. The results obtained from Figure 4.1 suggest that the MICP method successfully produces $CaCO_3$ under basic, acidic and neutral conditions, but favours the basic condition. The ability of the process to produce $CaCO_3$ in non-basic or neutral conditions can be explained by the fact that the alkalinity of the surrounding environment in the bacteria cells progressively increases due to the process of urea hydrolysis during the MICP process (Rebata-Landa, 2007). This means that as long as the final pH environment is between 7.5 and 9.3, $CaCO_3$ would still form (Ferris et al., 2004).

Apparently, when the $CaCO_3$ content was low (< 3%), the strength improvement was governed mainly by the homogeneity of the $CaCO_3$ distribution along the column, as shown in Figure 4.2. The distribution shown on the figure was made by the $CaCO_3$ crystals precipitation. The $CaCO_3$ precipitation distribution is mostly homogeneous in the neutral pH condition compared with the acidic and basic pH conditions. This could be possibly explained by the tendency of the bacteria attachment (on soil particles) to increase in ionic environment, as suggested by Harkes et al. (2010). The ionic environment in both the acidic and basic pH conditions was triggered by the presence of the NH_4^+ (acidic) and OH^- (basic) ions (Duan & Zhu, 2012; Hammad & Zoheir, 2013). Progressive formation of ionic environment encourages more bacteria to attach themselves to the soil particles, leading to concentrated accumulation of the bacteria in the top part of the bio-cemented column. Upon adding more supply of CS, these bacteria cells fuse together through the MICP reaction to form $CaCO_3$ crystals. The formation of the concentrated $CaCO_3$ crystals on the top part of the bio-cemented column limits the transport of subsequent bacteria to be mobilised deeper into the column, resulting in a non-homogenous $CaCO_3$ distribution.

"Publication has been removed due to copyright restrictions"

Figure 4.2: $CaCO_3$ precipitation distribution in different soil pH (after Mujah et al. 2016)

The actual distribution of the formed $CaCO_3$ affects the overall strength of the bio-cemented column. The effect of the homogeneity of the resulting cemented column in terms of $CaCO_3$ distribution (see Figure 4.2) may explain the reason behind the significant difference in bio-cemented soil strength between the neutral and basic conditions despite the difference in the formed $CaCO_3$ contents (2.5% and 1.3 %, respectively). It should be noted that the homogeneous distribution (in the case of the neutral pH condition) of the $CaCO_3$ precipitation increased the global UCS of the bio-cemented soil column. This is evidenced by the tensile crack failure of the bio-cemented sample, indicating that the shearing force was equally distributed along the shear plane [refer to Figure 3.13(a)]. Whereas, the bio-cemented columns in the acidic and basic conditions failed at the bottom part of the column, indicating a local failure as a result of the non-homogeneous $CaCO_3$ precipitation [refer to Figure 3.13(b)].

4.2.2 Surface Temperature

The initial surface temperature of soil treated by the MICP method plays a vital role in ensuring successful cementation. This is particularly important in field application because soils have different temperatures based on their location. For example, the temperature is invariably high on the Equator compared with other cold regions where the temperature can be extremely low. Prior to application of the MICP in these extreme surface temperature conditions, investigation into the performance of the MICP method in these temperatures is crucial.

To achieve the different extreme temperature conditions used in the current study, MICP treatment was conducted in: (1) inside a 4°C refrigerator; (2) room temperature at 25°C; and (3) inside a 50°C oven. These temperature degrees were selected to simulate cold regions (4°C), tropical regions (25°C) and arid regions (50°C). The coldest temperature of 4°C was selected, as the bacteria become inactive below it; the hottest temperature of 50°C was selected, because it is the limiting temperature for the bacteria survival. Above 50°C and below 4°C, the bacteria could either be respectively dead or inactive, rendering the MICP treatment process unfeasible (Rebata-Landa & Santamarina, 2006). Applicability of the MICP as a cementation treatment process is limited to the situations where the temperature range of (4°C- 50°C) is maintained. Performance of the MICP treated samples at these two extreme temperature conditions was assessed by performing some UCS tests, and the results are presented in Figure 4.3.

"Publication has been removed due to copyright restrictions"

Figure 4.3: Effect of soil surface temperature on the strength improvement of bio-cemented sands (after Cheng et al. 2017)

It can be seen from Figure 4.3 that the trend of increasing the strength exponentially with the $CaCO_3$ content is consistent for all tested temperatures. However, it is interesting to note that the strength improvement was higher at 25°C compared to the same $CaCO_3$ amount produced. It can be therefore argued that the $CaCO_3$ crystals formed at the highest temperature of 50°C were the least efficient in imparting the bio-cemented soil cohesive strength. In order to verify this argument, a microstructural study was warranted. This was accomplished by preparing SEM specimens from samples having the same $CaCO_3$ content that was produced at different temperatures. The microstructural images are presented in Figure 4.4.

Figure 4.4: SEM images of the bio-cemented sands treated at different surface temperatures: (a) and (b) 4°C, UCS = 200 kPa, and $CaCO_3$ content = 0.029 g/g sand; (c) and (d) 25°C, UCS = 250 kPa, and $CaCO_3$ content = 0.028 g/g sand; and (e) and (f) 50°C, UCS = 100 kPa, and $CaCO_3$ content = 0.03 g/g sand (after Cheng et al. 2017)

The crystals microstructural analysis indicates that MICP treatment at 50°C resulted in distributing the $CaCO_3$ crystals over the entire sand grain surface, with a typical individual crystal size of 2 and 5μm [Figure 4.4(e–f)]. The individual $CaCO_3$ crystals of this surface temperature of 50°C were of similar size; they distributed themselves spatially and coated the surface of the sand grains. However, analysis of the microscopic image shows that the sand grains were not effectively connected within the remaining large voids [Figure 4.4(e–f)]. For the samples treated at ambient temperature, the average size of the $CaCO_3$ crystals size increased by 10 times (individual $CaCO_3$ crystal size between 20 and 50μm), compared with those formed at 50°C. These large crystals precipitated on the grain surface, covering the contact areas of the sand grains [Figure 4.4(c–d)]. This pattern of distribution was also found in the samples treated at 4°C, whose crystal was also smaller in size [Figure 4.4(a–b)].

The kinetics of crystallisation indicates that both the activated energy (which is a function of temperature and relative supersaturation degree) has a strong impact on the rate of nucleation and crystal growth. It is the relationship between the competing kinetic rates of nucleation (birth of new crystal nuclei) and crystal growth (i.e. crystal size) that determines the distribution of crystals. Wojtowicz (1998) suggested that the higher the temperature, the lower the activation energy barrier as well as the faster the rate of nucleation of $CaCO_3$ precipitation. The faster nucleation rate may induce excess nucleation sites, which results in smaller crystal size, as found in the samples treated at 50°C. Although the nucleation rate was low at the low temperature of 4°C, the formed crystals also had a small size. This is possibly due to the slow crystal growth at low temperature due to the low relative supersaturation degree, which results from the low urease activity at low temperature (Sahrawat, 1984). It is believed that the decrease in the relative supersaturation led to a decrease in both the crystal nucleation rate and growth rate. As stated previously, the final crystal size distribution is dependent on the competition between these two rates. The formation of $CaCO_3$ in MICP is a very complex process, because of the role of the bacteria as nucleation sites and CO_3^{2-} ions as a producer. Therefore, if a different number of bacteria is supplied, the precipitation pattern can be different from what is obtained in the current study.

Generally, the temperature can affect many physical, chemical, and biological properties of the MICP system. For example, the temperature can affect the urease activity, which in turn influences the urea hydrolysis rate, CO_3^{2-} production rate and the resulting crystal growth rate. The solubility of $CaCO_3$ crystals also varies with the temperature. Overall, based on the temperature study performed here, it could be concluded that large-size crystals precipitated in the voids among the sand grains are more effective in producing the highest strength improvement of the bio-cemented sand.

4.2.3 Freeze-Thaw Cycles

Freeze-thaw cycles pose significant challenge to engineers living in regions having extreme topoclimatic positions, especially on sites involving formation of permafrost (Kellerer-Pirklbauer, 2017). The action of FT cycles can lead to rock weathering over a long period of time. FT cycles can also affect the performance of soil durability (short-term or long-term endurance of soil exposed to stresses). Therefore, it is important to consider the effect of FT cycles on bio-cemented sands prior to real field application. To this end, two uniform sands of 0.15 mm (fine sand) and 1.18 mm (coarse sand) as well as well-graded sand were tested after being treated with MICP. Each bio-cemented column of the two sands was prepared according to the procedures described in Section 3.11.

The UCS results of the tested samples are shown in Figure 4.5. It can be observed that an increase in the number of FT cycles is associated with a decrease in the compressive strength for all sand specimens [Figure 4.5(a) and (b)]. The main reason for the strength decreases after the FT cycles is formation and growth of micro cracks resulting from the ice forming during the freezing process, which induces micro cracks due to volume change of the ice crystals. In theory, higher porosity and permeability values allow more rapid water mass transfer in the sand matrix, which can increase the FT resistance. Lake et al. (2017) found that porous solids with high porosity or permeability usually have a good FT cycles resistance.

"Publication has been removed due to copyright restrictions"

"Publication has been removed due to copyright restrictions"

Figure 4.5: Effect of FT cycles on different sands: (a) fine sand (0.15 mm); (b) coarse sand (1.18 mm); and (c) well-graded sand (after Cheng et al. 2017)

The results presented in Figure 4.5 suggest that the fine sand (0.15 mm in size - smaller pore size and slightly less porosity) was more durable against the FT cycles than the coarse sand (1.18 mm in size- larger pore size and slightly higher porosity). This could be explained by the increase in the average number of contacts per soil particle (i.e. the coordination number) in the case of the fine sand due to the smaller inter-particular contact in the soil matrix as $CaCO_3$ crystals begin to precipitate. Assadi-Langroudi et al. (2018) found that the average number of contacts per sphere increases with the decrease in porosity. Therefore, the larger number of inter-particle contacts in the case of the fine sand helped the calcite crystals to bridge over the contact points, which increased the tensile resistance during the stress test caused during the durability experiment.

Figure 4.5(c) shows that the FT cycles have a minor impact on the well-graded sand. The main reason for the high durability of MICP well-graded sand is due to the unique characteristics of its soil particles which possess both fine soil particles (allowing a high number of inter-particle contact points) and coarse soil particles (ensuring high permeability due to the presence of the large pore size). Overall, it can be concluded that the influence of FT cycles on soil strength and durability depends on the soil porosity, pore size and bonding behaviour of MICP in the soil matrix.

Soils at high elevation normally freeze during winter. As such, geotechnical foundations that are exposed to FT cycles are prone to be subjected to significant structural damages. This is because FT cycles induce uneven stresses within the soil, resulting in a decrease in soil durability. As shown by the current study, UCS values of the bio-cemented soil samples were improved indicating the viability of MICP as a potential solution to minimise the impact of FT cycles. This is achieved by creating cemented soil bodies that have high durability against FT cycles which is attributed to the sufficient contact points in the soil matrix and the large pore size that ensure high permeability of the bio-cemented soil. These characteristics enhance the efficacy of MICP cementing agent in bridging the inter-particle contacts, and at the same time, allow a rapid water mass transfer within the soil matrix.

4.2.4 Rainwater Flushing

The effect of rainwater flushing on MICP treatment in the field is an important aspect, especially in the tropical region where the intensity of rainfall can become quite severe. Hence, it was deemed vital to study this effect in the laboratory prior to future field implementation. Tap water with pH ranging from 6.8–7.2 was used in the present study to simulate the effect of rainfall. In order to investigate the effect of extreme rainfall intensity on the MICP process, sand sample was subjected to a tap water stream for approximately 12 hours. Three sand samples were prepared at which: (1) the tap water flushing was commenced immediately after the bacterial placement; (2) the tap water flushing was commenced 24 hours after the bacterial placement; and (3) no tap water flushing was used (for control).

The effect of the rainwater flushing on the MICP process is shown in Figure 4.6. The figure shows that the control sample (i.e. no water flushing) was fully cemented [Figure 4.6(a)]. In contrast, the samples that encountered water flushing during the treatment process was partly cemented or completely non-cemented [Figure 4.6(b) and (c)]. For the control sample, the chemical conversion efficiency (CCE), which is defined as the percentage of injected $CO(NH_2)_2$ and $CaCl_2$ that precipitates as $CaCO_3$, was found to reduce from approximately 95% to only 5% throughout the MICP process [Figure 4.7(a)]. The decrease in the CCE may be explained by the loss of urease activity due to flushing. The water flushing caused the significant decrease in the CCE irrespective of the waiting period applied to the bacterial attachment. The negative impact of water flushing on bio-cementation was also demonstrated by the low degree of cementation and final $CaCO_3$ content measurements. Less than 0.3% (0.003 g/g sand) of $CaCO_3$ crystal was detected in the samples subjected to water flushing, whereas 10 times more (0.043 g/g sand) $CaCO_3$ crystals were found in the control sample with a measured UCS value of 262 kPa [Figure 4.7(b)].

Figure 4.6: Bio-cemented samples subjected to tap water flushing: (a) control sample with no tap water flushing; (b) sample with tap water flushing after 24 hours of bacteria placement; and (c) sample with tap water flushing immediately after bacteria placement (after Cheng et al. 2017)

Figure 4.7: Bio-cemented samples subjected to tap water flushing: (a) CCE; and (b) UCS and $CaCO_3$ content (after Cheng et al. 2017)

For successful bio-cementation, it is necessary that the bacteria are introduced into the soil first and kept without disturbance, followed by application of CS that contains $CO(NH_2)_2$ and $CaCl_2$. Torkzaban et al. (2008) demonstrated that the increase in the BS salinity increases bacteria adsorption onto the soil particles. By flushing low-salinity solutions after BC injection, a large part of the adsorbed bacteria could be remobilised from the solid surface into the liquid phase (Harkes et al., 2010). This suggests that, in real applications, rainwater flushing during MICP bio-cementation could reduce the effectiveness of MICP treatment by washing out the bacterial cells and reducing the CCE.

4.3 BC and CS Concentrations Optimisation

4.3.1 UCS Tests

A total number of 108 UCS specimens comprising from a broad range of cementation levels were tested. For the purpose of this study, the cementation levels were categorized based on the $CaCO_3$ content e.g. lightly cemented (2–4% $CaCO_3$ content), medium cemented (4–6% $CaCO_3$ content), and heavily cemented (> 6% $CaCO_3$ content). Figure 4.8 shows the results of the UCS tests, which indicates that the strength increases exponentially as the amount of $CaCO_3$ content increases as can be seen in Figure 4.8(a-c). Note that the specimens with < 2% $CaCO_3$ content was not reported here, as attempts to test them were unsuccessful as the specimens tended to deform locally registering negligible strength values; some specimens even collapsed immediately after being assembled in the testing machine. It is noted from Figure 4.8(a) that 32 U/mL BC provided the highest strength improvement at any $CaCO_3$ content compared to 16 and 8 U/mL BC when combined with 0.25 M CS. However, this trend is reversed in Figure 4.8(c), 8 U/mL BC provided the highest strength improvement at any $CaCO_3$ content compared to 16 and 32 U/mL BC when combined with 1 M CS. Plausible explanation of the reasons behind the different strength improvement efficiency of each combination is presented later.

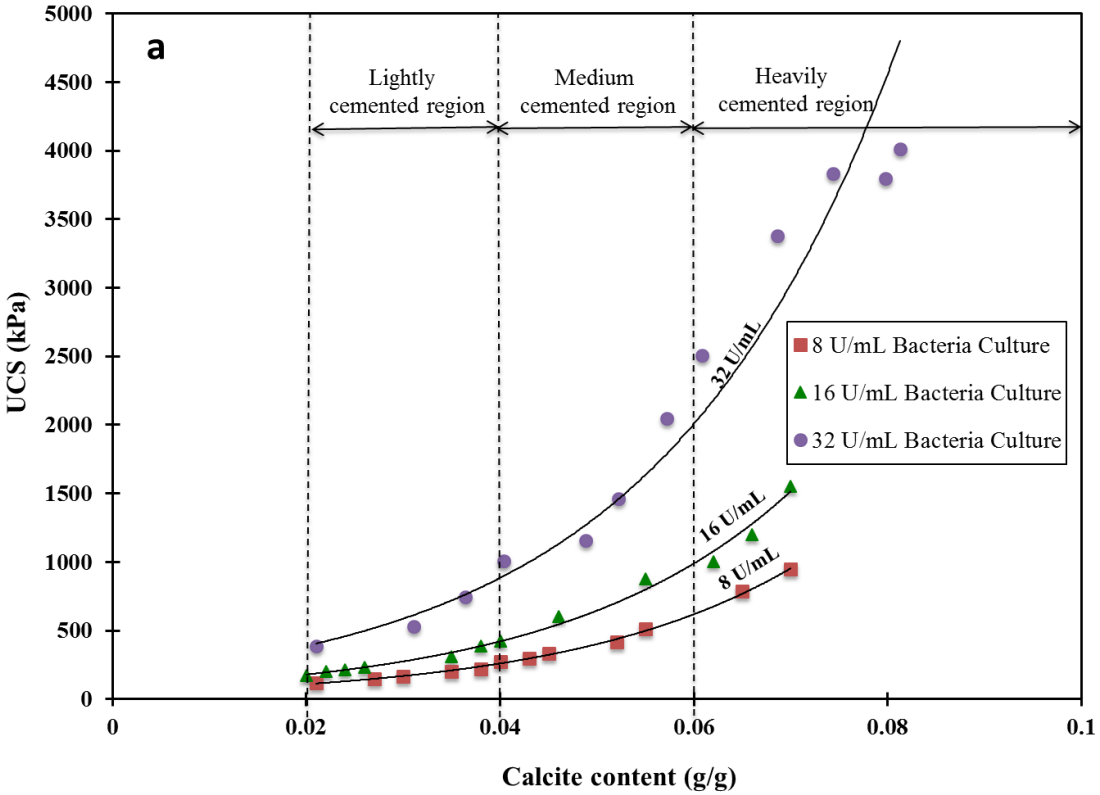
a
Lightly cemented region
Medium cemented region
Heavily cemented region
UCS (kPa)
Calcite content (g/g)
8 U/mL Bacteria Culture
16 U/mL Bacteria Culture
32 U/mL Bacteria Culture
32 U/mL
16 U/mL
8 U/mL
0
500
1000
1500
2000
2500
3000
3500
4000
4500
5000
0.02
0.04
0.06
0.08
0.1

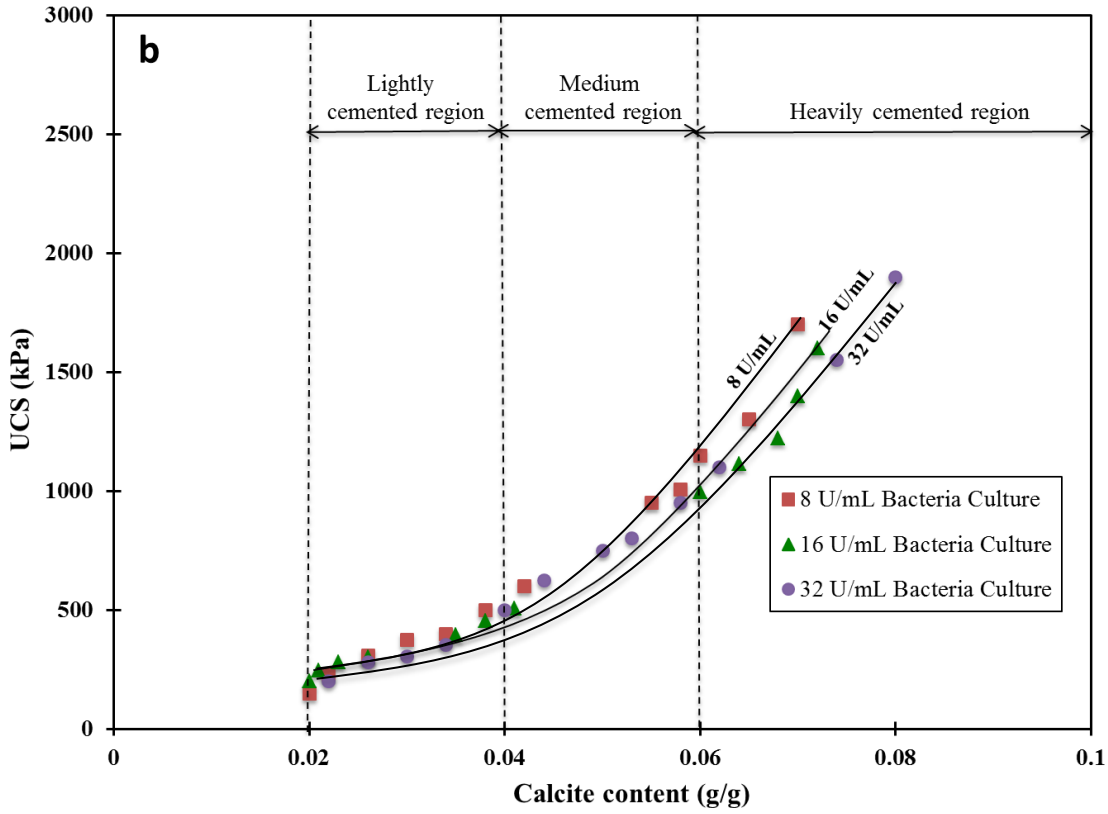
b
Lightly cemented region
Medium cemented region
Heavily cemented region
UCS (kPa)
Calcite content (g/g)
8 U/mL Bacteria Culture
16 U/mL Bacteria Culture
32 U/mL Bacteria Culture
8 U/mL
16 U/mL
32 U/mL
0
500
1000
1500
2000
2500
3000
0.02
0.04
0.06
0.08
0.1

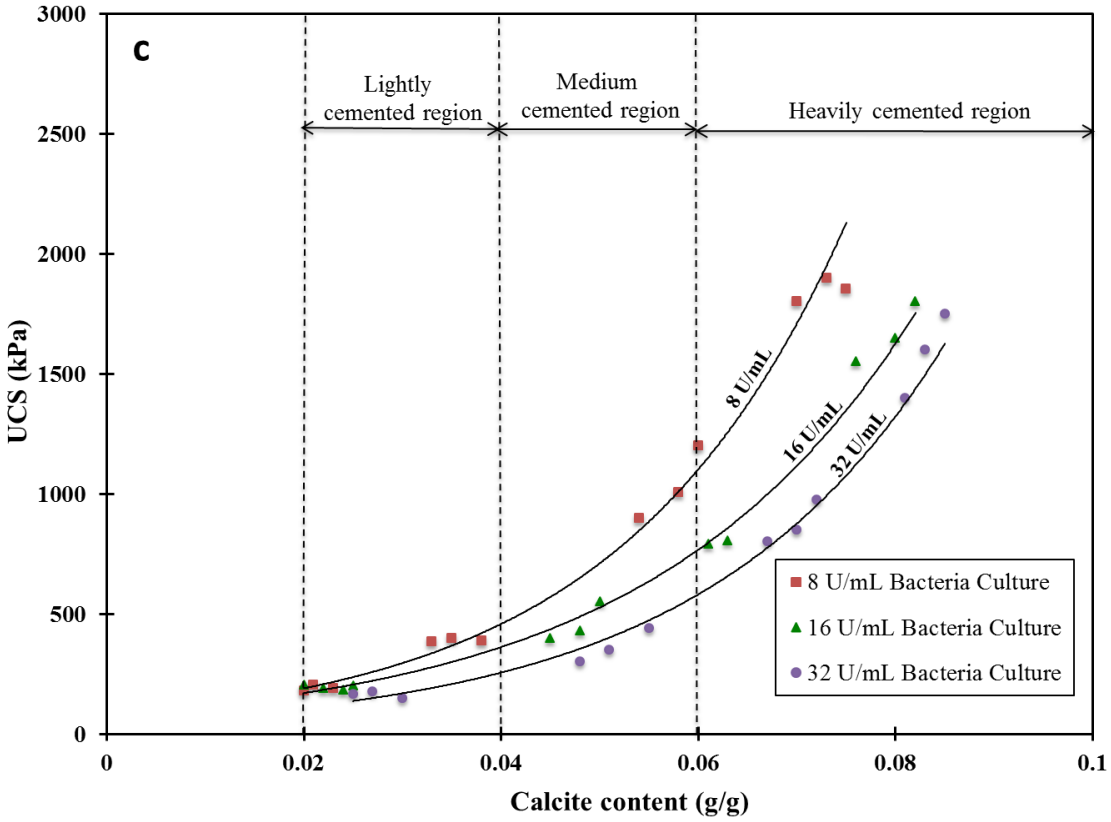

Figure 4.8: The effect of different BC (u/mL) and CS concentrations on UCS: (a) 0.25 M CS; (b) 0.5 M CS; and (c) 1 M CS

Figure 4.9 shows a comparison of all combinations of BC and CS concentrations. The strength response of bio-cemented specimens differs for different CS concentrations without a unique trend. For example, at lower CS concentration (i.e. 0.25 M), the specimens treated with higher BC concentrations were more effective in terms of the strength improvement per amount of calcite formed. However, the increase in strength in the case of CS = 0.5 M concentration was almost insensitive to the BC concentrations. In contrast to the tow trends above, at a higher CS concentration of 1 M, the specimens treated with lowest BC concentrations registered the highest strength. The lowest strength was registered for the combination of BC = 32 U/mL and CS = 1 M. Based on the UCS results, it is suggested that the combination of 32 U/mL BC and 0.25 M CS concentrations is the most effective in terms of the strength improvement.

Figure 4.9: Effect of different BC concentrations on the strength of bio-cemented specimens at various CS concentrations (after Mujah et al. 2019)

The microstructure of the specimens that exhibited the highest strength (BC: 32 U/mL and low CS: 0.25 M) and lowest strength (BC: 32 U/mL and high CS: 1 M) was examined under the SEM and the results are presented in Figure 4.10. It can be seen from Figure 4.10(a) and (b) that the favourable combination of high BC and low CS concentrations produced agglomeration of large clusters of $CaCO_3$ crystals (approximately > 20 μm). However, it should be mentioned that the relative size between the $CaCO_3$ crystals and the sand particles are more important than the absolute size of the crystals themselves, as the crystals need to be large enough to fill in the pore throats among different sand grains, which is a function of the grain size. Precipitation of large clusters of $CaCO_3$ crystals increases the area of contact between soil grains, leading to stronger load path and overall shear strength (Ismail et al., 2002a; Mitchell & Santamarina, 2005; Cheng et al. 2017). Figure 4.10(c and d) shows the precipitation of relatively smaller $CaCO_3$ crystals (approximately < 10 μm) for the combination of high BC and CS concentrations. The contrast between the crystal sizes of the two extreme combinations (in terms of specimen strength) is evident when one compares Figure 4.10(a) with Figure 4.10(c) and Figure 4.10(b) with Figure 4.10(d).

Figure 4.10: Microstructure of soil specimens at 5% CaCO3 content: (a, b) high BC (32 U/mL) and low CS (0.25 M) concentrations; and (c, d) high BC (32 U/mL) and high CS concentrations (1 M) (after Mujah et al. 2019)

The different sizes of the $CaCO_3$ crystals resulting from each concentration combination may be attributed to the competition between the crystal growth and crystal nucleation as a result of the complex interplay between the CS and BC concentrations. Gandhi et al. (1995) reported that the competition would occur if the nucleation of new crystals triumphs over the growth rate of the existing ones. In the case of high BC and low CS concentrations, a high number of bacterial cells are

introduced into the soil specimens and attach themselves to the sand grain surface. In principle, a high number of bacterial cells would provide abundance of nucleation sites in the soil matrix (Cheng et al., 2017). In the presence of CS, the urea hydrolysis reaction is triggered to produce CO_3^{2-} ions, which were then mainly consumed by the nucleation of new $CaCO_3$ crystals rather than by the growth of the existing ones. Initially, this leads to abundance of the small $CaCO_3$ crystals, but with continuous supply of low CS concentration, the numerous small crystals would develop to grow larger in size, as shown in Figure 4.10(b). The size of the $CaCO_3$ crystals precipitated using high BC and CS concentrations was comparatively smaller (approximately 10 µm) compared to the crystals formed under high BC and low CS concentrations, as shown in Figure 4.10(d). In both conditions, the amount of BC concentration was fixed to 32 U/mL, and the only difference was in the CS concentration. The CS concentration affects the super-saturation condition (difference between the actual concentration and solubility concentration) of the environment that favours MICP process (Bosak & Newman, 2005), which is usually affected by the Ca^{2+} and CO_3^{2-} ions sources from the $CaCl_2$ and $CO(NH_2)_2$. The higher the super-saturation, the greater the nucleation rate of $CaCO_3$ crystals, resulting in formation of small crystals (Al-Thawadi & Cord-Ruwisch, 2012). The correlation between the shear strength of the bio-cemented sand and the $CaCO_3$ content was investigated previously by Whiffin et al. (2007), Fujita et al. (2008) and Okwadha & Li (2010). They concluded that the $CaCO_3$ content may not necessarily contribute to the soil strength improvement. Cheng et al. (2013) and Cheng et al. (2017) showed how sand grains coated with $CaCO_3$ crystals had less strength efficiency than specimens experiencing accumulation of $CaCO_3$ crystals at the contact points. The accumulated clusters of $CaCO_3$ crystals act like a closed surface adhering to the host particles. On the microscale level, this surface could develop an arching mechanism to carry normal stresses and enhance the shear resistance because of the intrinsic shear stiffness of a closed surface (Ismail, 2000). The current study confirms the efficacy of the strength improvement by the formation of the effective $CaCO_3$ crystals. It is envisaged that accumulation of the effective $CaCO_3$ layers that adhere to the initial $CaCO_3$ precipitates increases the size of the $CaCO_3$ crystal as cycles of the low concentrated reagent are supplied, which eventually increases the total area of contacts among the $CaCO_3$ crystals and the host sand grains.

4.3.2 Permeability

Figure 4.11 shows the permeability test results obtained from the bio-cemented specimens listed earlier. Only the extreme cases between the highest (32 U/mL) and the lowest BC (8 U/mL) concentrations with their respective combinations are shown for clarity. The results show a general trend where the permeability decreases with the increase in the $CaCO_3$ content; the initial concentration of the BC supply affects the permeability trend, especially at high $CaCO_3$ content. Overall, the reduction in the permeability due to precipitation of the calcite is less than an order of magnitude within the tested $CaCO_3$ content, regardless of the BC concentration. It can be seen from Figure 4.11(a) and (b) that the change in the permeability at any $CaCO_3$ content is very small, irrespective of the BC or CS concentrations. This makes the focus for any permeability target to be placed on the amount of $CaCO_3$ that must be precipitated rather than on the specific combinations of BC and CS that should be used. Significant reduction in the permeability by more than an order of magnitude (for any practical application) will require significant amount of calcite. The benefit achieved from reducing the permeability must be weighed against the magnitude of strength acquired during the process of precipitation.

The 32 U/mL BC and 0.25 M CS concentration produced effective $CaCO_3$ crystals with distinct characteristics such as relatively large in size, rhombohedral shaped and were concentrated at the soil pore throat [Figure 4.12(a)]. This type of $CaCO_3$ distribution allows for more liquid passage [indicated by the rectangular box in Figure 4.12(a)] in the soil matrix as it does not completely fill the gaps between sand grains [Figure 4.12(b)]. Furthermore, this is evidenced by the fact that, for most of the specimens treated under this protocol, no sudden clogging was detected and the effective $CaCO_3$ crystals were successfully distributed throughout the entire specimen. Al Qabany et al. (2012) reported that lower concentration of CS (injected several times) would provide better overall strength due to the gradual increase in the pH environment around the bacteria cells that produced conditions favouring $CaCO_3$ precipitation. Detailed description on the unique features of the effective $CaCO_3$ crystals precipitation is presented later.

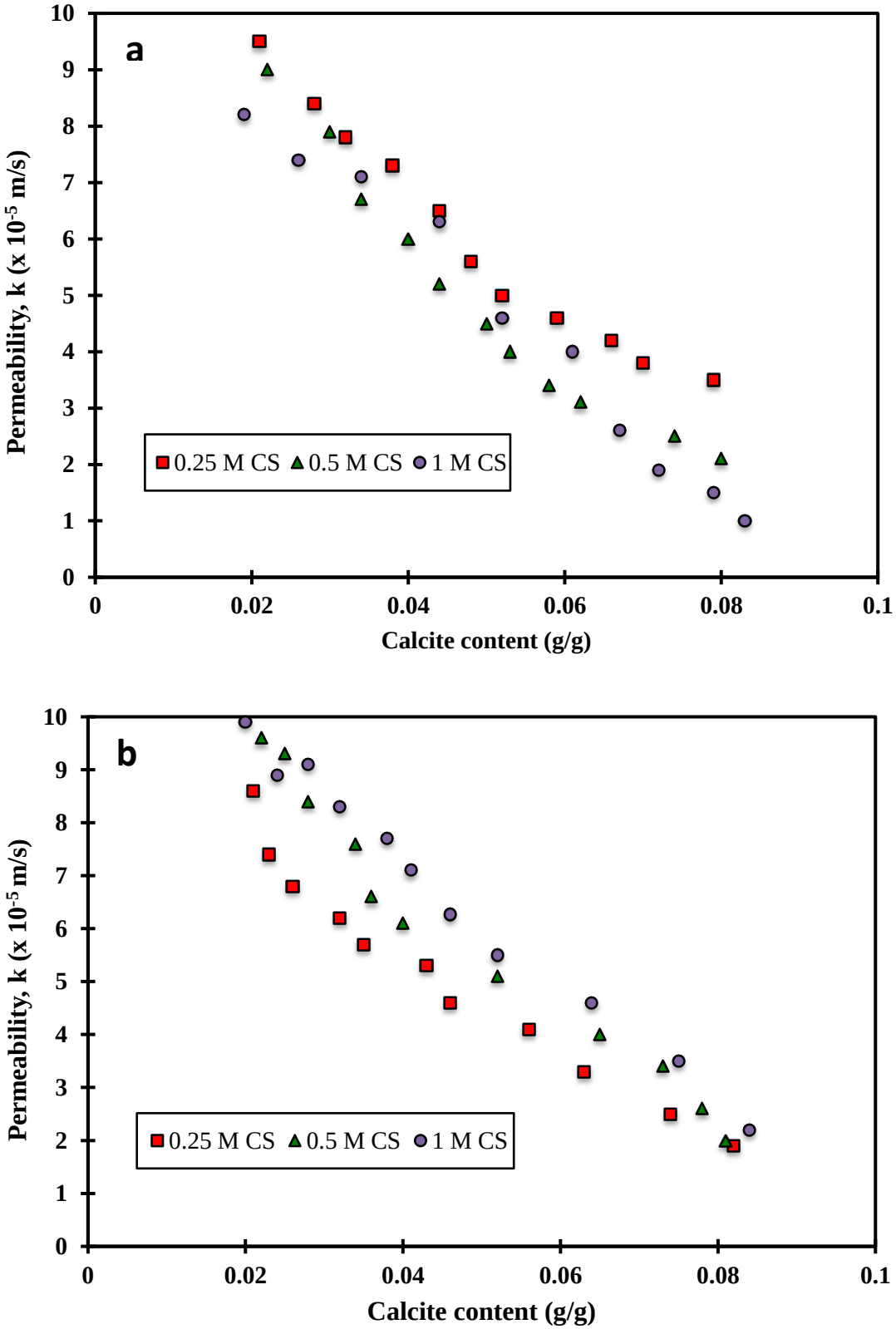

Figure 4.11: Permeability comparison of the bio-cemented specimens: (a) 32 U/mL BC concentration; and (b) 8 U/mL BC concentration

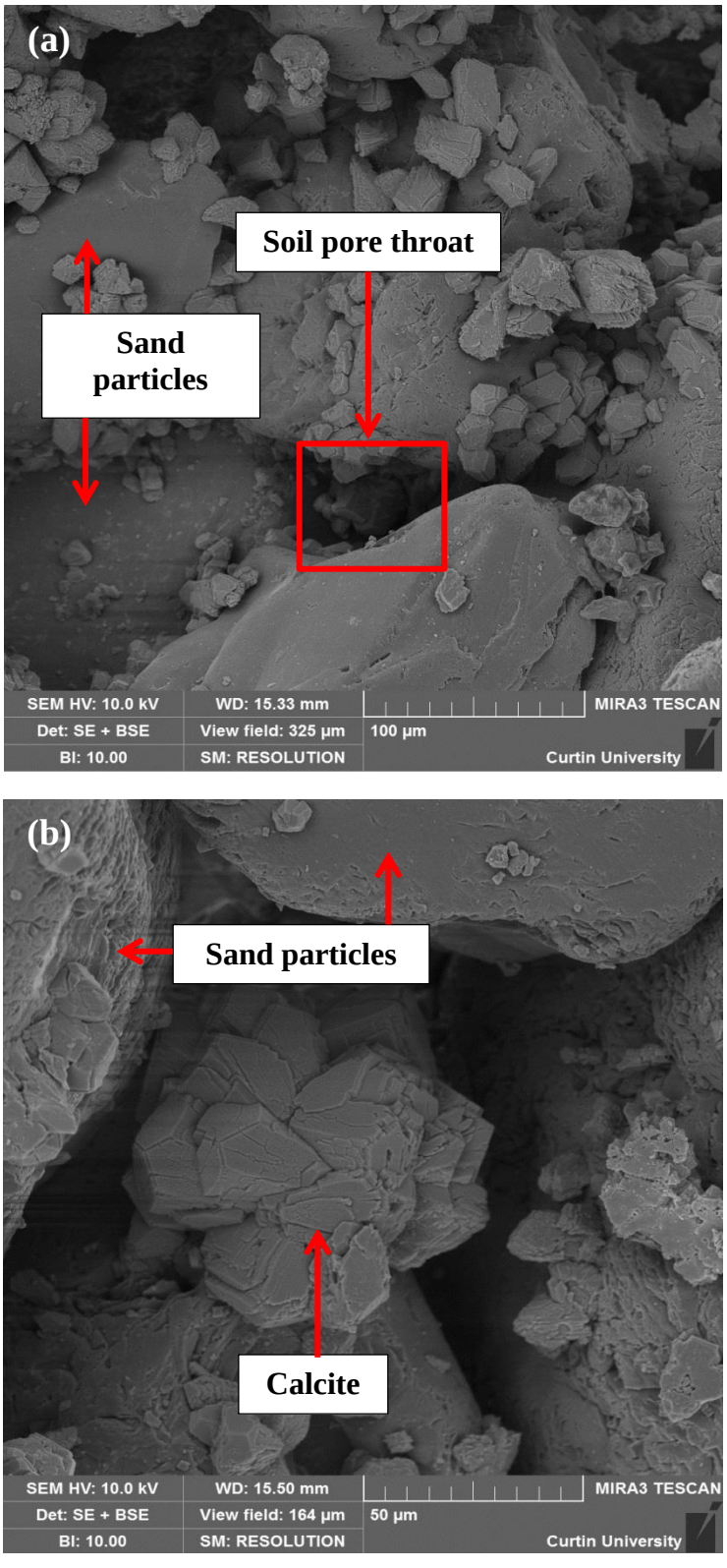

Figure 4.12: Characteristics of the effective $CaCO_3$ crystals precipitation: (a) precipitation at the soil pore throat; and (b) close up of the gap between the sand particles

4.3.3 Chemical Conversion Efficiency (CCE)

Based on the findings obtained from the treatment strategy employed in this study, it was clear that the different CCPPs are governed by the combined concentrations of BC and CS supplied during the MICP treatment. It is worth noting that in the present study, the BC solution was supplied once as one lot, and a constant input rate of 0.042 mol/L/h was maintained for all CS injections, to investigate the number of CS injection required to exhaust one BC solution injection. Therefore, it is imperative to study the CCE of the repeated injections of CS per injection of BC in order to produce a more cost-effective MICP process for field application.

Figure 4.13 shows the effect of the number of CS injection on CCE of the MICP process. Only the extreme cases involving the highest BC (32 U/mL) [Figure 4.13(a)] and the lowest BC (8 U/mL) [Figure 4.13(b)] concentrations are presented in order to discern the effect of the in-situ urease activity on CCE. Based on Figure 4.13 regardless of the BC concentration, the CCE of each treatment diminishes with the increasing number of CS treatments. Figure 4.13 also shows the cumulative mass of $CaCO_3$ precipitate (obtained from the CCE) of each condition; the decreasing CCE shown in the figure is related to the total amount of the produced $CaCO_3$. The gradual decrease in the CCE observed after each injection (which is in line with van Paassen et al. (2010a)) reflect the loss of the urease activity, possibly due to the bacterial cell encapsulation, elution of cells or/and cells death or lysis. It is observed from Figure 4.13(a) that only the combination of 32 U/mL BC and 0.25 M CS concentrations recorded > 50% CCE up to 4 number of CS injections. Although the MICP process continues after 4 number of CS injections (shown by the continued decline of the CCE), further supply of CS did not contribute towards the production of more $CaCO_3$ crystals, as the number of microbial cells become less available to encapsulate the urea during the hydrolysis reaction. Meanwhile, only two CS injections were recorded for the 8 U/mL BC concentration at CCE > 50% [Figure 4.13(b)]. The rapid decline in CCE for both BC concentrations (especially at 1 M CS condition) is presumably due to the intrinsic heterogeneity in any bacteria-related process, which can hamper exact replication of results.

Figure 4.13: Effect of the number of CS injections on CCE of the MICP process: (a) 32 U/mL BC; and (b) 8 U/mL BC concentrations (after Mujah et al. 2019)

The optimum number of CS injections is crucial for field application to ensure that it is sufficient to consume the supplied BC without wastage in each treatment cycle. Higher BC concentrations (e.g. 32 U/mL) can sustain a higher number of CS injections, whereby the CCE is expected to exceed 50% compared with lower BC concentration. The possible high number of CS injections achieved with the 32 U/mL BC concentration could be attributed to the higher number of bacteria cells in the BC solution. In fact, it is the number of bacteria cells available in the MICP environment that allows *p*rogression and continuity of the MICP process. On that basis, this study suggests that one injection of combination of 32 U/mL BC solution together with 4 injections of 0.25 M CS is ideal for a single treatment cycle. This is in line with the findings of Cheng et al. (2016) and Feng & Montoya (2016) who recommended multiple injections of bacteria to recover the in-situ urease activity and achieve a high level of cementation by continuing the MICP process. Also, recovery of the loss of the urease activity during the MICP process can be achieved by in-situ enrichment of ureolytic bacteria by providing a specific growth medium (Gomez et al., 2016) or by reintroducing the ex-situ cultivated bacterial culture.

4.3.4 Evolution of the Effective $CaCO_3$ Crystals

To study the morphology of the effective $CaCO_3$ crystal precipitates and their evolution as a function of the BC and CS injections over time, the specimens taken from the sand column after one, two, three and four injections were examined under the SEM. The reagents used in this study to produce the effective $CaCO_3$ crystals were based on the optimum results discussed in the preceding section (i.e. 32 U/mL BC and 0.25 M CS concentrations).

Figure 4.14: Evolution of the effective $CaCO_3$ crystals precipitation: (a) bacteria attachment onto the sand grain leading to formation of nucleation sites (image taken after the first injection); (b) formation of metastable primary spherical shaped precipitates (image taken after the second injection); (c) cluster of single crystals creating mesocrystals which successively form the effective $CaCO_3$ crystals (image taken after the third injection); and (d) precipitation of the effective $CaCO_3$ crystals concentrated at the soil pore throat (image taken after the fourth injection) (after Mujah et al. 2019)

Figure 4.14 shows evolution of the effective $CaCO_3$ crystals precipitation with successive injections. During the first treatment (one half void volumes of BC and CS were injected), the bacteria cells attached themselves to the sand grains due to their negatively charged state reacting to the positively charged Ca^{2+} ion during the urea hydrolysis reaction (DeJong et al., 2011; DeJong et al., 2013; Anbu et al., 2016; Rajasekar et al., 2017). The observed bacteria colonies are indicated by the red circles in Figure 4.14(a). In the second treatment (one full void volume of CS was injected), the metastable primary spherical shaped precipitates were detected [shown in red circle in Figure 4.14(b)] and these are speculated to be vaterite by van Paassen (2009) and Al Qabany et al. (2012). Further supply of CS helped the subsequent formation of the effective $CaCO_3$ crystals. This can be seen during the third treatment (two full void volumes of CS were injected) as portrayed in Figure 4.14(c), which displays the formation of mesocrystals as a result of the agglomeration of single crystals. Further details on this type of growth will be discussed later in Section 4.6. Eventually, in the fourth treatment (three full void volumes of CS were injected), the effective $CaCO_3$ crystals precipitation concentrated mainly in the soil pore throat, as captured in Figure 4.14(d).

Also, depending on the reagents input rate, $CaCO_3$ crystals transformation during the second treatment can be altered. For example, the formation of the metastable primary spherical shaped precipitates presented in Figure 4.14(b) was based on the constant input rate of 0.042 mol/L/h. However, if the input rate is increased, this will shorten the time required for the reagents to react during the MICP process, and this may produce a different transition mechanism. This is demonstrated in Figure 4.15, which shows the transition of the metastable primary spherical shaped single crystal into a much stable secondary rhombohedral shaped single crystal; this transition phase was captured during the second treatment using 0.167 mol/L/h input rate. This observation is in line with the transition phase reported by Terzis et al. (2016), who observed similar $CaCO_3$ crystals transformation.

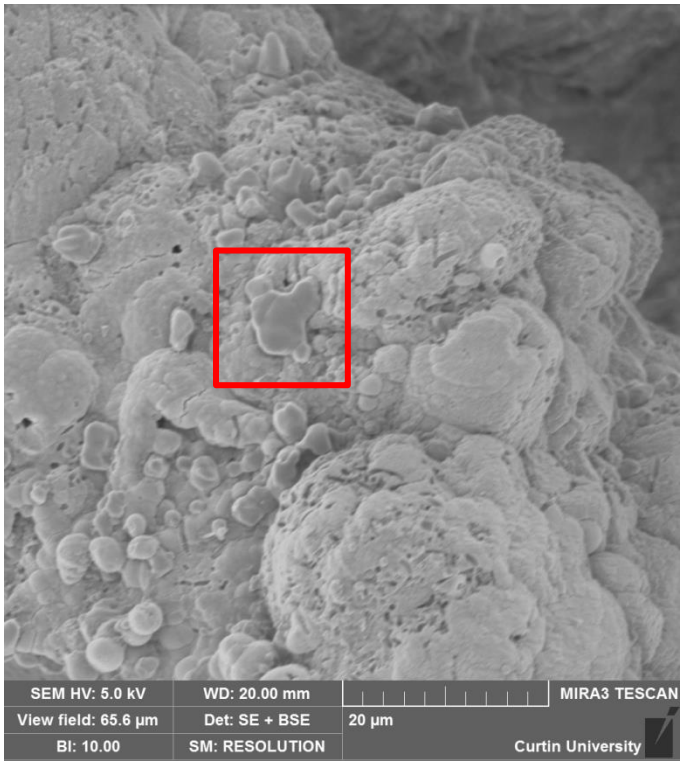

Figure 4.15: Transition of the metastable primary precipitate into a more stable secondary single crystal

Overall, the first supply of CS initially introduces Ca^{2+} ions into the bio-cemented specimen, to help create new $CaCO_3$ crystals. Further supply of CS together with the deposition of CO_3^{2-} ions from urea hydrolysis by bacteria onto the $CaCO_3$ crystal surface increases the size of the initially formed $CaCO_3$ crystals (Park et al., 2014a; Anbu et al., 2016). Unlike previously reported by DeJong et al. (2010) and Al Qabany & Soga (2013), growth of the $CaCO_3$ crystals in the current study stems from agglomeration of the single crystals (observed after the first and second treatment) creating mesocrystals (after the fourth treatment), which eventually form the effective $CaCO_3$ crystals (Figure 4.14).

4.3.5 Microstructural Features of the Effective $CaCO_3$ Crystals

In order to understand the mechanism associated with the precipitation of the effective $CaCO_3$ crystals, it is vital to make careful and thorough observations into the microstructural features that are unique to the precipitation process. It has been established earlier that the main characteristics of the effective $CaCO_3$ crystals precipitation are, but not limited to: (1) they are concentrated at the soil pore throats; (2) they are relatively large in size (normally > 20 µm); and (3) they have a rhombohedral shape. The current study has shown that these could be achieved in the laboratory by manipulating both BC and CS concentrations as discussed previously.

One of the most distinct features that allow for precipitation of the effective $CaCO_3$ crystals is the tendency of the bacteria cell to align in the vicinity of the soil pore throats, as shown in Figure 4.16a and b). This propensity is supported by two main factors: (1) availability of the rich nutrient (DeJong et al., 2010); and (2) the low stresses induced in the menisci region of the soil pore throat (Cheng et al., 2013).

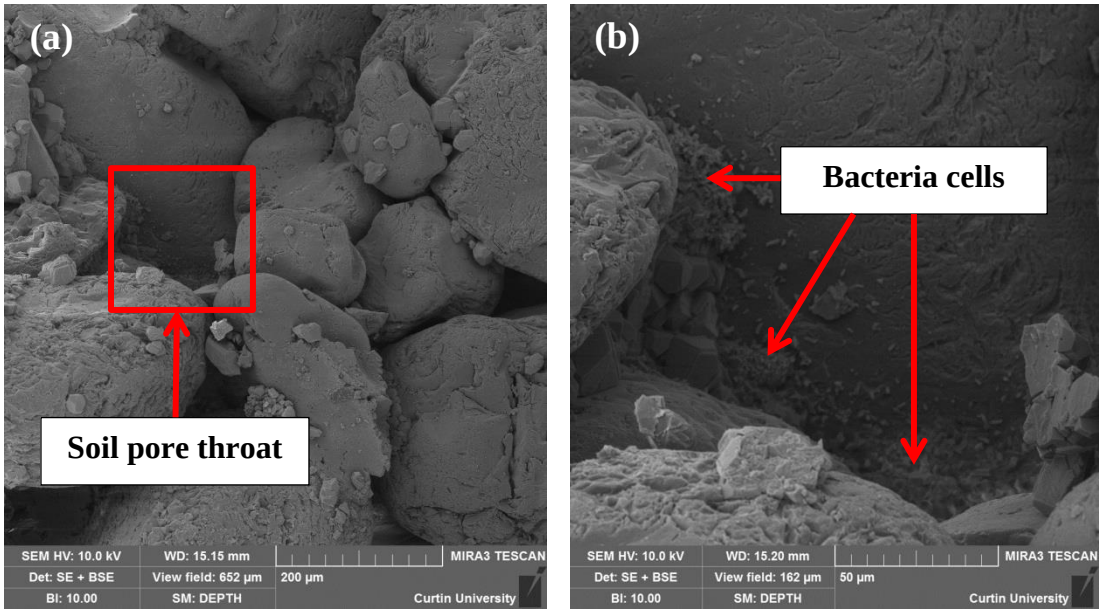

Figure 4.16: Feature of the effective $CaCO_3$ crystals precipitation: (a) alignment of bacteria cells in the soil pore throat region; and (b) a close up showing accumulation of bacteria cells after the second injection of BC solution during the second treatment cycle

Another interesting feature of the effective $CaCO_3$ crystals precipitation is the fact that they are relatively larger in size eventually. Based on the observations made in this study, this is attributed to the unique ability of the $CaCO_3$ crystals to cluster into agglomeration [Figure 4.17(a)], of large $CaCO_3$ mesocrystals [Figure 4.17(b)]. Agglomeration of the $CaCO_3$ precipitates shown in Figure 4.17(a) was the result of the low CS (0.25 M) injection (two full void volumes), while the clustered $CaCO_3$ mesocrystals shown in Figure 4.17(b) were achieved after three full void volumes of 0.25 M CS injections. The combination of high BC (32 U/mL) and low CS (0.25 M) favour this type of precipitation, because the high concentration of BC promotes accumulation of the bacteria cells near the soil pore throat region, as discussed earlier; on the other hand, the low concentration of CS injection supports the formation of the clustered $CaCO_3$ precipitates that eventually developed into $CaCO_3$ mesocrystals. This was achieved by progressively increasing the supersaturation condition; supersaturation is increased with the increase in both Ca^{2+} and CO_3^{2-} ions concentration (Al-Thawadi & Cord-Ruwisch, 2012) of the MICP process environment and thus, allowing accumulation of the succeeding precipitations over the initial small crystals.

Figure 4.18 depicts the growth of the effective $CaCO_3$ crystals during the second treatment cycle. As mentioned in Section 4.4, one treatment cycle equals one injection of 32 U/mL BC and four injections of 0.25 M CS. This protocol continues for the next treatment cycles. During the second treatment cycle, the effective $CaCO_3$ crystals continue to grow in size. This is evinced by the cascaded formation of the sheet-like pattern into a foliated structure (indicated by the red dotted circles in Figure 4.18). Unlike the evolving mechanism associated with the first treatment cycle, the effective $CaCO_3$ crystals formed in the subsequent treatment cycles copy the existing ones and adhere strongly to them, producing the foliated pattern described above. The increase in size of the initial crystals is the result of bacteria cells attachment to the initial crystals that occupied the pore throat after the first treatment cycle. The growth continues until all urea available in the CS are completely consumed by the bacteria cells.

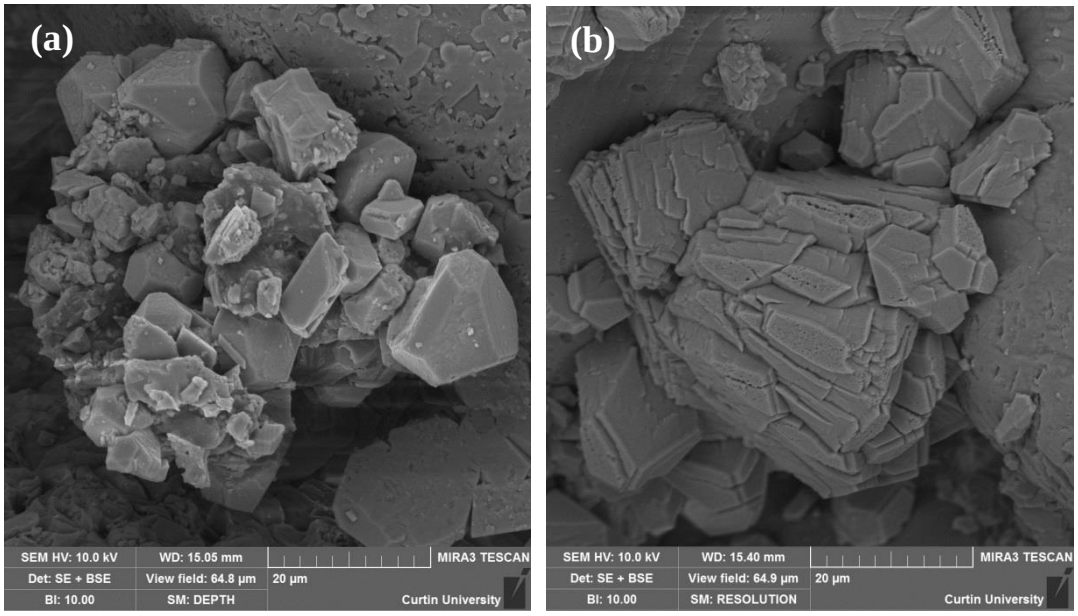

Figure 4.17: Feature of the effective $CaCO_3$ crystals precipitation: (a) $CaCO_3$ precipitates agglomeration; and (b) clustered crystals forming large $CaCO_3$ mesocrystals (size > 20 µm)

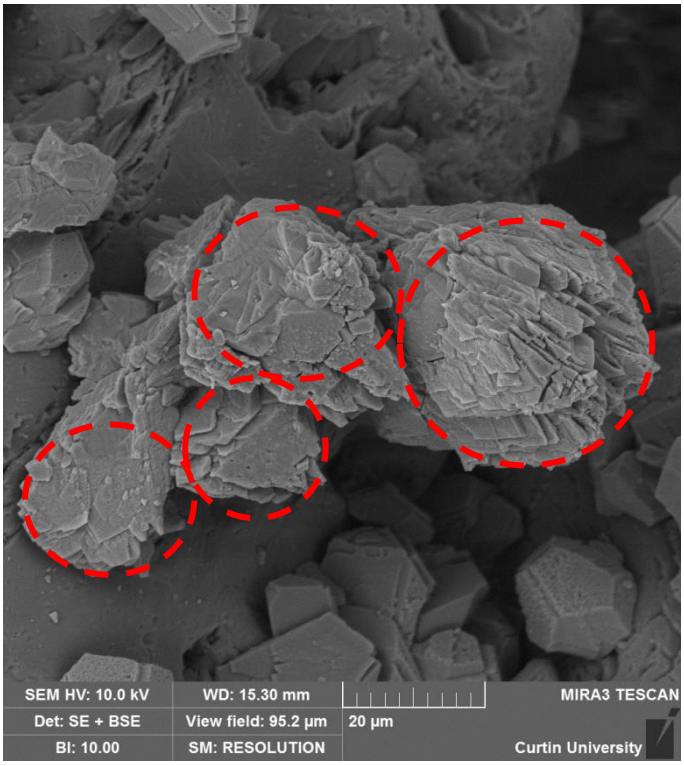

Figure 4.18: Sheet-like pattern reproducing a foliated structure due to successive growth of the effective $CaCO_3$ crystals

Eventually, the $CaCO_3$ mature (or develop) into a rhombohedral shape. Figure 4.19(a) shows that majority of the effective $CaCO_3$ crystals are rhombohedral in shape, especially those located at the soil pore throats. Figure 4.19(b) shows a close up of the region displaying the rhombohedral shape for large effective $CaCO_3$ crystals (size > 20 µm). Unlike the $CaCO_3$ crystals previously reported in the literature as being mainly circular in shape, the rhombohedral shape crystals are more robust due to their interlocking effect while connecting the sand grains (Figure 4.20), leading to a stronger cemented matrix overall. Explanation of the physiochemical nature of the mechanism of the effective $CaCO_3$ crystals and its interlocking nature is beyond the current study; however, based on the strength comparison between the optimised MICP and the OPC treated specimens, it is revealed that the optimised MICP imbued with the effective $CaCO_3$ crystals proved to impart significant strength improvement compared to the OPC treated specimens at similar cement content.

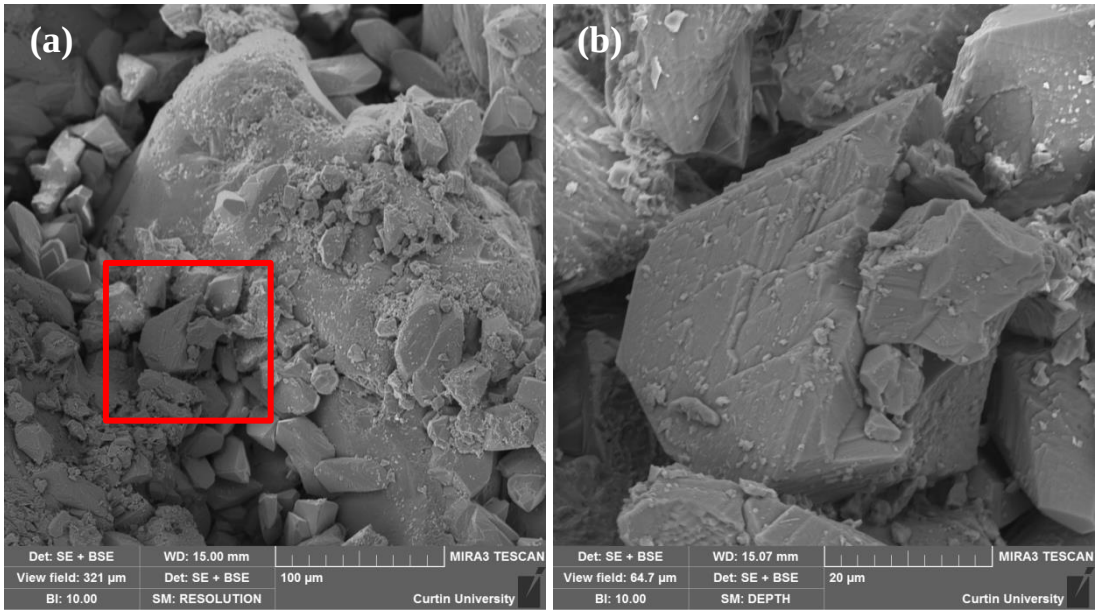

Figure 4.19: Shape feature of the effective $CaCO_3$ crystals precipitation: (a) rhombohedral shaped $CaCO_3$ crystals filing the gaps at the soil pore throat; and (b) a close up view of the large $CaCO_3$ mesocrystals (size > 20 µm)

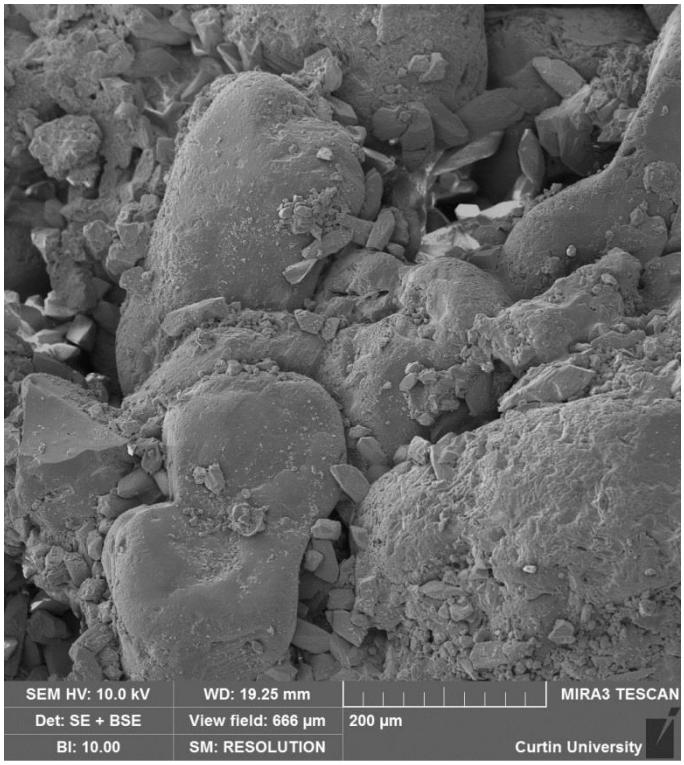

Figure 4.20: Effective $CaCO_3$ crystals precipitation interlocking the soil pore throats

The findings obtained from this study suggest that different $CaCO_3$ precipitation patterns can be engineered by controlling the BC and CS concentrations through the MICP treatment, which can result in a variety of macroscale strength responses. In general, the effective $CaCO_3$ crystal will develop into a pattern of large, clustered rhombohedral-shaped crystals. The $CaCO_3$ crystal precipitation pattern, including the relative size between crystals and sand particles, greatly impacts the target application of bio-cementation in the field. The specific features affects the strength of the cemented matrix, as it will influence the load transfer mechanism inside the soil matrix, which depends on the size of the contact area, linked by the precipitated $CaCO_3$ crystals (Ismail et al., 2002a). In terms of hydraulic conductivity, the shape, size and distribution of the precipitated $CaCO_3$ crystals near the soil pore throats will influence the flow properties of the cemented porous media, as reported by Al Qabany et al. (2012). It should be noted that in addition to the amount of effective $CaCO_3$ crystals formed, the spatial uniformity of the overall microbially induced $CaCO_3$ precipitates is also a critical factor controlling the ultimate soil strength of the cemented medium.

In civil engineering applications such as transportation subgrades and embankments, the ability to apply the MICP technique that produces the largest quantity of effective $CaCO_3$ precipitation is desirable to minimise the involved cost. The current study suggests that this can be achieved by the combination of high BC and low CS, which can increase the strength dramatically compared with its side effect of reducing the permeability. This is particularly advantageous in transportation subgrade and embankment applications, which normally need improved strength while maintaining high drainage characteristics.

4.4 MICP Method versus Ordinary Portland Cement

In order to further verify the optimised strength and permeability of the bio-cemented sand specimens, a series of MICP treated specimens were produced and tested in parallel with specimens cemented with ordinary Portland cement (OPC) for comparison; the OPC specimens were cured for 28 days. Figures 4.21 and 4.22 show a comparison of the stress-strain relationship of the MICP and OPC treated sands at various contents of the respective cementing agent. As expected, the increase in the content of either $CaCO_3$ or Portland cement increases the peak strength of the treated specimens. Based on the results of Figure 4.21, the peak strength recorded for the MICP treated sand at 4%, 6%, 8%, and 10% $CaCO_3$ are 850 kPa, 1200 kPa, 2200 kPa, and 4100 kPa, respectively. The corresponding values for the case of OPC are 500 kPa, 1100 kPa, 1500 kPa, and 3000 kPa, respectively (Figure 4.22). Also, it is noted that the OPC treated specimens exhibit relatively ductile behaviour compared with the bio-cemented specimens; this is in agreement with the findings obtained by Schnaid et al. (2001) and Ismail et al. (2002b).

Figure 4.21: Stress-strain relationship of the optimised MICP treated specimens (32 U/mL and 0.25 M CS) (after Mujah et al. 2019)

Figure 4.22: Stress-strain relationship of OPC treated specimens after 28 days (after Mujah et al. 2019)

Figure 4.23 shows the UCS and permeability results of the sand specimens treated with the optimised MICP effective $CaCO_3$ and OPC treated with 2-10% cement content after 28 days of curing. The optimised bio-cemented specimens have higher strength compared to the OPC treated specimens at all cementation levels. Moreover, the permeability of the optimised bio-cemented specimens is significantly higher than that of the OPC treated specimens at all cementation levels. For instance, at 6% cement content, the permeability of the OPC treated specimen is considerably reduced to 98%, while the optimised bio-cemented specimen retained about 50% of the initial permeability. At cement content > 8%, the OPC treated specimen would act as a very poor drainage material having a permeability value of less than 1×10^{-5} m/s.

Figure 4.23: Comparison of UCS and permeability of optimised bio-cemented (32 U/mL BC and 0.25 M CS) and OPC treated (at 28 days) sands (after Mujah et al. 2019)

The increase in the strength associated with significant reduction in the permeability of the OPC treated specimens are due to the cement hydration process, which continues for up to 28 days (and beyond) after the initial reaction between the cement and the soil (Nakarai & Yoshida, 2015; Mujah, 2016). According to Cheng et al. (2013), the cement hydration process produces water insoluble hydrates in the form of calcium silicate hydrate (C-S-H gel). This gel-like structure binds the sand particles, leading to an increase in strength and stiffness. It should be noted that the OPC cementation process presented here is representative of the traditional ground improving technique for soil stabilisation using chemical additives (e.g. cement, gypsum, or lime). Observation into the microscale level of the OPC treated specimens reveals that the C-S-H gel [Figure 4.24(a-b)] occupies most of the pore space, hence, limiting the permeability of the cemented material. Unlike the formation of the C-S-H structure, the precipitated $CaCO_3$ did not completely fill the gaps between the sand grains, hence, allowing relatively free passage of the liquid in the soil matrix [indicated by the red lines in Figure 4.24(c)]. The effective $CaCO_3$ crystals in their solid achieved stronger and stiffer post treatment mechanical responses compared with the C-S-H gel hydrates (for the reasons discussed above).

In summary, the results and discussion above indicate that the optimised bio-cementation process presented herein is more efficient than Portland cement in increasing both the strength and stiffness with much lower reduction in permeability. This is mainly attributed to the nature of the effective $CaCO_3$ crystals in terms of their large, rhombohedral shaped and clustered crystals and the strategic location of their formation at the pore throats compared with the OPC C-S-H gel that does not lend itself to a preferential growth pattern or location within the sand matrix.

Figure 4.24: SEM images showing the effect of cement on permeability: (a) formation of C-S-H gel in the OPC treated specimen (after 7 days); (b) formation of C-S-H gel in the OPC treated specimen (after 28 days); and (c) precipitation of the effective $CaCO_3$ crystals in the bio-cemented specimen. Cementing agent content fixed at 8% for all specimens (after Mujah et al. 2019)

It is essential to mention some of the limitations and postulates associated with the optimisation needed to produce the effective $CaCO_3$ crystals; these include: (1) the different BC concentrations used herein were harvested from one single bacterium type (e.g. *Sporosarcina pasteurii*); (2) the CS concentrations used were based on equimolar concentrations one part urea to one part $CaCl_2$ (to source the CO_3^{2-} ions and Ca^{2+} ions, respectively); and (3) the injection strategy implemented is based on a two-phase injection approach. It can be envisaged that using different types of ureolytic bacteria with either higher or lower BC concentrations or different non-equimolar concentrations of CS may yield different results. This is because different bacteria types have different rates of urea hydrolysis. Also, the use of not ureolytic bacteria should be taken into consideration as non-ureolytic bacteria did not use the same urea hydrolysis reaction pathway to produce $CaCO_3$ crystals. In addition, the use of different concentrations of the chemicals which made the CS e.g. urea and the calcium chloride were shown to affect the rate of the bio-cementation since different concentrations of CS require different reaction times to be fully consumed by the supplied bacteria. Different injection strategies such as the injection, pre-mixing or surface percolation methods may bring about different bacteria and CS distributions within the sand columns, changing the physical and mechanical outcomes of the cemented soil. It is noted that, the issue of treatment homogeneity which results from the homogeneous distribution of $CaCO_3$ crystals precipitation remains the major obstacle for MICP moving forward.

The conclusions of the current research might not be applicable to other types of sands (e.g., calcareous sand), which have different mineralogy properties and shapes, and the surface properties of the soil grain will have significant effect on the characteristics of the $CaCO_3$ precipitates thus, ensuing the characteristics of cementation. However, the methodology developed in the current study can be readily employed for other types of coarse-grained soils.

4.5 Strength Comparison with Previous Studies

A strength comparison chart in terms of the UCS values was produced and shown in Figure 4.25 for the optimised bio-cemented specimens treated with the combination of 32 U/mL BC and 0.25 M CS concentrations, along with results from previous studies. The main selection criterion for the list of the comparison is that those previous studies must have undergone similar optimisation; this can be in terms of their use of different treatment strategy, i.e. constant flow injection (Whiffin et al., 2007); reagents manipulation, i.e. using low BC and high CS concentrations (Al Qabany & Soga, 2013); using a different type of bacteria, i.e. *Bacillus Megaterium* (Duraisamy & Airey, 2015); using urease enzyme as a substitute for ureolytic bacteria (Zhao et al., 2014a); using a different type for the calcium source, e.g. soluble calcium derived from seawater (Cheng et al., 2014), calcium derived from egg shells (Choi et al., 2016)]; and using a low degree of saturation (S = 20%) treatment to produce effective $CaCO_3$ crystals (Cheng et al., 2013).

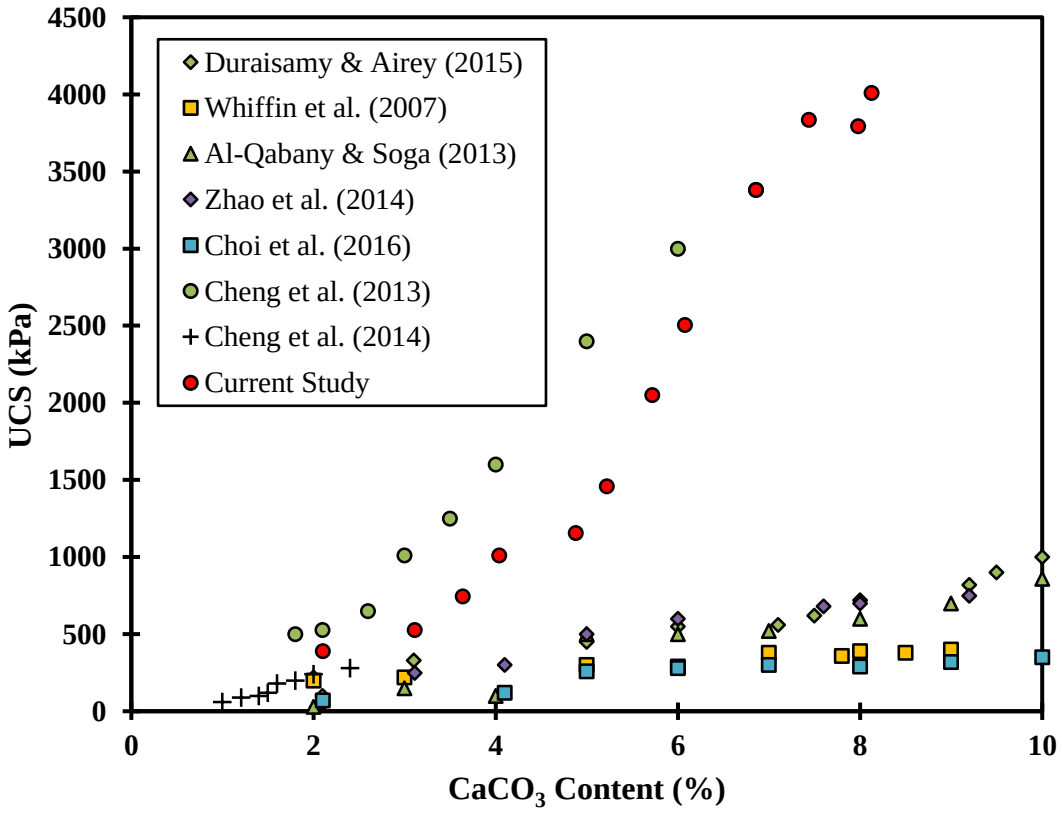

Figure 4.25: Strength comparison of the current results with previous studies

Figure 4.25 reveals that the strength values from the current study lie significantly above all previous studies, except those reported by Cheng et al. (2013), especially at $CaCO_3$ contents lower than 5%. The results from Cheng et al. (2013) were achieved by maintaining a partially saturated condition in the soil matrix during the MICP treatment. Apparently, the partially saturation condition triggered a strong coating effect, which is predominantly attributed to the homogeneously distributed solution on absorbed by the surface of the sand grains by the surface tension needed for the MICP solution to make such coating effect. It was also reported that the host grains' gaps were filled with $CaCO_3$ crystals, which were precipitated as a result of the retained MICP solution located at the grains in a menisci form, allowing the $CaCO_3$. Although the low degree of saturation condition proved to produce effective $CaCO_3$ crystals that are mainly precipitated at the soil pore throats, it will be practically of limited use, since it is difficult to control and maintain the inner soil matrix saturation condition that is critical for its effectiveness. However, using the method described in the current study will make the precipitation of the effective $CaCO_3$ crystals at the soil pore throats possible for field application due to the fact that it just require manipulation of the BC and CS concentrations with no other restrictive preparation in the field of the manner needed for the method described by Cheng et al. (2013). The excellent strength improvement achieved by the method presented herein stems from the fact that the optimised $CaCO_3$ crystals are relatively larger in size (> 20 μm), concentrated at the soil pore throats and rhombohedral in shape as compared to the previously reported $CaCO_3$ crystals precipitation patterns in the literature to date.

4.6 Summary

The effects of some key environmental parameters such as the initial soil pH, the degree of the surface temperature, the freeze-thaw (FT) cycles and the rainwater flushing on the potential application of MICP in such conditions were examined. The results showed that the MICP treatment favoured both basic soil pH and ambient surface temperature conditions. Also, it was revealed that bio-cemented fine sand (0.15 mm in diameter) is more durable compared with bio-cemented coarse sand (1.18 mm in diameter) under the action of up to 10 FT cycles while the impact was minor on the bio-cemented well-graded sand. It was also noted that MICP treatment failed to perform if rainwater was flushed even 24 hours and/or immediately after adding the bacteria. These findings are critical for application of the MICP in the field.

It was found that the combination of the 32 U/mL BC and the 0.25 M CS concentrations provided the highest strength improvement. Similarly, the same combination yielded the highest permeability retention, suggesting that the said combination is the most optimum for strength improvement and permeability retention. Examination into the CCE revealed that the optimum number of CS injection for the optimised combination of reagents used in the present study is 4. Further supply of CS proved less effective in forming more $CaCO_3$ crystals. The optimum number of CS injection is crucial for field application for both cost and environmental implications.

Microstructural study of the $CaCO_3$ crystals formation illustrated the specific mechanism associated with the effective $CaCO_3$ crystals precipitation. The SEM images captured the bacteria attachment onto the sand grains, which leads to the formation of the nucleation sites, formation of the metastable primary spherical shaped precipitates, the clustering of the single crystals into mesocrystals towards large effective $CaCO_3$ crystals, and the localisation of the effective $CaCO_3$ crystals at the ‘strategic’ soil pore throats.

Through microstructural imaging, the unique characteristics of the effective $CaCO_3$ crystals were determined and explained. These include the propensity of the bacteria cells to align themselves at the vicinity of the soil pore throats, the relatively large $CaCO_3$ crystals formed (> 20 μm in size) and the clustering of single crystal that eventually developed into rhombohedral mesocrystals. These unique characteristics of the effective $CaCO_3$ crystals are the underlying factors for the enhanced strength improvement of the bio-cemented presented herein.

The optimised bio-cemented specimens were compared to the conventional chemical stabilising technique using OPC treated specimens. The results showed that the optimised bio-cemented specimens performed better than the OPC treated specimens in terms of both strength and permeability; the effective $CaCO_3$ crystals were shown to provide more liquid passage compared with the C-S-H gel like structures found in the OPC treated specimens. The results of the proposed optimisation recipe utilised in the current study performed better than the previous MICP studies reported in the literature.

In the following chapter, the geotechnical behaviour of the optimised bio-cemented sand specimens is analysed through the triaxial testing considering the effect of different confining pressures and stress paths. Also, the experimental results conducted via the CU triaxial tests are compared to an analytical model for further validation.

Chapter 5
Geotechnical Behaviours of the Optimised Bio-Cemented Sand

5.1 Introduction

It has been demonstrated that the combination of both 32 U/mL BC and 0.25 M CS used in this study has produced an effective $CaCO_3$ crystal precipitation which increased both the strength improvement and the permeability retention of the bio-cemented sand compared to other previously known $CaCO_3$ precipitation. In this chapter, the geotechnical behaviour of the bio-cemented sand employing the optimised combination recipe were further examined through the triaxial tests, considering the effect of different confining pressures (100 kPa, 200 kPa, and 400 kPa) and stress paths (axial compression and constant-*p*). It is postulated that the optimised bio-cemented sand would behave similarly (in general) under the different confining pressures owing to the precipitation of the effective $CaCO_3$ crystals. However, the behaviour would be different under the different stress paths. Isotropic consolidated undrained (CU) triaxial tests were performed in order to capture the intended soil behaviour. A simple analytical model was presented at which, the results from the experiments were compared to predictions from the model. Finally, the shear strength parameters of the optimised bio-cemented sand were compared with results of previous studies found in the literature. The work presented in this chapter has formed the basis of the submitted article: Donovan Mujah, Mohamed A. Shahin, and Liang Cheng (2019). Experimental study and analytical model for strength behaviour of bio-cemented sand. *Proceedings of ICE - Ground Improvement*, under review (authorship attributions in Appendix D).

5.2 Triaxial Tests

Montoya & DeJong (2015) indicated the role of confining pressure and cementation level towards the shear strength and stiffness of MICP cemented sands. Earlier, van Paassen et al. (2010a) and Chou et al. (2011) reported the dependency of the behaviour of MICP cemented sands on confining stresses between 5 – 40 kPa in the direct shear tests. Furthermore, Feng & Montoya (2016) studied the effect of higher confining stresses, i.e. 100, 200 and 400 kPa, and the influence of cementation levels on the behaviour of the MICP cemented sands. They concluded that the stiffness, peak shear strength and dilation increase with an increase in the $CaCO_3$ content at a given effective confining pressure. Their results also noted that the dilation of the specimens is primarily suppressed with an increase in the effective confining pressure. The improvement in both the peak and residual friction angles and initial elastic modulus are dependent on both the cementation level and confining pressure.

The mechanical behaviour of bio-cemented sand specimens prepared by the method described in this thesis was investigated at different conditions of cementation level, confining pressure (100, 200, and 400 kPa) and varying loading paths (axial compression and constant-*p*). The consolidated isotropically undrained test (CU) was chosen over the drained test (CD) because it can be performed much quicker and it also provides both the total and effective stress paths information. The peak and residual shear stresses were quantified using the brittleness index, I_B, presented in Equation 5.1 (Bishop, 1971):

$$I_B = \frac{q_p - q_r}{q_p} \qquad \text{Equation 5.1}$$

Where;

I_B = Brittleness index;

q_p = Peak shear strength; and

q_r = Residual shear strength.

5.2.1 Influence of Confining Pressure

The effects of confining pressure on the stress-strain behaviour of the untreated and bio-cemented sands are shown in Figures 5.1 and 5.2. Based on the results in Figure 5.1(a), the strength of the untreated (uncemented) sand increases significantly in a ductile manner with the increase in confining pressure for the 3 confining pressures of 100, 200 or 400 kPa. The strength of the untreated sand was attained at approximately $\varepsilon = 3\%$, consistently for all confining pressures.

As can be seen from Figure 5.1(b), the untreated sand tends to contract up to $\varepsilon = 4\%$ with increasing the pore water pressure (and decreasing in effective stress). Further shearing of the specimen invokes a dilative and an increase in the effective stress. This observation is valid for all untreated sand specimens regardless of the confining pressure. On the other hand, and within the same range of cementation and tested confining pressure, the stress-strain behaviour of the optimised bio-cemented sand varies. Medium cemented specimens having $CaCO_3$ content between 5.2% and 5.5% were used for comparison with the behaviour presented above for the untreated sand. As expected, the cemented specimens always exhibit higher strength and stiffness compared with the untreated specimens at the same confining pressure. Generally, based on Figure 5.2(a), the optimised bio-cemented specimens exhibited a strain softening response after the peak stress, regardless of the confining pressure. However, the overall shearing response of all tested specimens was of a strain hardening fashion up to $\varepsilon = 1\%$.

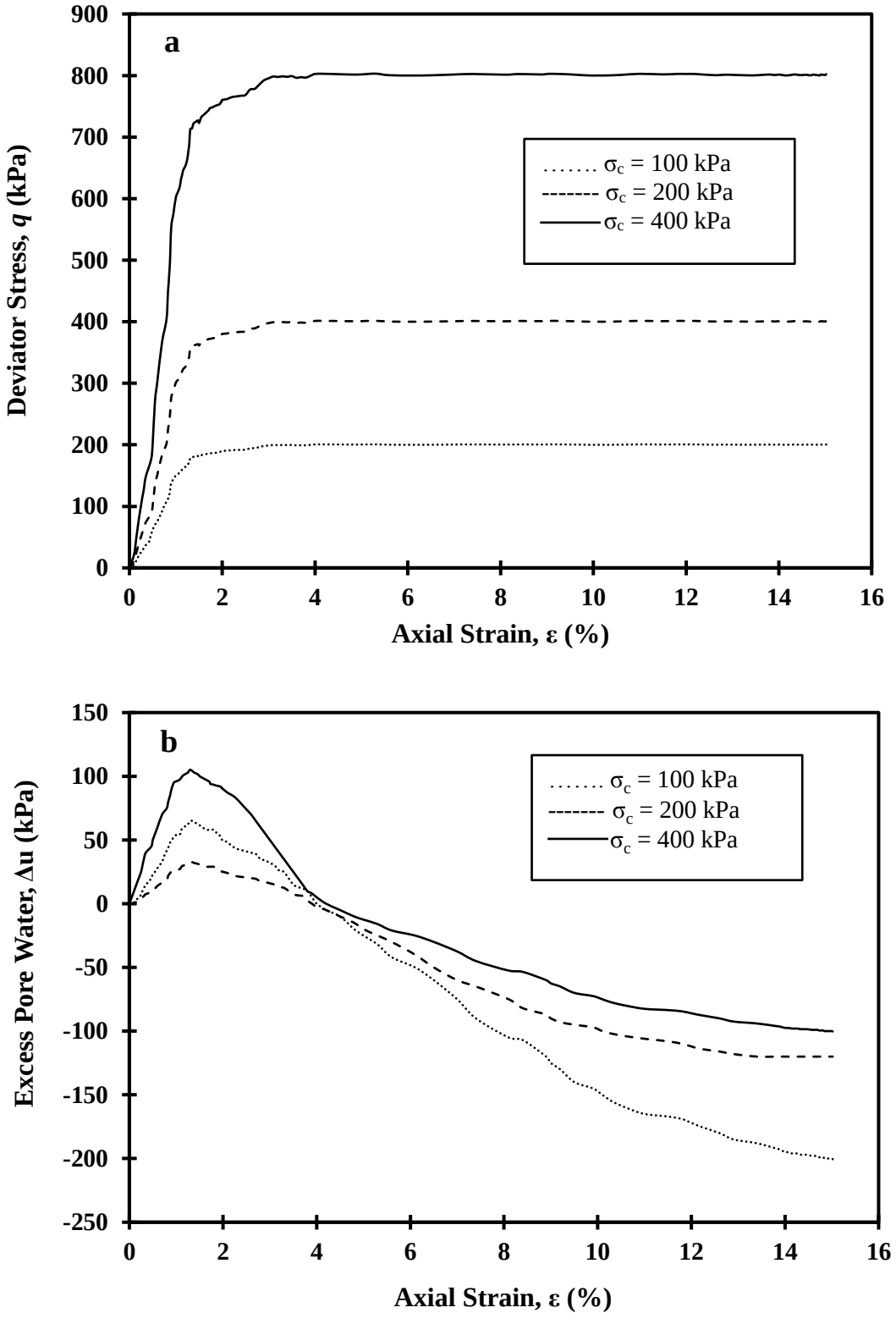

Figure 5.1: CU tests of the untreated sand:
(a) stress-strain curve; and (b) excess pore water pressure

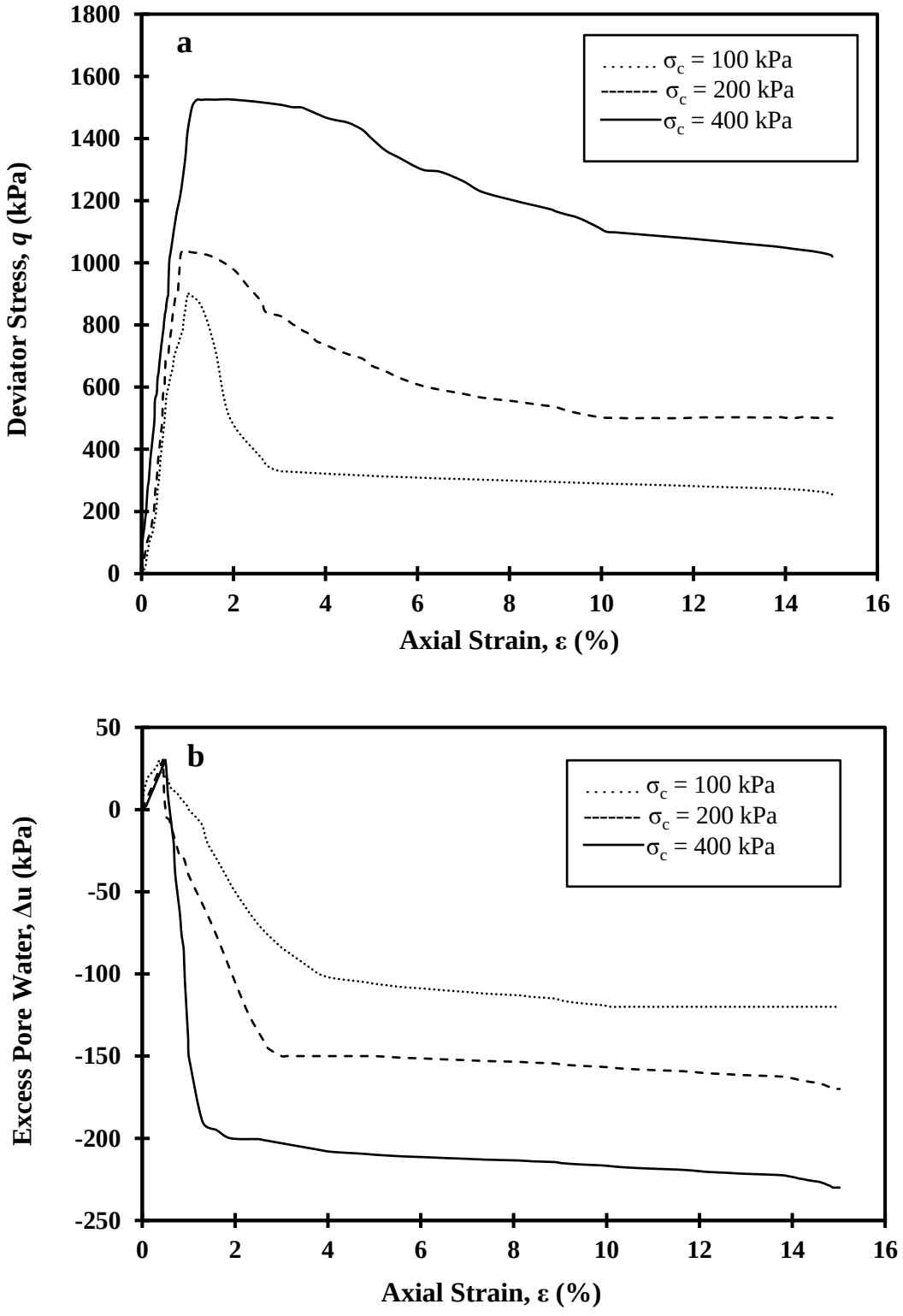

Figure 5.2: CU tests of the optimised bio-cemented sand: (a) stress-strain curve; and (b) excess pore water pressure

Based on the results in Figure 5.2(a), at a confining pressure = 100 kPa, the optimised bio-cemented specimen attained a peak strength q = 890 kPa at ε = 1%, followed by a strain softening behaviour. However, at higher confining pressures of 200 kPa and 400 kPa, the corresponding q = 1040 kPa and 1525 kPa were attained at ε = 0.95% and ε = 1.4%, respectively. Based on this observation, it can be said that, for a confining pressure of 100 kPa and 200 kPa, only minor change in the axial strain values was recorded at peak strength. However, at the higher confining pressure of 400 kPa, a much less axial strain value of 0.4% is required to increase the peak stress from 890 kPa to 1525 kPa, signifying the effect of the higher confining stress on the specimen stiffness. The sudden increase in stiffness under the 400 kPa confining pressure can be attributed to the degradation of the $CaCO_3$ bond inside the soil matrix, manifesting as fines that increased the soil grains roughness (DeJong et al., 2010; Montoya & DeJong, 2015).

Strong negative pore pressures were observed in all confining pressure conditions, as shown in Figure 5.2(b). The results indicated that higher confinement leads to a larger negative pore pressure. For instance, increasing the confining pressure from 100 kPa to 400 kPa resulted in no change in the positive peak values of. Δ_u ; however, the confining pressures seen to mobilise the development of higher negative Δ_u values at the residual state zone. The changes in pore pressure were due to the change in the mean total stress and/or the tendency of the volume of the soil to dilate post peak. In this case, the optimised bio-cemented specimens displayed more dilative tendency at the strain-softening zone due to the increase in stiffness as a result of the increase in the pore pressure.

Generally, cementation suppresses the tendency of the particles to crush from initial loading. This is reflected in an essentially elastic compression curve up to the yield point. Prior to the yield point, degradation of the cementation is brittle, followed by a strain softening response. The strain softening behaviour observed after the brittle yielding could either continue towards the residual value or change to strain hardening due to mobilisation of friction.

5.2.2 Brittleness Index

The brittleness index, $I_{B,}$ relates the residual shear strength value q_r to the peak shear strength value, q_p, as represented by Equation 5.1. Figure 5.3 compares the I_B values of the untreated and the bio-cemented sands (the optimised, high BC + high CS, and low BC + low CS combinations). Based on Figure 5.3, the confining pressure has no impact in the case of the untreated sand. However, as expected, the I_B values in the case of bio-cemented specimens is much higher than those in the case of no treatment and gradually reduces with confining pressure (I_B = 0.72, 0.52 and 0.33 at confining pressures of 100 kPa, 200 kPa and 400 kPa, respectively). The combination of high BC + high CS treatment produced the most brittle specimens regardless of the confining pressures due to the precipitation of much smaller $CaCO_3$ crystals cementing the sand grains. The high I_B value indicates that more degradation in the $CaCO_3$ bond has occurred in the residual stress zone, which eventually led to specimen failure.

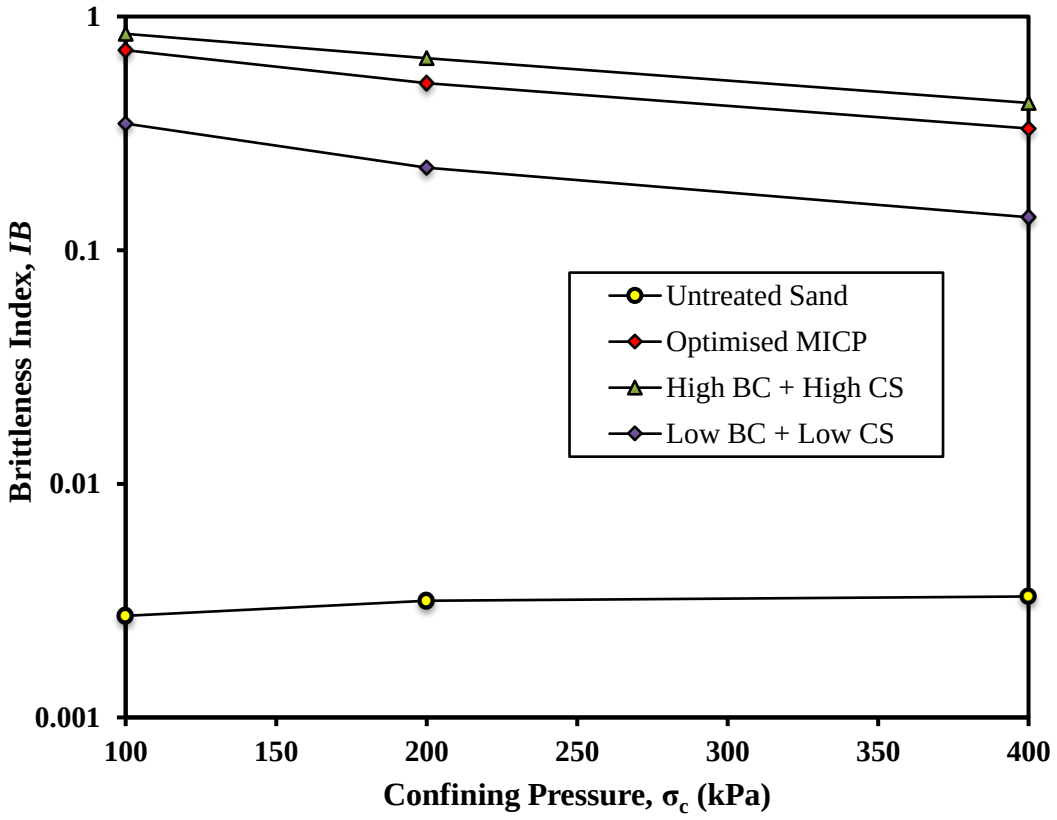

Figure 5.3: Brittleness index of the untreated and the bio-cemented sands

5.2.3 Undrained Peak Failure Envelope

The improved response of the loose treated sand with MICP could occur from two effects i.e. densification (as a result of soil dilation under loading not considering any binding/cementation effects created by the $CaCO_3$ crystals), and cementation (as a result of the $CaCO_3$ crystals binding). Precipitated $CaCO_3$ crystals reduced the sand void ratio and upon undrained shearing, the mean stress will increase until the critical state line (CSL) is reached due to the propensity of sand to dilate (DeJong et al., 2010). Figure 5.4 shows the undrained peak failure envelope for both the untreated and bio-cemented sands, along with the full stress path of the tested specimens. Based on the peak failure envelope of the untreated sand, it is determined that the α (*q-p'* space intercept) and ζ (*q-p'* space slope angle) values are zero kPa and 27°, respectively. The equivalent shear strength parameters are $c' = 0$ and $\phi' = 31°$. On the other hand, the corresponding values of α and ζ for the bio-cemented sand are 278 kPa and 44°, respectively.

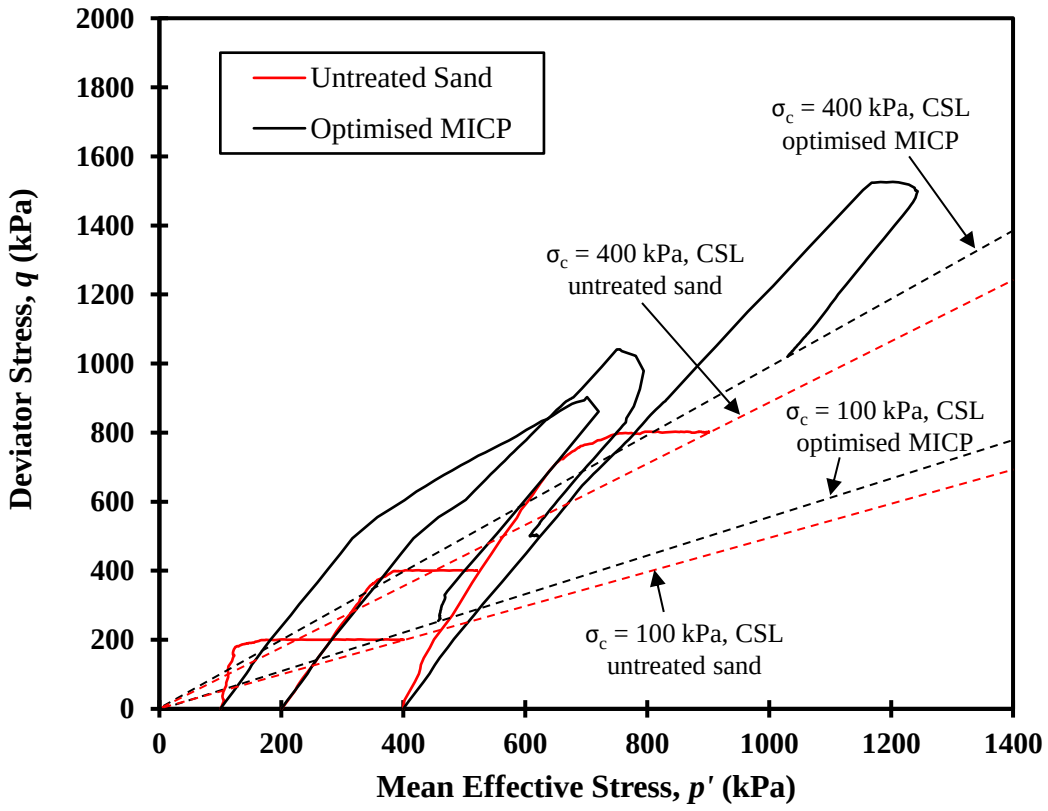

Figure 5.4: Undrained stress path and peak failure envelope for the untreated and optimised bio-cemented sands

The failure envelope of the MICP treated sand was greater than that of the untreated sand since the increased density and particle angularity (from the precipitated $CaCO_3$) increases the resistance to shearing. The CSL prior to and after MICP treatment was shifted due to the $CaCO_3$ changing the particle properties (e.g. shape) and gradation of the sand tested. Cementation of the sand particles together further increases soil strength. The cementation increases the initial stiffness of soil at small strains and the maximum deviatoric stress (q) that can be applied before the specimen begins to yield (Figure 5.4). As the maximum shear resistance is reached, localised shearing and breakage of the $CaCO_3$ cementation bonding initiates. As bonds continue to break, the shear resistance continues to decrease until the soil has completely failed, and the benefit of cementation is lost. However, at this failed state, the benefits of densification are still taking effect as shown by the much higher CSL.

5.3 Response to Different Stress Paths

Figure 5.5 shows the undrained shear stress behaviour of the optimised bio-cemented sand under the constant-p stress path (achieved by increasing σ_1 while decreasing σ_3 at a constant total mean stress where σ_1 and σ_3 are the major and minor principal stresses, respectively; this produces the total stress path shown in Figure 5.6, since $\frac{\Delta\sigma_3}{\Delta\sigma_1} = -0.5$). Based on Figure 5.5(a), the peak q value increases at low axial strain values (1 – 1.3%) with the increase in the confining pressures from 100 kPa to 400 kPa. The peak shear stress occurred at approximately 1% axial strain for both the 100 kPa and 200 kPa confining pressures whereas, for the 400 kPa confining pressure, the peak shear stress transpired at 1.4% axial strain. Clear strain hardening followed by peak shear stress value that eventually developed into strain softening can be seen at the 400 kPa confining pressure condition. However, the behaviour of the optimised bio-cemented specimen under the 100 kPa and 200 kPa confining pressures slightly deviate in terms of no significant peak shear stress was noticed and that the q value levelled off until failure with no visible strain softening observed. It is also noted from Figure 5.5(b) that the excess pore water pressure registered only negative values (signifying high dilation) at the shearing stage, leading to a deviation from its behaviour under the axial compression loading path.

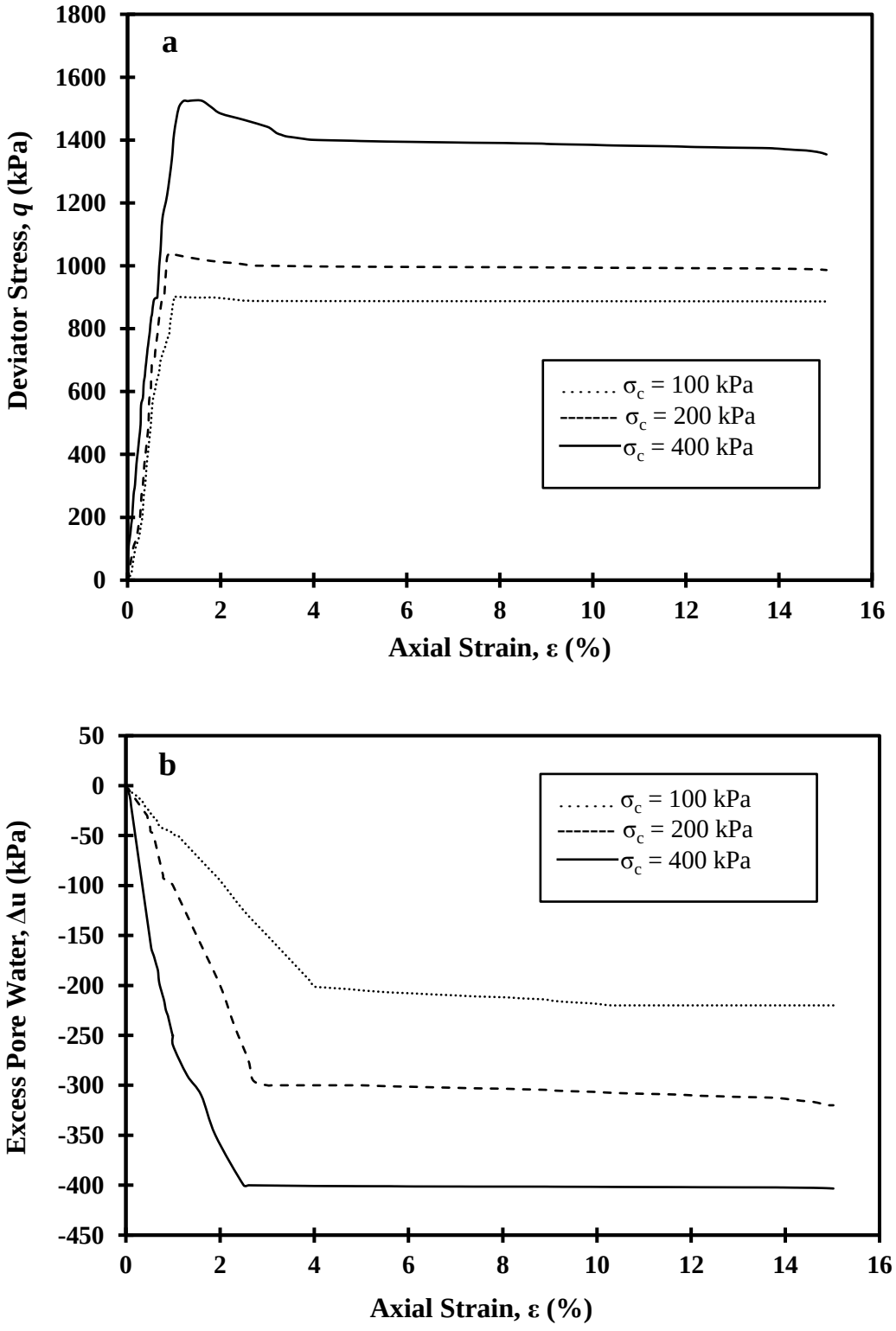

Figure 5.5: Undrained constant-*p* test of the optimised bio-cemented sand: (a) stress-strain curve, and (b) excess pore water pressure

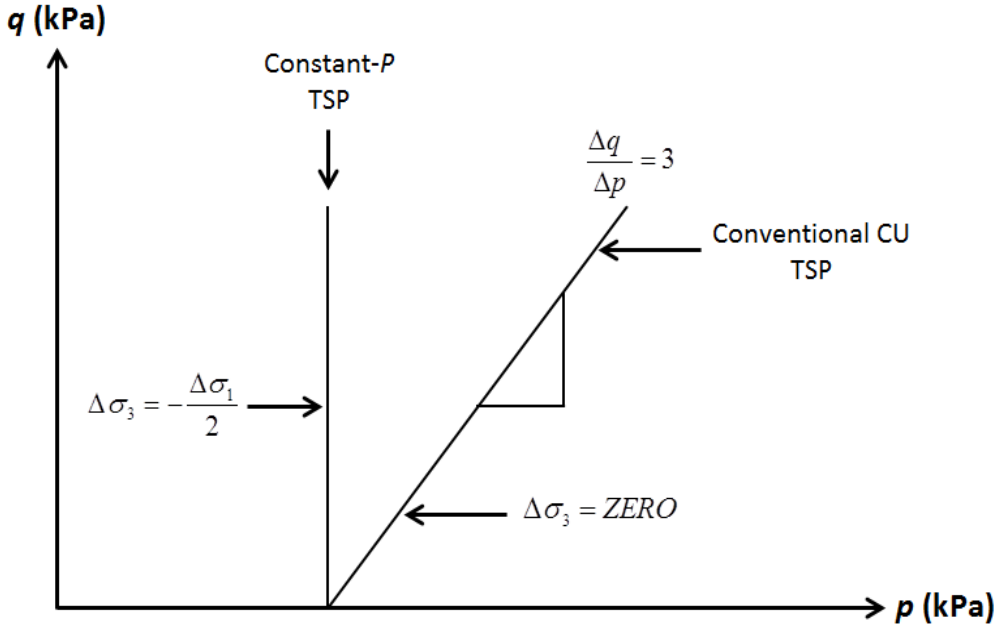

Figure 5.6: Schematic diagram showing the total stress paths

Figure 5.7 shows the effective stress paths for both the axial compression CU and constant-*p* tests. It can be observed from the figure that, for a confining pressure of 100 kPa, the optimised bio-cemented specimens coincidentally behave quite similar in both stress paths loading conditions. Similar behaviour was reported by Montoya & DeJong (2015) under 100 kPa confining pressure. This behaviour under small confining pressure can be attributed to the much slower rate of stiffness reduction due to cementation degradation prior to failure. However, it is noted that for the axial compression CU test, after a certain critical point, the drop in the q value is significant as the p' value increases meanwhile, for the constant-*p* test, q value remains constant. The abrupt reduction in p' when maximum q was reached signifies that the benefit of $CaCO_3$ cementation is lost as bonds continue to break until the soil has completely failed.

Interestingly, the behaviour of the bio-cemented specimens changed in much higher confining pressures, i.e. 200 kPa and 400 kPa. It seemed that in both confining pressure conditions, q value drops significantly in the axial compression CU test while, the drop is less significant in constant-*p* test as the p' value increases.

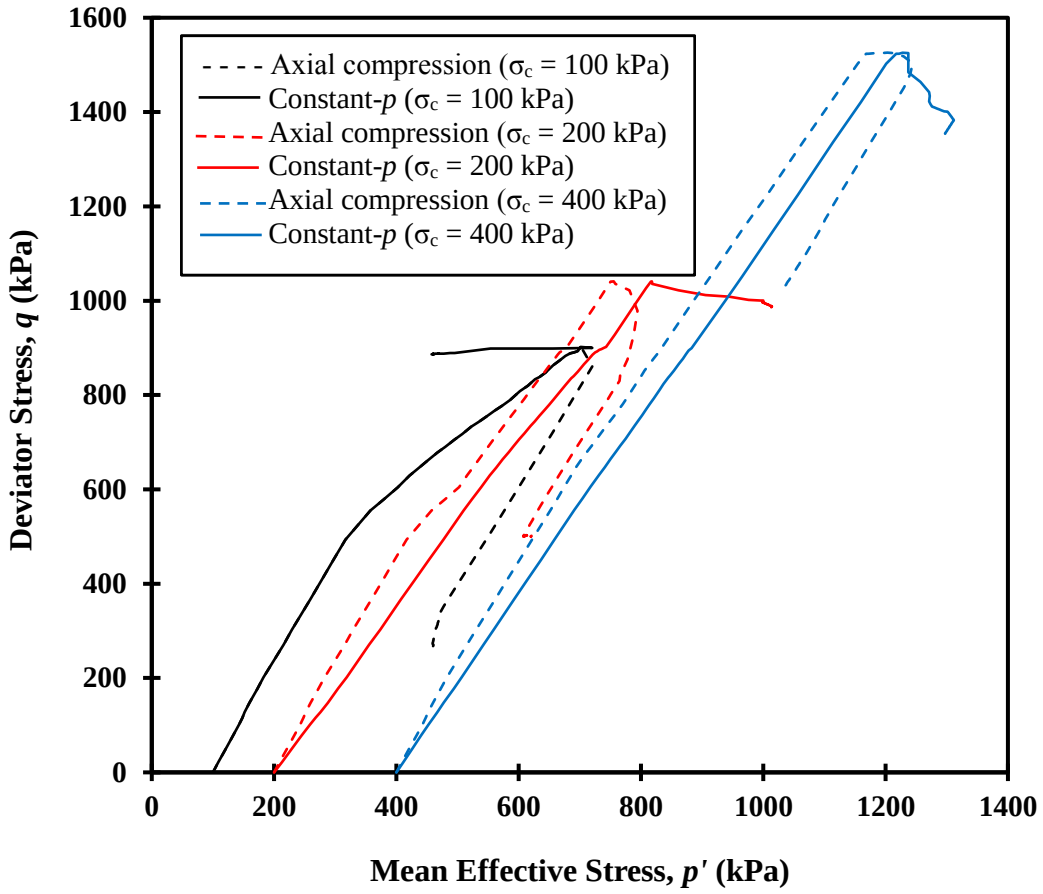

Figure 5.7: Effective stress paths for the axial compression and constant-*p* tests

5.4 Relationship between E_{max} and q_{max} for various geomaterials

To further validate the improved geotechnical properties of the bio-cemented sand using the recipe tested in the current study, the relationship between the maximum elastic modulus, E_{max} (the maximum soil stiffness i.e. the ratio between stress and strain in the elastic soil region), and the maximum deviator stress, q_{max}, for various geo-materials was examined (Figure 5.8). It can be seen that the bio-cemented sands (1 GPa < E_{max} < 10 GPa) behave reasonably well in terms of the soil elastic modulus when compared to other geo-materials; the bio-cemented sand treated using the recipe developed in this study can be positioned in between that of artificially soft rock and also 5 to 6 flushes of using the technique called calcite in-situ precipitation system (CIPS) (Ismail, 2000).

Although the improvement of the mechanical behaviour of the bio-cemented sand proposed by this study performed much lower than that of the concrete, it was revealed that MICP treatment has higher permeability retention compared to that of using cement based reinforcing agent for soil stabilisation (Mujah *et al.*, 2019). Also, the present study could be performed slightly at par with 3 to 4 flushes of CIPS, despite having much lower calcite content, proves that the amount of calcite content does not necessarily correlate to the strength and stiffness improvement; rather, it is the efficacy of the precipitate that is more dominant.

Figure 5.8: Relationship between E_{max} and q_{max} for various geomaterials (modified after Ismail, 2002)

5.5 Comparison of the Shear Strength Parameters

A comparison of the various shear strength parameters obtained from this research and other previous studies in the literature is presented in Table 5.1. The shear strength parameters obtained from the current study (based on the results of the axial compression CU triaxial tests) are the highest when the $CaCO_3$ contents were compared, even for higher $CaCO_3$ from the literature. This signifies the effectiveness of the precipitated $CaCO_3$ crystals formed in the present study. Although the heavily cemented specimen produced by Feng & Montoya (2016) recorded an average $CaCO_3$ content of 5.3% equal the one used in the present study, the improvement in the shear strength parameters was not as significant. This further proves that the unique precipitation pattern of the optimised bio-cemented specimen produced with the recipe presented in the current study is more efficient. However, caution must be made in this generalisation as the properties of the sands used (soil grains size, shapes, and relative densities) could play significant role in the achievement of the improved strength.

Table 5.1: Comparison of the various shear strength parameters

Cementation level	**Reference**	**$CaCO_3$ content (%)**	**c' (kPa)**	**ϕ' (°)**
Lightly cemented	Feng & Montoya (2016)	1.4	5	34
Medium cemented	Feng & Montoya (2016)	2.4	9	38
Medium cemented	**Present study**	**5.1**	**278**	**44**
Medium cemented	Feng & Montoya (2016)	5.3	59	41
Heavily cemented	Terzis et al. (2016)	8.5	253	44
Heavily cemented	Cui et al. (2017)	8	200	42

5.6 Prediction of q_u

The ultimate strength, q_u, of the artificially cemented granular soils is positively influenced by an increase in cement content and decrease in porosity (Wang & Leung, 2008; Rios et al., 2012). It was shown by Consoli et al. (2007) that the adjusted porosity/cement ratio, n/C_{iv}^{c}, could be plotted against q_u to describe a unique hyperbolic relationship for a given soil and cement type, as shown in Equation 5.2 (Consoli et al., 2007):

$$q_u = B\left(\frac{n}{C_{iv}^{c}}\right)^{b} \qquad \text{Equation 5.2}$$

where; n is the sample porosity and C_{iv} is the percentage of the cement volume over the total volume of the specimen. The exponent, c, can be approximated to 1.0 for clean granular soils (Consoli et al., 2013). The term b is the empirical exponent derived from the experiments while the term B is the multiplying factor controlled by the sand matrix properties. The theoretical model presented in the current study was modified from the model developed by Diambra et al. (2017) to predict q_u of artificially cemented sand using Portland cement. The proposed theoretical model to predict the overall constitutive behaviour of the cemented soil herein is based on the consideration that the cemented soil acts as a multiphase material imposing the superposition of the stress contributions of cement bonds as well as the sand grains.

5.6.1 Theoretical Model

The proposed theoretical model assumed that the bio-cemented soil composite is made of the soil phase and the cement phase with the following characteristics:

1. The soil composite is isotropic.
2. The behaviour of the bio-cemented soil at failure is governed by the superposing of both phases contributed by their strengths [following the stress superposition approach proposed by Vatsala et al. (2001)].
3. The failure of the bio-cemented soil composite occurs as a result of the simultaneous failure of both the cemented and soil matrix phases [following the proposed failure mechanism by DeJong et al. (2010)].
4. The strain tensors are compatible with the soil and cement phases [following the parallel spring approach proposed by Vatsala et al. (2001)].

The failure stress state of the bio-cemented soil composite, σ, can be derived from the failure stresses of its constituents, i.e. failure stress of the soil matrix phase, σ_m, and the failure stress of the cement phase, σ_c, following the volumetric averaging approach as shown in Equation 5.3 (Diambra et al., 2013):

$$\sigma = \mu_m \sigma_m + \mu_c \sigma_c \qquad \text{Equation 5.3}$$

where, μ_m and μ_c are the volumetric concentrations of the soil and cement in the bio-cemented soil composite respectively. Equation 5.3 can be expanded in terms of the total mean stress, p, and deviatoric stress, q, components to satisfy the axisymmetric stress conditions of the UCS test procedures, as expressed in Equation 5.4:

$$\begin{bmatrix} q \\ p \end{bmatrix} = \mu_m \begin{bmatrix} q_m \\ p_m \end{bmatrix} + \mu_c \begin{bmatrix} q_c \\ p_c \end{bmatrix} \qquad \text{Equation 5.4}$$

5.6.2 Failure of the Soil Phase

It is assumed that in the soil phase, the grain crushing does not occur during loading; thus, its effect on the strength of the soil matrix and the overall failure mode is therefore, negligible. The density-dependent deviatoric stress and mean stress ratio, $\frac{q_m}{p_m}$, is normally used to represent the strength of granular soils. Diambra et al. (2017) introduced a state parameter, ψ, which is the ratio between the current density state with the density at the critical state, to link the strength of the material as shown in Equation 5.5:

$$\psi = \frac{n_{cs}}{n} \qquad \text{Equation 5.5}$$

where; n represents the current soil porosity and n_{cs} refers to the critical state soil porosity. $\psi > 1$ represents the state on the loose side of the critical state line (CSL) and $\psi < 1$ represents the state on the dense side of the CSL. According to Diambra et al. (2017), the granular soil stress ratio at failure can then be expressed by Equation 5.6:

$$\frac{q_m}{p_m} = M^* = M\left(\frac{n_{cs}}{\eta}\right)^a \qquad \text{Equation 5.6}$$

where; $M^*$is the peak strength, M is the critical state strength and a is the model parameter that links the peak strength to the state parameter.

5.6.3 Failure of the Cement Phase

The strength of the cement phase can be described using the Drucker-Prager failure criterion, as presented by Diambra et al. (2017) in Equation 5.7:

$$q_c = c_c + M_c p_c \qquad \text{Equation 5.7}$$

where; c_c is the cohesion of cement phase and M_c is the slope of the failure line for cement phase in the $q_c - p_c$ plane, can be linked to the uniaxial compressive strength, σ_c^c, and the uniaxial tensile strength, σ_c^t, of the cementing agent by the following expressions:

$$c_c = 2\left(\frac{\sigma_c^c}{1-\beta}\right) \qquad \text{Equation 5.8}$$

and

$$M_c = 3\left(\frac{\beta+1}{\beta-1}\right) \qquad \text{Equation 5.9}$$

where; β is the ratio between the uniaxial compressive and the tensile strengths:

$$\beta = \frac{\sigma_c^c}{\sigma_c^t} \qquad \text{Equation 5.10}$$

5.6.4 Strength Relationship for the Bio-Cemented Sand

Substituting Equations 5.6 and 5.7 into Equation 5.4, q_u can be derived as:

$$q_u = 3\mu_c \left(\frac{c_c + M_c p_c - M^* p_c}{3 - M^*} \right) \quad \text{Equation 5.11}$$

An estimation of the confining stress of the current cement phase, p_c, is required to ensure that Equation 5.11 is expressed in terms of the soil and cement phase strength only. Hence, it is assumed that the artificially cemented soil exhibits a quasi-elastic behaviour up to the peak strength under the UCS test conditions. Therefore, the radial strain of the cemented soil, ε_r, and the axial strain of the cemented soil, ε_a, can be linked in Equation 5.12 (Diambra et al., 2017):

$$\varepsilon_r = -\nu \varepsilon_a \quad \text{Equation 5.12}$$

where; ν is the bio-cemented soil composite Poisson' ratio. It is possible to derive the cement stress ratio, K_c (Equation 5.13) based on the approximation between the ratio of deviatoric stress, q_c, and isotropic stress, p_c, assuming the strain compatibility condition that both the soil and cement phases experienced the same strain field at which, they are behaving elastically up to the peak strength (Diambra et al., 2017):

$$\frac{q_c}{p_c} = K_c = 3\left(\frac{1+\nu}{1+\nu_c} \right)\left(\frac{1-2\nu_c}{1-2\nu} \right) \quad \text{Equation 5.13}$$

where; ν_c is the cement Poisson' ratio. The combination of Equation 5.7 and Equation 5.13 yields the expression for isotropic stress at failure for the cement phase Equation 5.14 (Diambra et al., 2017):

$$p_c = \frac{c_c}{K_c - M_c} \qquad \text{Equation 5.14}$$

By substituting Equation 5.14 into Equation 5.11, the following relationship for q_u is obtained:

$$q_u = \left(\frac{6\mu_c \sigma_c^c}{K_c(1-\beta)+3(\beta+1)} \right) \left[\frac{K_c - M\left(\frac{n_{cs}}{n}\right)^a}{3 - M\left(\frac{n_{cs}}{n}\right)^a} \right] \qquad \text{Equation 5.15}$$

Equation 5.15 provides a direct expression for q_u of the bio-cemented soil as a function of the porosity, n and the volumetric concentration of the cement, μ_c provided that the parameters given in Table 5.2 are constant relative to the soil and cement phases. The value of the soil porosity at the critical state is considered a soil constant independent of the mean effective stress.

Table 5.2: Proposed model parameters

Phase	**Variable**	**Symbol**	**Values**		
			LC	**MC**	**HC**
Soil phase	Critical state soil strength ratio	M	1.36	1.36	1.36
	Critical state soil porosity	n_{cs}	40%	40%	40%
	Parameter governing dependence of soil strength and density	a	1.2	2.3	3.1
Cement phase	Compressive cement strength	σ_c^c	1.2 MPa	1.8 MPa	3.5 MPa
	Tensile cement strength	σ_c^t	0.3 MPa	0.4 MPa	0.7 MPa
	Cement strength ratio	β	4	4.5	5
	Cement stress ratio	K_c	-6	-5	-3

LC = Lightly cemented silica sand
MC = Medium cemented silica sand
HC = Heavily cemented silica sand

5.6.5 Calibration of Model Parameters

The values of the critical state strength ratio, M (linked to the critical state friction angle, ϕ) and the critical state porosity, n_{cs}, were derived from the triaxial tests conducted in the laboratory. A series of 3 sets of triaxial tests comprising of different degree of cementation; lightly cemented (2–4% calcite content), medium cemented (4–6% calcite content), and heavily cemented (> 6% calcite content) were prepared in the laboratory. The estimation of the parameter a for the soil was made from the calibration exercise of the data obtained through Equation 5.6 with the UCS values shown in Figure 5.9. The value of the parameter β relative to the cement phase was selected based on the typical ranges of the uniaxial compression and tensile cement strength values for bio-cemented soil based on the UCS and the tensile strength tests conducted in the laboratory (Appendix F). Since the value of the parameter K_c is dependent on the Poisson's ratios of the cemented soil and the cement phase, a constant value of $K_c \cong 4$ is adopted (Diambra et al., 2017). The strength parameter of the cementing phase, σ_c^c, was determined by matching the UCS given by Equation 5.15 with the experimental results.

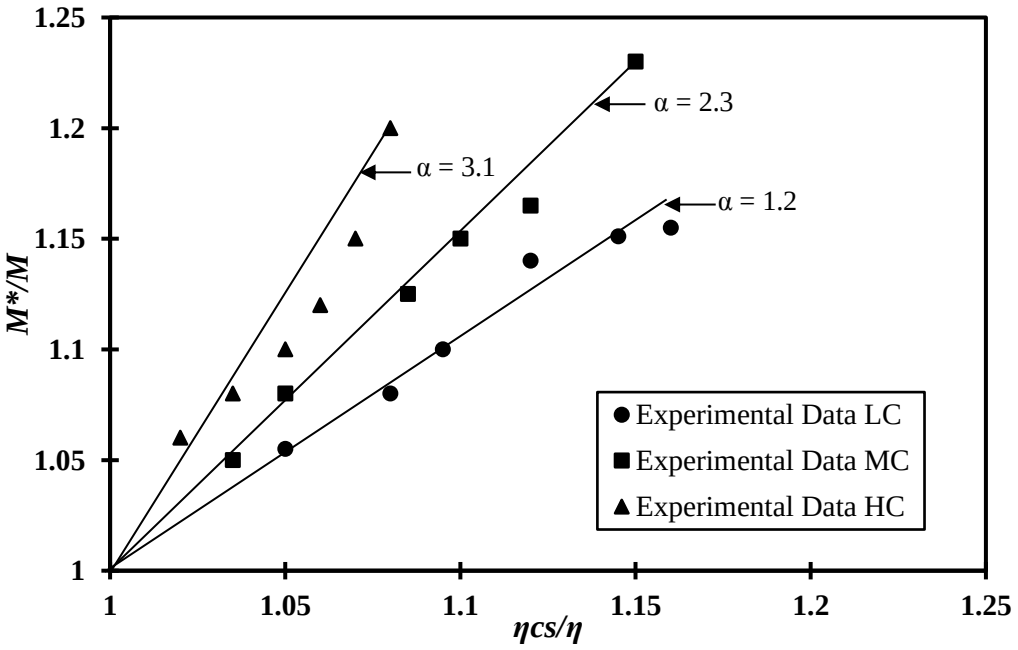

Figure 5.9: Calibration of the parameter a for soil using peak strength data from triaxial test

5.7 Theoretical Model Prediction

The model predictions and the experimental results versus the n/C_{iv} ratio for the three cementation levels are shown in Figure 5.10. Figure 5.10(a-c) shows clearly that the model predicts the q_u values reasonably well. For example, in the lightly cemented sand condition [Figure 5.10(a)], both data converge into a similar curve, though the slope of the experimental data is steeper than the model prediction especially from 15 to 20 n/C_{iv} values. In the case of medium cementation, Figure 5.10(b) shows that the model underestimates the experimental data at strength levels higher than 1500 kPa; however, the model begins to converge well with the experiment data at 8 to 10 n/C_{iv} values. In the heavily cemented sand condition [Figure 5.10(c)], the model slightly overestimated the experimental data. Figure 5.10(d) shows the direct comparison between the model predictions and the experiment results. The results demonstrate that the compared data relates well with each other. Nevertheless, it must be noted that slight discrepancies exist in the data arising from the difficulty in estimating the exact percentage of cementation. This difficulty has been circumvented by combining the strength of the cemented bonds to be considered as a unique model parameter.

The observations made in this study were based on the use of Silica sand with mostly round soil grains shape cemented with the effective $CaCO_3$ crystals. The accuracy of the model prediction may differ if: (1) different soil properties, e.g. soil grains size and shape were used. Ismail et al. (2002a) reported the influence of the soil particle size and shape (round or non-angular grains) towards the strength of the cemented soil; and (2) different cementation bonding parameters were applied based on the type of the CCPP. It is shown that the different type of CCPP would produce different strength improvement as concluded in Section 4.3, as it affects the peak strength of the bio-cemented specimens.

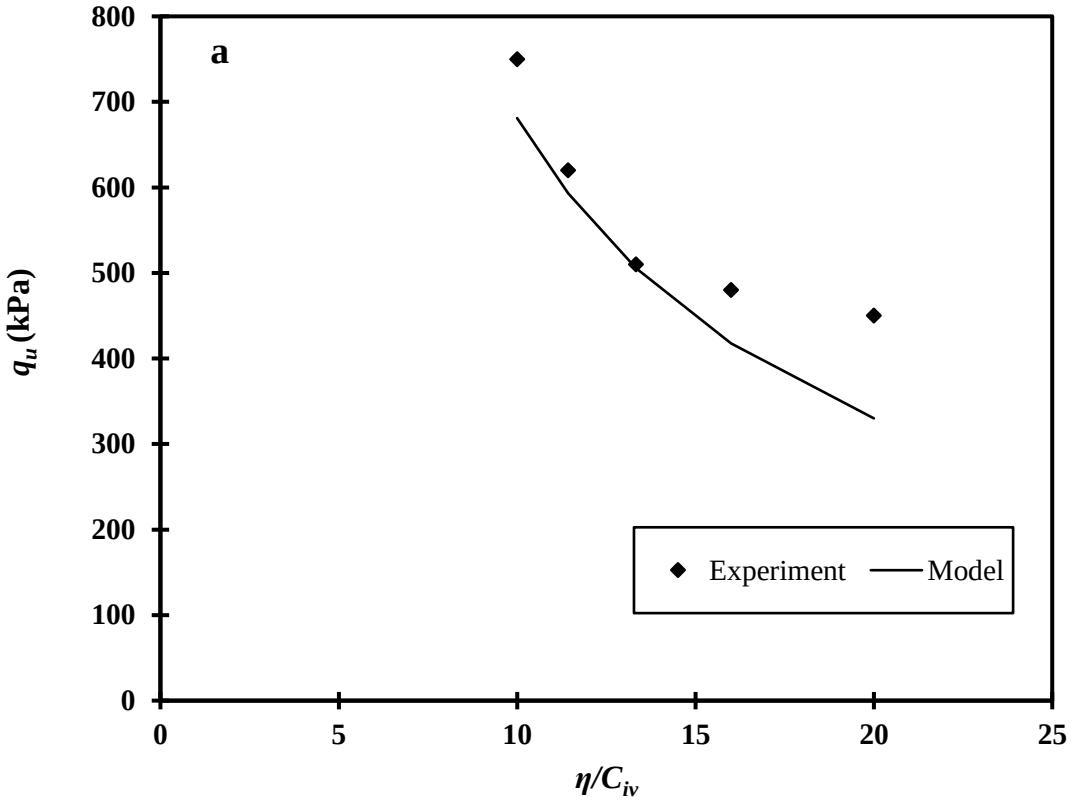
a
800
700
600
500
400
300
200
100
0
q_u (kPa)
0
5
10
15
20
25
η/C_{iv}
Experiment
Model

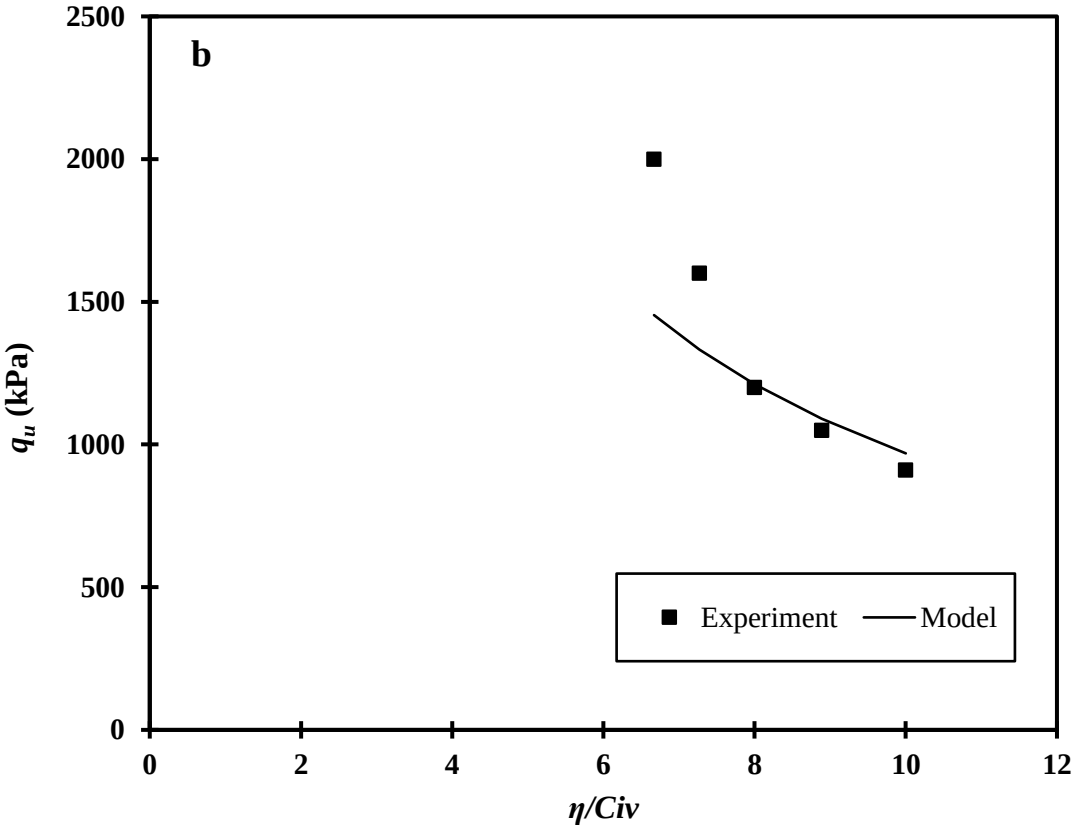
b
2500
2000
1500
1000
500
0
q_u (kPa)
0
2
4
6
8
10
12
η/Civ
Experiment
Model

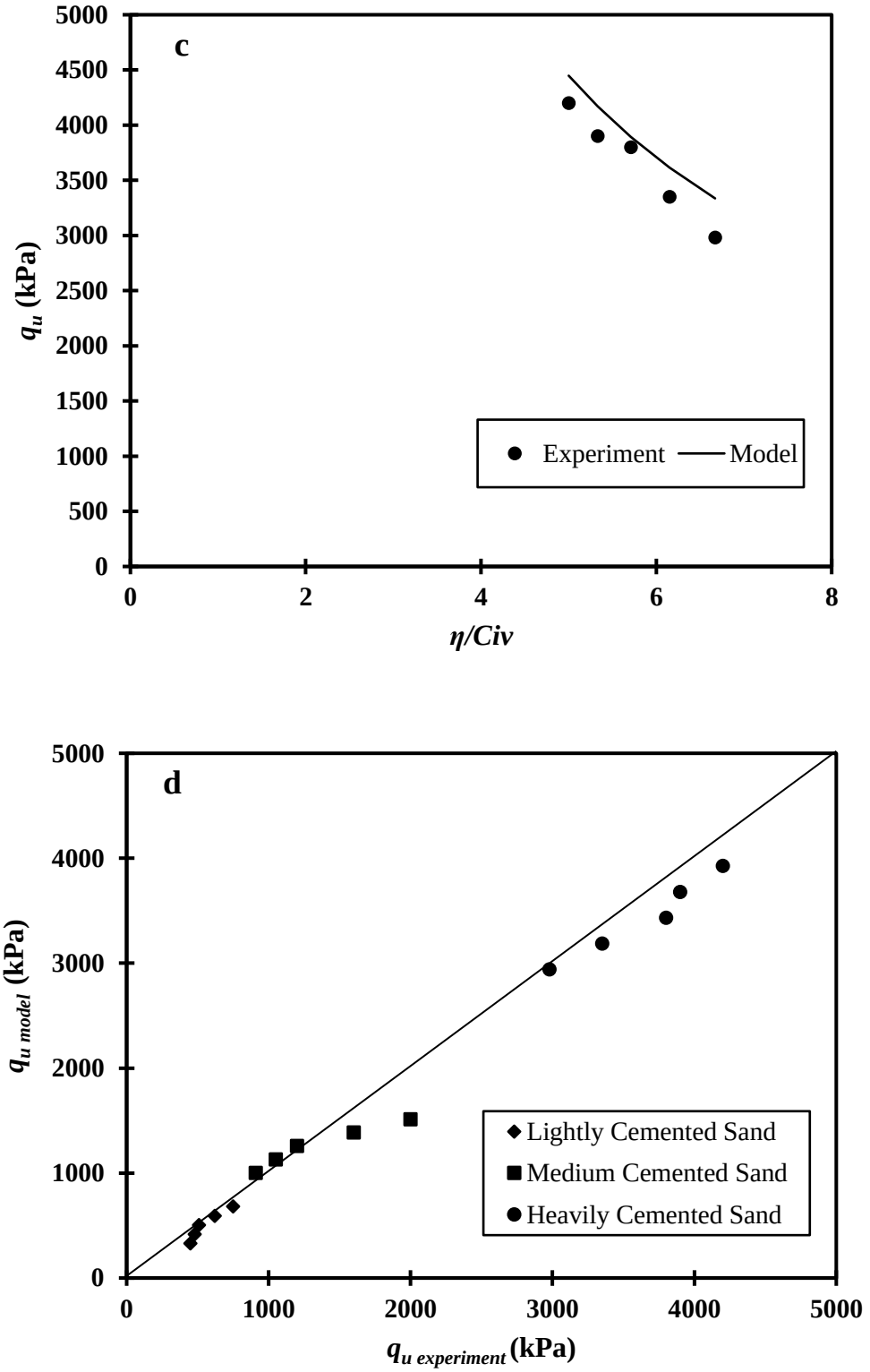

Figure 5.10: Comparison between model predictions and experimental results: (a) lightly cemented sand; (b) medium cemented sand; (c) heavily cemented sand; and (d) direct comparison between model predictions and experimental results

5.8 Summary

The geotechnical behaviour of the optimised bio-cemented specimens was examined in this chapter. Experimental programs consisting of the isotropically consolidated undrained compression tests (CU) under different confining pressures (100, 200 and 400 kPa) and specialist stress paths were performed. The stress path analyses include the axial compression and constant-*p* analysis. The experimental data were compared with the available data published in the literature in terms of their respective shear strength parameters (ϕ' and c') in order to verify the effectiveness of the optimised bio-cemented specimens treated with the combination of 32 U/mL BC and 0.25 M CS concentrations. The results confirmed that the proposed MICP recipe has greatly improved the shear strength parameters of the optimised bio-cemented sand compared to the untreated sand and previous studies.

An analytical model to predict the q_u value of bio-cemented sand was analysed and compared with the experimental data. The results showed reasonable convergence of the compared data. It must be noted that discrepancy arises from the difficulty in estimating the exact percentage of cementation has been circumvented by combining the strength of the cemented bonds to be considered as a unique model parameter. In the following chapter, general summary and comprehensive conclusions with recommendations for future work are presented.

Chapter 6

Summary, Conclusions and Recommendations

6.1 Summary

This thesis investigated a new (or modified) technique whereby sands can be cemented artificially by calcite ($CaCO_3$). This technique is achieved through the precipitation of effective $CaCO_3$ crystals. It is based on using urease bacteria in a biochemistry reaction to produce the effective $CaCO_3$. The thesis presented the results of a comprehensive study aimed at understanding the different $CaCO_3$ crystals precipitation patterns. The work focused on determining the optimum design of the process (procedure, concentrations and the effective $CaCO_3$ crystal precipitation) for potential field application. In terms of the depositional environment for the artificial $CaCO_3$, the results showed that the MICP treatment favoured basic soil pH and ambient surface temperature conditions. Also, it was revealed that fine sand (0.15 mm in diameter) is more durable than coarse sand in resisting harsh conditions while the impact was minor in well-graded sand. It was also noted that MICP treatment failed to perform if rainwater was flushed, immediately after the bacteria placement or even 24 hours after.

In this study, effective $CaCO_3$ was proposed by successfully combining the different bacteria culture (BC) and cementation solution (CS) concentrations in the laboratory. The results revealed that the combination of a high BC concentration (32 U/mL) and a low CS concentration (0.25 M) produced the most effective CCPP with distinctive characteristics of the produced crystals: (1) relatively large crystals; (2) rhombohedral crystal shape and (3) effectively concentrated at the soil pore throats. This combination also yielded the highest strength improvement and the lowest reduction in permeability, suggesting that the said combination is the most optimum for field application requiring strength improvement and permeability retention.

Examination into the chemical coefficient efficiency (CCE) revealed that the optimum number of CS injection for the optimised combination of reagents used in the present study is 4. More injections proved less effective in forming more $CaCO_3$ crystals. Obviously, knowledge of the optimum number of CS injection is vital for feasibility of field applications, to ensure full consumption of the supplied BC without economic wastage in each treatment cycle.

The optimised bio-cemented specimens were compared to the conventional chemical stabilisation technique using ordinary Portland cement (OPC) treated specimens after 28-day curing. The results showed that the optimised bio-cemented specimens performed better in terms of higher strength and higher permeability. The superiority of the bio-cementation is believed to result from the intrinsic features of the effective $CaCO_3$ crystals compared with the formation of the calcium silicate hydrate (C-S-H) gel like structure found in the OPC treated specimens.

A comprehensive electron microscope (SEM) study was undertaken to study the precipitation mechanism of the various calcite crystal precipitation patterns (CCPP) produced as a result of the precipitated $CaCO_3$ crystals proposed in this study. The SEM images successfully captured the process of bacteria attachment onto the sand grains, which instigates formation of: nucleation sites, metastable primary spherical shaped precipitates; and cluster of effective $CaCO_3$ crystals that precipitate strategically at the soil pore throats. The unique characteristics of the effective $CaCO_3$ crystals were determined through the microstructural imaging.

A theoretical model based on the concept of superposition of strength contributions from both the soil and cement phases was also developed. The model assumes that the soil behaves in accordance with the critical state soil concept, while the strength of the cemented phase is described using the Drucker-Prager failure criterion. In this model, the ultimate strength, q_u , of the bio-cemented sand is a function of the adjusted porosity/cement parameter. The model successfully predicted the experimental and theoretical data reasonably well.

The mechanical behaviour of the untreated and the optimised bio-cemented specimens was assessed using triaxial testing. CU tests under different confining pressures of 100, 200 and 400 kPa and stress paths (axial compression and constant-*p*) were performed. The results showed that increasing the confining pressures from 100 kPa to 400 kPa increased the yield stress of both the untreated and optimised bio-cemented specimens. For the optimised bio-cemented specimen, under 100 kPa and 200 kPa confining pressures, insignificant effect on the increased stiffness was observed. However, under the 400 kPa confining pressure, a noticeable change in the axial strain value is required to increase the peak stress, demonstrating the effect of the high confining stress on the optimised bio-cemented specimen stiffness. Strong negative pore pressures were observed in all confining pressures and the 400 kPa confining pressure lead to a larger negative pore pressure.

The dilation tendency of the bio-cemented specimens occurred at different strain values regardless of the confining pressures. The high brittleness index, value observed in the 400 kPa confining pressure indicates that more degradation in the $CaCO_3$ bond occurs in the residual stress zone, which leads to failure. It is also noted that the residual stress values for the optimised bio-cemented specimen recorded higher values at high strains compared to the peak stress values attained in the untreated sand sample. The behaviour of the optimised bio-cemented specimens are characterised by a strain softening response with gradual degradation towards the residual strength until failure.

Examination into the mechanical improvement of the optimised bio-cemented sands treated using the recipe developed in this study behaves reasonably well compared to other geomaterials. Based on the comparison of the various geomaterials, it can be concluded that the optimised bio-cemented sands produced by the current study can be positioned in between that of artificially soft rock and 5 to 6 flushes of using the calcite in-situ precipitation (CIPS) technique. Moreover, using the proposed CCPP developed in this study, the shear strength parameters of the optimised bio-cemented sands are generally higher than their counterparts from earlier MICP treatments.

6.2 Conclusions

The work presented in this thesis explores the different types of the $CaCO_3$ crystals precipitation patterns (CCPP) and how they affect the engineering properties of bio-cemented sands. For this purpose, different combinations of MICP reagents (BC and CS) were examined and the optimum combination that produced the desired engineering properties improvement as outlined in this thesis was presented. Investigation into the MICP treatment process optimisation led to the following findings:

- For optimum results, MICP treatment is best conducted at neutral soil conditions (pH around 7).
- For optimum results, MICP treatment is best performed at ambient surface temperature (25°C). This temperature is the most optimum condition for the bacterium species used in this study, i.e. *Bacillus sp*.
- Fine sand (0.15 mm in diameter) is more durable than the coarse sand (1.18 mm in diameter) under the action of up to 10 FT cycles. While the impact is minor towards well-graded sand.
- MICP treatment would fail to perform if rainwater is flushed 24 hours and/or immediately after the bacteria placement into the treated sand column.
- Different CCPPs produced different engineering properties in the bio- cemented sand. The combination of 32 U/mL BC and 0.25 M CS yielded the highest strength improvement in terms of UCS value. The combination of 32 U/mL BC and 0.25 M CS yielded the lowest permeability reduction value of about 40%.
- Precipitation of relatively large, rhombohedral $CaCO_3$ crystals that concentrate at the soil pore throats proved to be highly effective in terms of enhancing the engineering properties of the bio-cemented sand.
- The optimised bio-cementation provided better levels of improvement compared with earlier studies.
- One excellent feature of the optimised MICP process is that the increase in the produced amount of $CaCO_3$ is associated with the increase in the size of their crystals, a critical reason for superiority of the technique.

- The optimised bio-cemented sand samples shown brittle behaviour compared with the OPC treated sand samples within the tested cementation levels.
- Comparison of the optimised bio-cemented specimens with the previous MICP treated specimen by other studies revealed that the optimised bio-cemented material performed better in terms of the strength improvement, except against the partial saturation technique; however, such a technique was shown to be impractical for field application.

Investigation into the microstructural analysis of the precipitation mechanism of the effective $CaCO_3$ crystals evolution and their unique features led to the following findings:

- After the first injection, bacteria attachment onto the sand grains that leads to the birth of nucleation sites is shown.
- After the second injection, the formation of metastable primary spherical shaped precipitates before they morph into the secondary more stable precipitate form was demonstrated.
- After the third injection, a cluster of single crystal creating mesocrystals that successively form the effective $CaCO_3$ crystals was captured.
- After the fourth injection, the precipitation of the effective $CaCO_3$ crystals concentrated at the soil pore throat was noted.
- Transition of the metastable primary precipitate towards the more stable secondary single crystal was also captured after the second injection using 0.167 mol/L/h input rate. This transition phase is only observed when the input rate is more than 0.042 mol/L/h.
- The microstructural analysis revealed that the concentration of the $CaCO_3$ crystals at the soil pore throat stems from two main factors: (1) availability of the rich nutrient in that area; and (2) the lower stresses existing in the menisci region of the soil pore throats.

- Another feature of the effective $CaCO_3$ crystals is their relatively large size (normally > 20 μm) compared to the available recorded size of the previous $CaCO_3$ crystals (normally 5 < size < 10 μm). This can be attributed to the progressive increase in the supersaturation condition as a result of the increase in the concentrations of the Ca^{2+} and CO_3^{2-} ions in the MICP environment thus, leading to the accumulation of succeeding precipitations over the initial small $CaCO_3$ crystals.
- Another feature of the effective $CaCO_3$ crystals is their final development into a rhombohedral shape that provides better interlocking mechanism for more shear resistance.

Investigation into the effect of the effective $CaCO_3$ crystals precipitation into the optimised bio-cemented sand geotechnical behaviours led to the following findings:

- Increasing the confining pressure from 100 kPa to 400 kPa generally increase the peak stress values of all the untreated and optimised bio-cemented specimens.
- At confining pressure = 100 kPa, the optimised bio-cemented specimen attained peak q = 890 kPa at ε = 1%, followed by strain softening behaviour.
- At higher confining pressures of 200 kPa and 400 kPa, peak q = 1040 kPa and peak q = 1525 kPa were attained at ε = 0.95% and ε = 1.4%, respectively.
- Strong negative pore pressures were observed in all confining pressures.
- Dilation tendency occurred at different strain values of 4%, 3% and 2% axial strains for the confining pressures of 100 kPa, 200 kPa and 400 kPa respectively.
- 100 kPa confining pressure shows the highest I_B value of 0.72, followed by I_B value for the 200 kPa confining pressure of 0.52 and the I_B value for the 400 kPa confining pressure of 0.33.
- The residual stress values for the optimised bio-cemented specimen still show higher values at high strains compared to the peak stress values attained in the untreated sand sample.
- The optimised bio-cemented sand developed higher failure envelope than that of the untreated sand.

- The loading paths influence the behaviour of the MICP treated specimen. Under constant-*p* stress path, clear strain hardening followed by peak shear stress value that eventually developed into strain softening can be seen under the 400 kPa confining pressure condition. No significant peak shear stress was noticed under 100 kPa and 200 kPa confining pressures and that the *q* value levelled off until failure with no visible strain softening observed.
- *E* and the shear strength parameters values (c' = 278 kPa and ϕ' = 44°) of the optimised bio-cemented specimen performed and improved well as compared to previous studies within the tested range.

6.3 Recommendations for Future Work

Although this thesis has provided a significant contribution regarding the development of the newly proposed effective $CaCO_3$ crystals to improve the engineering properties of the bio-cemented sand, further issues should be addressed for future work, including the following items:

1. The proposed combination of the MICP reagents used in the current study, i.e. 32 U/mL BC and 0.25 M CS, was sourced from one type of bacterium species and that the CS concentration was based on the equimolar ratio of $CO(NH_2)_2$ and $CaCl_2$. Using different types of ureolytic bacteria with either higher or lower BC concentrations and different non-equimolar concentrations of CS may yield different results.

2. Natural silica sand was used as the main soil for the purpose of this study. Different types of soils might react differently to the different CCPP as the soils have different shape, size and mineralogy characteristics. One interesting type of soil recommended for future work is calcareous sand, which mostly or partly contains calcite particles. It is worthwhile to understand the effect of the calcite particles already present in the sand grains as to whether they can produce soluble calcium that can be used as calcium source for the MICP process to improve the properties of the bio-cemented sands.

3. Although the current injection technique that employed the method called the two-phase injection seemed to have fully cemented the bio-cemented specimens (laboratory-scaled column), the fact remains that this technique was deemed unsuccessful when a long column of 1 m in height was tried (results not shown). The main issue with the current technique is that it cannot distribute the effective $CaCO_3$ crystals homogenously throughout the entire column. The two-phase injection method was carried out by injecting a half void volume of BC, followed by injecting a half void volume of CS during the first injection. The sample was left to cure for 24 hours to allow for the bacteria to attach to the soil grains. After 24 hours, full void volume of CS was then injected into the sand column. The sample was left to cure for 24 hours to allow for $CaCO_3$ precipitation (second injection). After 24 hours, another full void volume of CS was supplied and left to cure for 24 hours (third injection). These procedures were repeated several times for each individual sand column in order to gain different degrees of cementation, which leads to the different desired strength and stiffness. The effective $CaCO_3$ crystals non-homogeneous precipitation pattern stems from the failure to distribute the bacteria cells (eventually become the nucleation sites for new crystal growth) throughout the entire column depth. The reality is that most of the precipitation occurred within the top half of the column depth (fully cemented part) leaving the bottom half of the column either partially cemented or completely uncemented. Hence, it is recommended that future work focus on searching for a new technique to improve the process.

4. Current study focuses more on the microscale analysis of the newly proposed CCPP without looking at the behaviour of the proposed CCPP on real field application. It is recommended that future work would examine the implementation of using the newly proposed CCPP on real field test to assay its relevance towards field application. Although the current study did not test the newly proposed CCPP for field trial, the understanding of its precipitation mechanism, its microstructural characteristics and the bio-cemented sand performance treated with its recipe are well documented.

References

Australian Standards (2001). Methods of testing soils for engineering purposes (Soil strength and consolidation tests - Determination of permeability of a soil - Constant head method for a remoulded specimen) AS 1289.6.7.1.

Australian Standards (2008). Methods for preparation and testing of stabilized materials (Unconfined compressive strength of compacted materials) AS 5101.4.

Australian Standards (1998). Soil strength and consolidation tests – Determination of the compressive strength of a soil (Compressive strength of a saturated specimen tested in undrained triaxial compression with measurement of pore water pressure) AS 1289.6.4.2.

Achal, V., Mukerjee, A. and Sudhakara Reddy, M. (2013). Biogenic treatment improves the durability and remediates the cracks of concrete structures. *Construction and Building Materials,* 48, 1-5.

Achal, V., Mukherjee, A., Kumari, D. and Zhang, Q. (2015). Biomineralization for sustainable construction – A review of processes and applications. *Earth-Science Reviews,* 148, 1-17.

Achal, V., Mukherjee, A. and Reddy, M. S. (2011). Microbial concrete: Way to enhance the durability of building structures. *Journal of Materials in Civil Engineering,* 23(6), 730-734.

Akiyama, M. and Kawasaki, S. (2012). Novel grout material comprised of calcium phosphate compounds: In vitro evaluation of crystal precipitation and strength reinforcement. *Engineering Geology,* 125, 119-128.

Al-Thawadi, S. M. (2008). *High strength in-situ biocementation of soil by calcite precipitating locally isolated ureolytic bacteria.* PhD Thesis, Murdoch University, Australia. p. 272.

Al-Thawadi, S. M. (2011). Ureolytic bacteria and calcium carbonate formation as a mechanism of strength enhancement of sand. *Journal of Advanced Science and Engineering Research,* 1, 98-114.

Al-Thawadi, S. M. (2013). Consolidation of sand particles by aggregates of calcite nanoparticles synthesized by ureolytic bacteria under non-sterile conditions. *Journal of Chemical Science and Technology,* 2(3), 141-146.

Al-Thawadi, S. M. and Cord-Ruwisch, R. (2012). Calcium carbonate crystals formation by ureolytic bacteria isolated from Australian soil and sludge. *Journal of Advanced Science and Engineering Research,* 2, 12-26.

Al Qabany, A. and Soga, K. (2013). Effect of chemical treatment used in MICP on engineering properties of cemented soils. *Géotechnique,* 63(4), 331-339.

Al Qabany, A., Soga, K. and Santamarina, C. (2012). Factors affecting efficiency of microbially induced calcite precipitation. *Journal of Geotechnical and Geoenvironmental Engineering,* 138(8), 992-1001.

Amin, M., Zomorodian, S. M. A. and O'Kelly, B. C. (2017). Reducing the hydraulic erosion of sand using microbial-induced carbonate precipitation. *Proceedings of the Institution of Civil Engineers - Ground Improvement,* 170(2), 112-122.

Amini, Y. and Hamidi, A. (2014). Triaxial shear behavior of a cement-treated sand–gravel mixture. *Journal of Rock Mechanics and Geotechnical Engineering,* 6(5), 455-465.

Anbu, P., Kang, C. H., Shin, Y. J. and So, J. S. (2016). Formations of calcium carbonate minerals by bacteria and its multiple applications. *Springerplus,* 5, 250.

Assadi-Langroudi, A., Ng'ambi, S. and Smalley, I. (2018). Loess as a collapsible soil: Some basic particle packing aspects. *Quaternary International,* 469, 20-29.

Bishop, A. (1971). The influence of progressive failure on the choice of the method of stability analysis. *Geotechnique,* 21(2), 168-172.

Bhaduri, S., Debnath, N., Mitra, S., Liu, Y. and Kumar, A. (2016). Microbiologically induced calcite precipitation mediated by sporosarcina pasteurii. *Journal of Visualized Experiments,* 10.3791/53253(110).

Bosak, T. and Newman, D. K. (2005). Microbial kinetic controls on calcite morphology in supersaturated solutions. *Journal of Sedimentary Research,* 75, 190-199.

Burbank, M. B. (2010). *Precipitation of calcite by indigenous microorganisms to strengthen soils.* PhD Thesis, University of Idaho, USA. p. 104.

Burbank, M. B., Weaver, T. J., Green, T. K., Williams, B. C. and Crawford, R. L. (2011). Precipitation of calcite by indigenous microorganisms to strengthen liquefiable soils. *Geomicrobiology Journal,* 28(4), 301-312.

Burbank, M. B., Weaver, T. J., Williams, B. C. and Crawford, R. L. (2012). Urease activity of ureolytic bacteria isolated from six soils in which calcite was precipitated by indigenous bacteria. *Geomicrobiology Journal,* 29(4), 389-395.

Cheng, L. (2012). *Innovative ground enhancement by improved microbially induced CaCO3 precipitation technology.* PhD Thesis, Murdoch University, Australia. p. 252.

Cheng, L. and Cord-Ruwisch, R. (2012). In situ soil cementation with ureolytic bacteria by surface percolation. *Ecological Engineering,* 42, 64-72.

Cheng, L. and Cord-Ruwisch, R. (2013). Selective enrichment and production of highly urease active bacteria by non-sterile (open) chemostat culture. *Journal of Industrial Microbiology & Biotechnology,* 40(10), 1095-1104.

Cheng, L. and Cord-Ruwisch, R. (2014). Upscaling effects of soil improvement by microbially induced calcite precipitation by surface percolation. *Geomicrobiology Journal,* 31(5), 396-406.

Cheng, L., Cord-Ruwisch, R. and Shahin, M. A. (2013). Cementation of sand soil by microbially induced calcite precipitation at various degrees of saturation. *Canadian Geotechnical Journal,* 50(1), 81-90.

Cheng, L. and Shahin, M. A. (2016). Urease active bioslurry: a novel soil improvement approach based on microbially induced carbonate precipitation. *Canadian Geotechnical Journal,* 10.1139/cgj-2015-0635, 1-10.

Cheng, L. and Shahin, M. A. (2017). Stabilisation of oil-contaminated soils using microbially induced calcite crystals by bacterial flocs. *Géotechnique Letters,* 7(2), 1-6.

Cheng, L., Shahin, M. A. and Cord-Ruwisch, R. (2014). Bio-cementation of sandy soil using microbially induced carbonate precipitation for marine environments. *Géotechnique,* 64(12), 1010-1013.

Cheng, L., Shahin, M. A. and Cord-Ruwisch, R. (2016). Surface percolation for soil improvement by biocementation utilizing in situ enriched indigenous aerobic and anaerobic ureolytic soil microorganisms. *Geomicrobiology Journal,* 34(6), 546-556.

Cheng, L., Shahin, M. A. and Mujah, D. (2017). Influence of key environmental conditions on microbially induced cementation for soil stabilization. *Journal of Geotechnical and Geoenvironmental Engineering,* 143(1), 04016083.

Cho, G.-C., Dodds, J. and Santamarina, J. C. (2006). Particle shape effects on packing density, stiffness, and strength: natural and crushed Sands. *Journal of Geotechnical and Geoenvironmental Engineering*, 132(5), 591-602.

Choi, S.-G., Wu, S. and Chu, J. (2016). Biocementation for sand using an eggshell as calcium source. *Journal of Geotechnical and Geoenvironmental Engineering*, 10.1061/(asce)gt.1943-5606.0001534, 06016010.

Chou, C.-W., Seagren, E. A., Aydilek, A. H. and Lai, M. (2011). Biocalcification of sand through ureolysis. *Journal of Geotechnical and Geoenvironmental Engineering*, 137(12), 1179-1189.

Chu, J., Ivanov, V., Naeimi, M., Stabnikov, V. and Liu, H.-L. (2013). Optimization of calcium-based bioclogging and biocementation of sand. *Acta Geotechnica*, 9(2), 277-285.

Consoli, N. C., Festugato, L., da Rocha, C. G. and Cruz, R. C. (2013). Key parameters for strength control of rammed sand–cement mixtures: Influence of types of portland cement. *Construction and Building Materials*, 49, 591-597.

Consoli, N. C., Foppa, D., Festugato, L. and Heineck, K. S. (2007). Key parameters for strength control of artificially cemented soils. *Journal of Geotechnical and Geoenvironmental Engineering*, 133(2).

De Muynck, W., Leuridan, S., Van Loo, D., Verbeken, K., Cnudde, V., De Belie, N. and Verstraete, W. (2011). Influence of pore structure on the effectiveness of a biogenic carbonate surface treatment for limestone conservation. *Applied Environmental Microbiology*, 77(19), 6808-6820.

DeJong, J. T., Burbank, M., Kavazanjian, E., Weaver, T., Montoya, B. M., Hamdan, N., Bang, S. S., Esnault-Filet, A., Tsesarsky, M., Aydilek, A., Ciurli, S., Tanyu, B., Manning, D. A. C., Larrahondo, J., Soga, K., Chu, J., Cheng, X., Kuo, M., Al Qabany, A., Seagren, E. A., Van Paassen, L. A., Renforth, P., Laloui, L., Nelson, D. C., Hata, T., Burns, S., Chen, C. Y., Caslake, L. F., Fauriel, S., Jefferis, S., Santamarina, J. C., Inagaki, Y., Martinez, B. and Palomino, A. (2013). Biogeochemical processes and geotechnical applications: progress, opportunities and challenges. *Géotechnique*, 63(4), 287-301.

DeJong, J. T., Fritzges, M. B. and Nüsslein, K. (2006). Microbially induced cementation to control sand response to undrained shear. *Journal of Geotechnical and Geoenvironmental Engineering*, 132(11), 1381-1392.

DeJong, J. T., Martinez, B. C., Ginn, T. R., Hunt, C., Major, D. and Tanyu, B. (2014). Development of a scaled repeated five-spot treatment model for examining microbial induced calcite precipitation feasibility in field applications. *Geotechnical Testing Journal*, 37(3), 1-12.

DeJong, J. T., Mortensen, B. M., Martinez, B. C. and Nelson, D. C. (2010). Bio-mediated soil improvement. *Ecological Engineering*, 36(2), 197-210.

DeJong, J. T., Soga, K., Banwart, S. A., Whalley, W. R., Ginn, T. R., Nelson, D. C., Mortensen, B. M., Martinez, B. C. and Barkouki, T. (2011). Soil engineering in vivo: harnessing natural biogeochemical systems for sustainable, multi-functional engineering solutions. *Journal of the Royal Society Interface*, 8(54), 1-15.

Dhami, N. K., Reddy, M. S. and Mukherjee, A. (2013). Biomineralization of calcium carbonates and their engineered applications: A review. *Frontiers in Microbiology*, 4, 1-13.

Diambra, A., Ibraim, E., Peccin, A., Consoli, N. C. and Festugato, L. (2017). Theoretical derivation of artificially cemented granular soil strength. *Journal of Geotechnical and Geoenvironmental Engineering,* 10.1061/(asce)gt.1943-5606.0001646, 04017003.

Diambra, A., Ibraim, E., Russell, A. R. and Muir Wood, D. (2013). Fibre reinforced sands: from experiments to modelling and beyond. *International Journal for Numerical and Analytical Methods in Geomechanics,* 37(15), 2427-2455.

Duan, T. and Zhu, W. K. (2012). Optimization of calcium carbonate precipitation for Bacillus pasteurii. *Applied Mechanics and Materials,* 178-181, 676-679.

Duraisamy, Y. and Airey, D. W. (2015). Performance of biocemented Sydney sand using ex-situ mixing technique. *Journal of the Deep Foundations Institute,* 9(1), 48-56.

Farah, T., Souli, H., Fleureau, J.-M., Kermouche, G., Fry, J.-J., Girard, B., Aelbrecht, D., Lambert, J. and Harkes, M. (2016). Durability of bioclogging treatment of soils. *Journal of Geotechnical and Geoenvironmental Engineering,* 10.1061/(ASCE)GT.1943-5606.0001503.

Feng, K. and Montoya, B. M. (2016). Influence of confinement and cementation level on the behavior of microbial-induced calcite precipitated sands under monotonic drained loading. *Journal of Geotechnical and Geoenvironmental Engineering,* 142(1), 04015057.

Feng, K. and Montoya, B. M. (2017). Quantifying level of microbial-induced cementation for cyclically loaded sand. *Journal of Geotechnical and Geoenvironmental Engineering,* 10.1061/(asce)gt.1943-5606.0001682, 06017005.

Ferris, F. G., Phoenix, V., Fujita, Y. and Smith, R. W. (2004). Kinetics of calcite precipitation induced by ureolytic bacteria at 10 to 20°C in artificial groundwater. *Geochimica et Cosmochimica Acta,* 68(8), 1701-1710.

Fujita, Y., Ferris, F. G., Lawson, R. D., Colwell, F. S. and Smith, R. W. (2000). Subscribed content calcium carbonate precipitation by ureolytic subsurface bacteria. *Geomicrobiology Journal,* 17(4), 305-318.

Fujita, Y., Taylor, J. L., Gresham, T. L. T., Delwiche, M. E., Colwell, F. S., Mcling, T. L., Petzke, L. M. and Smith, R. W. (2008). Stimulation of microbial urea hydrolysis in groundwater to enhance calcite precipitation. *Environment Science and Technology,* 42(8), 3025-3032.

Gandhi, K. S., Kumar, R. and Ramkrishna, D. (1995). Some basic aspects of reaction engineering of precipitation processes. *Industrial & Engineering Chemical Research,* 34(10), 3223-3230.

Ginn, T. R., Murphy, E. M., Chilakapati, A. and Seeboonruang, U. (2001). Stochastic-convective transport with nonlinear reaction and mixing: application to intermediate-scale experiments in aerobic biodegradation in saturated porous media. *Journal of Contaminant Hydrology,* 48, 121-149.

Glatstein, D. A. and Francisca, F. M. (2014). Hydraulic conductivity of compacted soils controlled by microbial activity. *Environmental Technology,* 35(13-16), 1886-1892.

Gomez, M. G., Anderson, C. M., Graddy, C. M. R., DeJong, J. T., Nelson, D. C. and Ginn, T. R. (2016). Large-scale comparison of bioaugmentation and biostimulation approaches for biocementation of sands. *Journal of Geotechnical and Geoenvironmental Engineering,* 10.1061/(asce)gt.1943-5606.0001640, 04016124.

Gomez, M. G., Dworatzek, S. M., Martinez, B. C., deVlaming, L. A., DeJong, J. T., Hunt, C. E. and Major, D. W. (2014). Field-scale bio-cementation tests to improve sands. *Proceedings of the ICE - Ground Improvement*, 10.1680/grim.13.00052, 1-11.

Grabiec, A. M., Starzyk, J., Stefaniak, K., Wierzbicki, J. and Zawal, D. (2017). On possibility of improvement of compacted silty soils using biodeposition method. *Construction and Building Materials*, 138, 134-140.

Hamdan, N., Kavazanjian, E., Rittmann, B. E. and Karatas, I. (2016). Carbonate mineral precipitation for soil improvement through microbial denitrification. *Geomicrobiology Journal*, 34(2), 139-146.

Hammad, I. A. T., Fatma N. and Zoheir, A. E. (2013). Urease activity and induction of calcium carbonate precipitation by Sporosarcina pasteurii NCIMB 8841. *Journal of Applied Science Research*, 9(3), 1525-1533.

Hammes, F., Boon, N., de Villiers, J., Verstraete, W. and Siciliano, S. D. (2003a). Strain-specific ureolytic microbial calcium carbonate precipitation. *Applied Environmental Microbiology*, 69(8), 4901-4909.

Hammes, F., Seka, A., de Knijf, S. and Verstraete, W. (2003b). A novel approach to calcium removal from calcium-rich industrial wastewater. *Water Research*, 37, 699–704.

Hammes, F. and Verstraete, W. (2002). Key roles of pH and calcium metabolism in microbial carbonate precipitation. *Reviews in Environmental Science and Bio/Technology*, 1, 3-7.

Han, Z., Cheng, X. and Ma, Q. (2016). An experimental study on dynamic response for MICP strengthening liquefiable sands. *Earthquake Engineering and Engineering Vibration*, 15(4), 673-679.

Harbottle, M. J., Lam, M. T., Botusharova, S. P. and Gardner, D. R. (2014). *Self-healing soil: Biomimetic engineering of geotechnical structures to respond to damage*. Proceedings of the 7th International Congress of Environmental Geotechnics, Melbourne. pp. 1121-1128.

Harkes, M. P., van Paassen, L. A., Booster, J. L., Whiffin, V. S. and van Loosdrecht, M. C. M. (2010). Fixation and distribution of bacterial activity in sand to induce carbonate precipitation for ground reinforcement. *Ecological Engineering*, 36(2), 112-117.

Harris, D., Ummadi, J. G., Thurber, A. R., Allau, Y., Verba, C., Colwell, F., Torres, M. E. and Koley, D. (2016). Real-time monitoring of calcification process by sporosarcina pasteurii biofilm. *Analyst*, 141(10), 2887-2895.

Hillgartner, H., Dupraz, C. and Hug, W. (2001). Microbially induced cementation of carbonate sands: Are micritic meniscus cements good indicators of vadose diagenesis? *Sedimentology*, 48, 117-131.

Hooke, J. and Sandercock, P. (2017). *Combating desertification and land degradation spatial strategies using vegetation*. Switzerland: Springer.

Ismail, M. A. (2000). *Strength and deformation behaviour of calcite-cemented calcareous soil.* PhD Thesis, University of Western Australia, Australia. p. 353.

Ismail, M. A. (2002). Performance of an offshore stabilised calcareous soil. *Ground Improvement*, 6(4), 175-186.

Ismail, M. A., Joer, H. A., Randolph, M. F. and Meritt, A. (2002a). Cementation of porous materials using calcite. *Géotechnique*, 52(5), 313-324.

Ismail, M. A., Joer, H. A., Sim, W. H. and Randolph, M. F. (2002b). Effect of cement type on shear behavior of cemented calcareous soil. *Journal of Geotechnical and Geoenvironmental Engineering,* 128(6), 520-529.

Ivanov, V. and Chu, J. (2008). Applications of microorganisms to geotechnical engineering for bioclogging and biocementation of soil in situ. *Reviews in Environmental Science and BioTechnology*, 7(2), 139-153.

Ivanov, V., Chu, J. and Stabnikov, V. (2015a). Basics of construction microbial biotechnology. In F. P. Torgal, J. A. Labrincha, M. V. Diamanti, C. P. Yu, & H. K. Lee (Eds.), *Biotechnologies and Biomimetics for Civil Engineering* (10.1007/978-3-319-09287-4_2pp. 21-56). Switzerland: Springer International Publishing.

Ivanov, V., Chu, J., Stabnikov, V., He, J. and Naeimi, M. (2010). *Iron-based bio-grout for soil improvement and land reclamation.* Second International Conference on Sustainable Construction Materials and Technologies, Italy. pp. 415-420.

Ivanov, V., Chu, J., Stabnikov, V. and Li, B. (2015b). Strengthening of soft marine clay using bioencapsulation. *Marine Georesources & Geotechnology*, 33(4), 320-324.

Jiang, N. J. and Soga, K. (2014). *Seepage-induced erosion control by microbially induced calcite precipitation: An experimental investigation*. Proceedings of the 7th International Congress of Environmental Geotechnics, Melbourne. pp. 1113-1120.

Jiang, N. J. and Soga, K. (2017). The applicability of microbially induced calcite precipitation (MICP) for internal erosion control in gravel–sand mixtures. *Géotechnique*, 67(1), 42-55.

Jiang, N. J., Soga, K. and Kuo, M. (2016). Microbially induced carbonate precipitation for seepage-induced internal erosion control in sand–clay mixtures. *Journal of Geotechnical and Geoenvironmental Engineering,* 10.1061/(ASCE)GT.1943-5606.0001559.

Kanmani, S., Gandhimathi, R. and Muthukkumaran, K. (2014). Bioclogging in porous media: influence in reduction of hydraulic conductivity and organic contaminants during synthetic leachate permeation. *Journal of Environmental Health Science & Engineering,* 12(126), 1-11.

Kellerer-Pirklbauer, A. (2017). Potential weathering by freeze-thaw action in alpine rocks in the European Alps during a nine year monitoring period. *Geomorphology,* 296, 113-131.

Keykha, H. A., Huat, B. B. K. and Asadi, A. (2014). Electrokinetic stabilization of soft soil using carbonate-producing bacteria. *Geotechnical and Geological Engineering,* 32(4), 739-747.

Lake, C. B., Yousif, M. A.-M. and Jamshidi, R. J. (2017). Examining freeze/thaw effects on performance and morphology of a lightly cemented soil. *Cold Regions Science and Technology,* 134, 33-44.

Lee, M. J., Choi, S. K. and Lee, W. (2009). Shear strength of artificially cemented sands. *Marine Georesources & Geotechnology,* 27(3), 201-216.

Lee, M. L., Ng, W. S. and Tanaka, Y. (2013). Stress-deformation and compressibility responses of bio-mediated residual soils. *Ecological Engineering,* 60, 142-149.

Lin, H., Suleiman, M. T., Brown, D. G. and Kavazanjian, E. (2015). Mechanical behavior of sands treated by microbially induced carbonate precipitation. *Journal of Geotechnical and Geoenvironmental Engineering,* 10.1061/(asce)gt.1943-5606.0001383, 04015066.

Maleki, M., Ebrahimi, S., Asadzadeh, F. and Emami Tabrizi, M. (2016). Performance of microbial-induced carbonate precipitation on wind erosion control of sandy soil. *International Journal of Environmental Science and Technology,* 13(3), 937-944.

Martin, D., Dodds, K., Butler, I. B. and Ngwenya, B. T. (2013). Carbonate precipitation under pressure for bioengineering in the anaerobic subsurface via denitrification. *Environmental Science and Technology,* 47(15), 8692-8699.

Martinez, B. C. (2012). *Up-scaling of microbial induced calcite precipitation in sands for geotechnical ground improvement.* PhD Thesis, University of California Davis, USA. p. 256.

Martinez, B. C., DeJong, J. T., Ginn, T. R., Montoya, B. M., Barkouki, T. H., Hunt, C., Tanyu, B. and Major, D. (2013). Experimental optimization of microbial-induced carbonate precipitation for soil improvement. *Journal of Geotechnical and Geoenvironmental Engineering,* 139(4), 587-598.

Mitchell and Santamarina, J. C. (2005). Biological considerations in geotechnical engineering. *Journal of Geotechnical and Geoenvironmental Engineering,* 131(10), 1222-1233.

Mitchell, A. C. and Ferris, F. G. (2006). The influence of Bacillus pasteurii on the nucleation and growth of calcium carbonate. *Geomicrobiology Journal,* 23(3-4), 213-226.

Montoya, B. M. (2012). *Bio-mediated soil improvement and the effect of cementation on the behavior, improvement, and performance of sand.* PhD Thesis, University of California Davis, USA. p. 252.

Montoya, B. M. and DeJong, J. T. (2013). Healing of biologically induced cemented sands. *Géotechnique Letters,* 3(3), 147-151.

Montoya, B. M. and DeJong, J. T. (2015). Stress-strain behavior of sands cemented by microbially induced calcite precipitation. *Journal of Geotechnical and Geoenvironmental Engineering,* 141(6).

Montoya, B. M., DeJong, J. T. and Boulanger, R. W. (2013). Dynamic response of liquefiable sand improved by microbial-induced calcite precipitation. *Géotechnique,* 63(4), 302-312.

Mortensen, B. M., Haber, M. J., DeJong, J. T., Caslake, L. F. and Nelson, D. C. (2011). Effects of environmental factors on microbial induced calcium carbonate precipitation. *Journal of Applied Microbiology,* 111(2), 338-349.

Mujah, D. (2016). Compressive strength and chloride resistance of grout containing ground palm oil fuel ash. *Journal of Cleaner Production,* 112, 712-722.

Mujah, D., Shahin, M. A. and Cheng, L. (2016). State-of-the-art review of bio-cementation by microbially induced calcite precipitation (MICP) for soil stabilization. *Geomicrobiology Journal,* 34(6), 524-537.

Mujah, D., Cheng, L. and Shahin, M. A. (2019). Microstructural and geomechanical study on biocemented sand for optimization of MICP process. *Journal of Materials in Civil Engineering,* 31(4).

Nakarai, K. and Yoshida, T. (2015). Effect of carbonation on strength development of cement-treated Toyoura silica sand. *Soils and Foundations,* 55(4), 857-865.

National Health and Medical Research Council (2011). Australian Drinking Water Guidelines 6 (pp. 1126). Canberra.

National Meteorological Library (2015). Australian Government Bureau of Meteorology Guidelines (pp. 1187). Canberra.

Nemati, M. and Voordouw, G. (2003). Modification of porous media permeability, using calcium carbonate produced enzymatically in situ. *Enzyme and Microbial Technology,* 33(5), 635-642.

Ng, W. S., Lee, L. M., Tan, C. K. and Hii, S. L. (2013). Improvements in engineering properties of soils through microbial-induced calcite precipitation. *KSCE Journal of Civil Engineering,* 17(4), 718-728.

Ng, W. S., Lee, M. L. and Hii, S. L. (2012). An overview of the factors affecting microbial-induced calcite precipitation and its potential application in soil improvement. *World Academy of Science, Engineering and Technology,* 6(2), 683-689.

Ng, W. S., Lee, M. L., Tan, C. K. and Hii, S. L. (2014). Factors affecting improvement in engineering properties of residual soil through microbial-induced calcite precipitation. *Journal of Geotechnical and Geoenvironmental Engineering,* 140(5).

Okwadha, G. D. and Li, J. (2010). Optimum conditions for microbial carbonate precipitation. *Chemosphere,* 81(9), 1143-1148.

Park, K., Jun, S. and Kim, D. (2014a). Effect of strength enhancement of soil treated with environment-friendly calcium carbonate powder. *Scientific World Journal,* 2014, 526491.

Park, S., Choi, S. and Nam, I. (2014b). Effect of plant-induced calcite precipitation on the strength of sand. *Journal of Materials in Civil Engineering,* 26(8), 06014017.

Pham, V. P., Nakano, A., van der Star, W. R. L., Heimovaara, T. J. and van Paassen, L. A. (2016). Applying MICP by denitrification in soils: a process analysis. *Environmental Geotechnics,* 10.1680/jenge.15.00078, 1-15.

Phillips, A. J., Cunningham, A. B., Gerlach, R., Hiebert, R., Hwang, C., Lomans, B. P., Westrich, J., Mantilla, C., Kirksey, J., Esposito, R. and Spangler, L. (2016). Fracture sealing with microbially-induced calcium carbonate precipitation: A field study. *Environmental Science & Technology,* 50(7), 4111-4117.

Piriyakul, K. and Iamchaturapatr, J. (2013). Biocementation through microbial calcium carbonate precipitation. *Journal of Industrial Technology,* 9(3), 195-218.

Qiu, M., Hu, C., Liu, J., Chen, C. and Lou, X. (2017). Removal of high concentration of ammonia from wastewater by the ion exchange resin. *Nature Environment and Pollution Technology,* 16(1), 261-264.

Rajasekar, A., Moy, C. K. S. and Wilkinson, S. (2017). MICP and advances towards eco-friendly and economical applications. *IOP Conference Series: Earth and Environmental Science,* 78, 012016.

Rebata-Landa, V. (2007). *Microbial activity in sediments: Effects on soil behavior*. PhD Thesis, Georgia Institute of Technology, USA. p. 173.

Rebata-Landa, V. and Santamarina, J. C. (2006). Mechanical limits to microbial activity in deep sediments. *Geochemistry, Geophysics, Geosystems,* 7(11), 1-12.

Reddy, M. S., Achal, V. and Mukherjee, A. (2012). Microbial concrete, a wonder metabolic product that remediates the defects in building structures. In T. S. e. al. (Ed.), *Microorganisms in Environmental Management: Microbes and Environment* (10.1007/978-94-007-2229-3_24pp. 547-568). India: Springer.

Rios, S., Viana da Fonseca, A. and Baudet, B. A. (2012). Effect of the porosity/cement ratio on the compression of cemented soil. *Journal of Geotechnical and Geoenvironmental Engineering,* 138(11), 1422-1426.

Rong, H., Qian, C.-X. and Li, L.-z. (2012). Study on microstructure and properties of sandstone cemented by microbe cement. *Construction and Building Materials,* 36, 687-694.

Rong, H. and Qian, C. (2013). Microstructure evolution of sandstone cemented by microbe cement using X-ray computed tomography. *Journal of Wuhan University of Technology-Mater. Sci. Ed.,* 28(6), 1134-1139.

Ruistuen, H., Teufel, L. W. and Rhett, D. (1999). Influence of reservoir stress path on deformation and permeability of weakly cemented sandstone reservoirs. *SPE Reservoir Evaluation & Engineering,* 2(3), 266-272.

Sahrawat, K. L. (1984). Effects of temperature and moisture on urease activity in semi-arid tropical soils. *Plant and Soil,* 78, 401-408.

Salifu, E., MacLachlan, E., Iyer, K. R., Knapp, C. W. and Tarantino, A. (2016). Application of microbially induced calcite precipitation in erosion mitigation and stabilisation of sandy soil foreshore slopes: A preliminary investigation. *Engineering Geology,* 201, 96-105.

Santamarina, C. and Cho, G. C. (2004). *Soil behaviour: The role of particle shape.* Skempton Conference, London. pp. 1-14.

Schnaid, F., Prietto, P. D. M. and Consoli, N. C. (2001). Characterization of cemented sand in triaxial compression. *Journal of Geotechnical and Geoenvironmental Engineering,* 127(10), 857-868.

Sel, I., Ozhan, H. B., Cibik, R. and Buyukcangaz, E. (2014). Bacteria-induced cementation process in loose sand medium. *Marine Georesources & Geotechnology,* 33(5), 403-407.

Shahrokhi-Shahraki, R., O'Kelly, B. C., Niazi, A. and Zomorodian, S. M. A. (2015). Improving sand with microbial-induced carbonate precipitation. *Proceedings of the ICE - Ground Improvement,* 168(3), 217-230.

Sham, E., Mantle, M. D., Mitchell, J., Tobler, D. J., Phoenix, V. R. and Johns, M. L. (2013). Monitoring bacterially induced calcite precipitation in porous media using magnetic resonance imaging and flow measurements. *Journal of Contaminant Hydrology,* 152, 35-43.

Sharma, R., Baxter, C. and Jander, M. (2011). Relationship between shear wave velocity and stresses at failure for weakly cemented sands during drained triaxial compression *Soils and Foundations,* 51(4), 761-771.

Shen, P., Zhang, L. M., Chen, H. X. and Gao, L. (2017). Role of vegetation restoration in mitigating hillslope erosion and debris flows. *Engineering Geology,* 216, 122-133.

Smith, A., Pritchard, M., Edmondson, A. and Bashir, S. (2017). The reduction of the permeability of a lateritic soil through the application of microbially induced calcite precipitation. *Natural Resources,* 08(05), 337-352.

Stewart, T. L. and Fogler, H. S. (2001). Biomass plug development and propagation in porous media. *Biotechnology and Bioengineering,* 72(3), 353-363.

Stocks-Fischer, S., Galinat, J. K. and Bang, S. S. (1999). Microbial precipitation of CaCo3. *Soil Biology and Biochemistry,* 31, 1563-1571.

Terzis, D., Bernier-Latmani, R. and Laloui, L. (2016). Fabric characteristics and mechanical response of bio-improved sand to various treatment conditions. *Géotechnique Letters,* 6(1), 50-57.

Terzis, D. and Laloui, L. (2018). 3-D micro-architecture and mechanical response of soil cemented via microbial-induced calcite precipitation. *Scientific Reports,* 8(1).

Tobler, D. J., Cuthbert, M. O. and Phoenix, V. R. (2014). Transport of sporosarcina pasteurii in sandstone and its significance for subsurface engineering technologies. *Applied Geochemistry,* 42, 38-44.

Tobler, D. J., Maclachlan, E. and Phoenix, V. R. (2012). Microbially mediated plugging of porous media and the impact of differing injection strategies. *Ecological Engineering*, 42, 270-278.

Torkzaban, S., Tazehkand, S. S., Walker, S. L. and Bradford, S. A. (2008). Transport and fate of bacteria in porous media: Coupled effects of chemical conditions and pore space geometry. *Water Resources Research,* 44(4), 1-12.

Tuller, M., Or, D. and Dudley, L. M. (1999). Adsorption and capillary condensation in porous media: Liquid retention and interfacial configurations in angular pores. *Water Resources Research*, 35(7), 1949-1964.

Valdes, J. R. and Santamarina, C. (2006). Particle clogging in radial flow: Microscale mechanisms. *SPE Journal*, 193-198.

van Paassen, L. A. (2009). *Biogrout: Ground improvement by microbially induced carbonate precipitation.* PhD Thesis, Delft University of Technology, Netherlands. p. 203.

van Paassen, L. A., Daza, C. M., Staal, M., Sorokin, D. Y., van der Zon, W. and van Loosdrecht, M. C. M. (2010a). Potential soil reinforcement by biological denitrification. *Ecological Engineering*, 36(2), 168-175.

van Paassen, L. A., Ghose, R., van der Linden, T. J. M., van der Star, W. R. L. and van Loosdrecht, M. C. M. (2010b). Quantifying biomediated ground improvement by ureolysis: Large-scale biogrout experiment. *Journal of Geotechnical and Geoenvironmental Engineering,* 136(12), 1721-1728.

Van Tittelboom, K., De Belie, N., De Muynck, W. and Verstraete, W. (2010). Use of bacteria to repair cracks in concrete. *Cement and Concrete Research,* 40(1), 157-166.

Vatsala, A., Nova, R. and Murthy, B. R. S. (2001). Elastoplastic model for cemented soils. *Journal of Geotechnical and Geoenvironmental Engineering,* 127(8), 679-687.

Waller, J. T. (2011). *Influence of bio-cementation on shearing behavior in sand using X-ray computed tomography*. MSc Thesis, University of California Davis. p. 52.

Wang, Y. H. and Leung, S. C. (2008). Characterization of cemented sand by experimental and numerical investigations. *Journal of Geotechnical and Geoenvironmental Engineering,* 134(7), 992-1004.

Wei, S., Cui, H., Jiang, Z., Liu, H., He, H. and Fang, N. (2015). Biomineralization processes of calcite induced by bacteria isolated from marine sediments. *Brazillian Journal of Microbiology*, 46(2), 455-464.

Whiffin, V. S. (2004). *Microbial CaCO3 precipitation for the production of biocement.* PhD Thesis, Murdoch University, Australia. p. 162.

Whiffin, V. S., van Paassen, L. A. and Harkes, M. P. (2007). Microbial carbonate precipitation as a soil improvement technique. *Geomicrobiology Journal,* 24(5), 417-423.

Wojtowicz, J. A. (1998). Factors affecting precipitation of calcium carbonate. *Journal of the Swimming Pool and Spa Industry*, 3(1), 18-23.

Yang, Z. and Cheng, X. (2013). A performance study of high-strength microbial mortar produced by low pressure grouting for the reinforcement of deteriorated masonry structures. *Construction and Building Materials*, 41, 505-515.

Yasuhara, H., Neupane, D., Hayashi, K. and Okamura, M. (2012). Experiments and predictions of physical properties of sand cemented by enzymatically-induced carbonate precipitation. *Soils and Foundations*, 52(3), 539-549.

Zhao, Q., Li, L., Li, C., Li, M., Amini, F. and Zhang, H. (2014a). Factors affecting improvement of engineering properties of MICP-treated soil catalyzed by bacteria and urease. *Journal of Materials in Civil Engineering*, 10.1061/(asce)mt.1943-5533, 1-10.

Zhao, Q., Li, L., Li, C., Zhang, H. and Amini, F. (2014b). A full contact flexible mold for preparing samples based on microbial-induced calcite precipitation technology. *Geotechnical Testing Journal*, 37(5), 1-5.

APPENDIX A

Review Paper

Donovan Mujah, Mohamed A. Shahin, and Liang Cheng (2016) 'State-of-the-Art Review of Biocementation by Microbially Induced Calcite Precipitation (MICP) for Soil Stabilization' Geomicrobiology Journal, 34(6): 524-537

Author/ Attribution	conception & design	data acquisition & method	data conditioning & manipulation	data analysis & statistical method	data interpretation & discussion	final approval	revision & review
Donovan Mujah	×	×	×	N/A	×	×	×
I acknowledge that these represent my contributions to the above research output. Affiliation: Curtin University Signature:							
Dr. Mohamed A. Shahin	N/A	N/A	×	N/A	×	×	×
I acknowledge that these represent my contributions to the above research output. Affiliation: Curtin University Signature:							
Dr. Liang Cheng	N/A	N/A	×	N/A	×	×	×
I acknowledge that these represent my contributions to the above research output. Affiliation: Jiangsu University Signature:							

APPENDIX B

Technical Paper

Liang Cheng, Mohamed A. Shahin, and Donovan Mujah (2017) 'Influence of Key Environmental Conditions on Microbially Induced Cementation for Soil Stabilization' Journal of Geotechnical and Geoenvironmental Engineering 143(1) doi: 10.1061/(ASCE)GT.1943-5606.0001586

Author/ Attribution	conception & design	data acquisition & method	data conditioning & manipulation	data analysis & statistical method	data interpretation & discussion	final approval	revision & review
Dr. Liang Cheng	×	×	×	×	×	×	×
I acknowledge that these represent my contributions to the above research output. Affiliation: Jiangsu University Signature:							
Dr. Mohamed A. Shahin	×	N/A	×	×	×	×	×
I acknowledge that these represent my contributions to the above research output. Affiliation: Curtin University Signature:							
Donovan Mujah	×	×	×	×	×	×	×
I acknowledge that these represent my contributions to the above research output. Affiliation: Curtin University Signature:							

APPENDIX C

Technical Paper

Donovan Mujah, Liang Cheng, and Mohamed A. Shahin (2019). Microstructural and geo-mechanical study on bio-cemented sand for optimization of MICP process. Journal of Materials in Civil Engineering, 31(4) doi: 10.1061/(ASCE)MT.1943-5533.0002660

Author/ Attribution	conception & design	data acquisition & method	data conditioning & manipulation	data analysis & statistical method	data interpretation & discussion	final approval	revision & review
Donovan Mujah	×	×	×	×	×	×	×
I acknowledge that these represent my contributions to the above research output. Affiliation: Curtin University Signature:							
Dr. Liang Cheng	×	N/A	×	×	×	×	×
I acknowledge that these represent my contributions to the above research output. Affiliation: Jiangsu University Signature:							
Dr. Mohamed A. Shahin	×	N/A	×	×	×	×	×
I acknowledge that these represent my contributions to the above research output. Affiliation: Curtin University Signature:							

APPENDIX D

Technical Paper

Donovan Mujah, Mohamed A. Shahin, and Liang Cheng (2019). Experimental study and analytical model for strength behaviour of bio-cemented sand. *Proceedings of ICE - Ground Improvement*, under review.

Author/ Attribution	conception & design	data acquisition & method	data conditioning & manipulation	data analysis & statistical method	data interpretation & discussion	final approval	revision & review
Donovan Mujah	×	×	×	×	×	×	×
I acknowledge that these represent my contributions to the above research output. Affiliation: Curtin University Signature:							
Dr. Mohamed A. Shahin	×	N/A	×	×	×	×	×
I acknowledge that these represent my contributions to the above research output. Affiliation: Curtin University Signature:							
Dr. Liang Cheng	×	N/A	×	×	×	×	×
I acknowledge that these represent my contributions to the above research output. Affiliation: Jiangsu University Signature:							

APPENDIX E

Refereed Conference Proceedings

Donovan Mujah, Mohamed Shahin, and Liang Cheng (2016). Performance of bio-cemented sand under various environmental conditions. In Proceedings of XVIII Brazilian Conference on Soil Mechanics and Geotechnical Engineering, COBRAMSEG, 19-22 October 2016, Belo Horizonte, Brazil ISSN: 2595-0843 doi: 10.20906/CPS/GJ-05-0002

Author/ Attribution	conception & design	data acquisition & method	data conditioning & manipulation	data analysis & statistical method	data interpretation & discussion	final approval	revision & review
Donovan Mujah	×	×	×	×	×	×	×
I acknowledge that these represent my contributions to the above research output. Affiliation: Curtin University Signature:							
Dr. Mohamed Shahin	×	N/A	×	×	×	×	×
I acknowledge that these represent my contributions to the above research output. Affiliation: Curtin University Signature:							
Dr. Liang Cheng	×	N/A	×	×	×	×	×
I acknowledge that these represent my contributions to the above research output. Affiliation: Jiangsu University Signature:							